DISSERTATIONES SCHOLAE DOCTORALIS AD SANITATEM INVESTIGANDAM
UNIVERSITATIS HELSINKIENSIS

SANNA KOSKELA

THE LIMITS OF VISUAL SENSITIVITY AND ITS CIRCADIAN CONTROL

MOLECULAR AND INTEGRATIVE BIOSCIENCES RESEARCH PROGRAMME
FACULTY OF BIOLOGICAL AND ENVIRONMENTAL SCIENCES
DOCTORAL PROGRAM BRAIN AND MIND
UNIVERSITY OF HELSINKI

Molecular and Integrative Biosciences Research Programme
Faculty of Biological and Environmental Sciences
University of Helsinki
Helsinki, Finland

Doctoral Program Brain and Mind
Doctoral School of Health Sciences

THE LIMITS OF VISUAL SENSITIVITY AND ITS CIRCADIAN CONTROL

Sanna Koskela

DOCTORAL DISSERTATION

To be presented for public discussion with the permission of the Faculty of Biological and Environmental Sciences of the University of Helsinki, in Hall 1, Metsätalo, on the 9th of October 2020, at 16 o'clock.

Helsinki 2020

Supervisors	Associate Professor Petri Ala-Laurila Faculty of Biological and Environmental Sciences University of Helsinki, Finland Department of Neuroscience and Biomedical Engineering Aalto University School of Science, Finland Professor Kristian Donner Faculty of Biological and Environmental Sciences University of Helsinki, Finland
Thesis Advisory Committee	Docent Soile Nymark Faculty of Medicine and Health Technology Tampere University, Finland Docent Vootele Voikar Neuroscience Center Helsinki Institute of Life Science University of Helsinki, Finland
Reviewers	Associate Professor Tiffany Schmidt Department of Neurobiology Northwestern University, Evanston, IL, USA Professor Eric Warrant Department of Biology, Faculty of Science Lund University, Lund, Sweden
Opponent	Chief, Dr. Samer Hattar Section on Light and Circadian Rhythms National Institute of Mental Health National Institutes of Health, Bethesda, MD, USA
Custos	Professor Juha Voipio Faculty of Biological and Environmental Sciences University of Helsinki, Finland

Cover illustration by Sanna Koskela

Published in Dissertationes Scholae Doctoralis Ad Sanitatem Investigandam Universitatis Helsinkiensis.

ISBN 978-951-51-6548-0 (paperback)

ISBN 978-951-51-6549-7 (PDF)

ISSN 2342-3161 (print)

ISSN 2342-317X (online)

Painosalama Oy

Helsinki 2020

THE BRAIN – is wider than the Sky –
For – put them side by side –
The one the other will contain
With ease – and You – beside –

Emily Dickinson, c. 1863.
Poem #598 (R.W. Franklin edition)

ABSTRACT

At the sensitivity limit of vision, the quantal fluctuations of light and neural noise in the retina and the brain limit the detection of light signals. The challenge for vision, as for all senses, lies in separating the weakest signals from the neural noise originating within the sensory system. In this thesis, I studied sparse signal detection in the vertebrate visual system (mouse and frog) at low light levels from single retinal neurons to behavioral performance.

First, we determined the sensitivity limit of amphibian color vision at low light levels. Unlike most vertebrates, amphibians are potential dichromats even at night, with two spectrally distinct classes of rod photoreceptors: common vertebrate rods (peak sensitivity at 500 nm) and an additional class called "green rods" (peak sensitivity at 430 nm). We showed that frogs in a phototaxis experiment can distinguish blue from green down to their absolute visual threshold, meaning that they have wavelength discrimination as soon as they start seeing anything. Remarkably, the behavioral blue/green discrimination approached theoretical limits set by photon fluctuations and rod noise, highlighting the sensitivity of the system comparing signals from the two different photoreceptors. Additionally, we show that the amphibian threshold for color discrimination is task- and context-dependent, underlining that sensory discrimination is not universally driven to absolute physical limits, but depends on evolutionary trade-offs and flexible brain states.

In the second paper, we studied the impact of the circadian rhythm on the sensitivity limit of mouse vision. The retina has its own intrinsic circadian rhythms, which has led to the hypothesis that the sensitivity limit of vision would be under circadian control. We used a simple photon detection task, which allowed us to link well-defined retinal output signals to visually guided behavior. We found that mice have strikingly better performance in the visual task at night, so that they can reliably detect 10-fold dimmer light in the night than in the day. Interestingly, and contrary to previous hypotheses, this sensitivity difference did not arise in the retina, as assessed by spike recordings from retinal ganglion cells. Instead, mice utilize a more efficient search strategy in the task during the night. They are even able to apply the more efficient strategy at day once they have first performed the task during the night. Measured differences in search strategy explain only part of the day/night difference, however. We hypothesize that in addition there are diurnal changes in the state of brain circuits reading out the retinal input and making decisions.

In the third paper, we determined the sensitivity limit of decrement (shadow) detection of mouse vision. Compared with the question of ultimate limit for detecting light, the question of sensitivity limits for detecting light decrements (negative contrast) has been remarkably neglected. We recorded

the OFF responses of the most sensitive retinal ganglion cells at dim background light levels and correlated the thresholds to visually guided behavior in tightly matched conditions. We show that compared with an ideal-observer model most of the losses happen in the retina and remarkably, the behavioral performance is very close to an optimal read-out of the retinal ganglion cells.

I have shown across visual tasks and in two different species how closely behavior in specific conditions can approach the performance limit set by physical constraints, rejecting noise and making use of every available photon. However, the actual performance strongly depends on the behavioral context and relevance of the task and state of the brain.

TIIVISTELMÄ

Näön herkkyyden rajalla valokvanttien vähäinen määrä asettaa erityisen suuren haasteen näköjärjestelmän toiminnalle. Tällöin näköjärjestelmän on kyettävä erottamaan heikoimmatkin signaalit aistijärjestelmän sisäisestä kohinasta. Väitöskirjassani kysyn miten biologiset mekanismit vastaavat näihin haasteisiin. Selvitän hermoverkkojen signaalinkäsittelykykyä käyttäytymistä määrittävänä tekijänä, käyttäen mallina selkärankaisen (sammakko, hiiri) silmän verkkokalvon suorituskykyä lähellä näönherkkyyden rajaa. Tutkin näköaistin suorituskykyä yksittäisten verkkokalvon hermosolujen tasolta koko eläimen näönvaraiseen käyttäytymiseen.

Ensimmäisessä osaprojektissa määritin heikoimman valointensiteetin missä sammakko pystyy erottamaan värejä. Toisin kuin muilla selkärankaisilla, sammakkoeläimillä on kaksi erityyppistä hämäränäköön erikoistunutta sauva-valoreseptoria: vihreän valon aallonpituutta parhaiten absorboiva viherherkkä sauvareseptori (kuten meillä) sekä lyhyempiä, sinisiä aallonpituuksia absorboiva siniherkkä sauva. Osoitimme, että sammakot pystyvät erottamaan värejä valaistuksessa, missä ihmiset eivät pysty. Tämä sini/viher-erotuskyky lähestyi teoreettisia fysikaalisia raja-arvoja. Lisäksi näytimme, että sammakkoeläinten värinäön kynnysherkkyys riippuu käyttäytymistehtävästä, korostaen kuinka aistinvarainen erotuskyky riippuu myös evolutiivisista valinnoista ja eläimen käyttäytymistilasta.

Toisessa osatyössä tutkin vuorokausirytmin vaikutusta hiiren näönherkkyyteen. On oletettu, että verkkokalvon sopeutuu ennakoivasti valtaviin valon intensiteettimuutoksiin yön ja päivän välillä. Tässä työssä käytimme yksinkertaista, himmeiden valojen havaitsemistehtävää, joka mahdollisti verkkokalvon aivoihin lähettämän signaalin yhdistämisen näönvaraiseen käyttäytymiseen tiukan kvantitatiivisesti. Havaitsimme, että yöllä hiiret erottivat hyvin heikkoja valoja pimeässä jopa kymmenen kertaa paremmin kuin päivällä. Yllätykseksemme tämä ei johtunut muutoksista verkkokalvon maksimaalisessa herkkyydessä, vaan parempi suorituskyky yöllä johtui tehokkaammasta käyttäytymisstrategiasta sekä tarkemmasta näkötiedon käsittelystä aivoissa. Näytimme lisäksi, että hiiret pystyvät hyödyntämään tehokkaampaa strategiaa myös päiväsaikaan, jos ovat ensin suorittaneet tehtävän yöllä.

Näkeminen vaatii sekä valojen että varjojen havaitsemista. Kolmannessa osaprojektissa määritin kuinka paljon fotoneja pitää poistaa heikosta taustavalosta, jotta hiiri havaitsee eron. Tämä kysymys on jäänyt verrattain huomiotta, verrattuna kymmenien vuosien tutkimukseen pienimmästä havaittavasta valomäärästä. Vertasimme herkimpien

verkkokalvosolujen suorituskykyä näönvaraiseen käyttäytymiseen vastaavissa olosuhteissa. Näytimme verkkokalvon prosessointiin perustuvaa mallinnusta hyväksi käyttäen, että verrattuna teoreettisesti täydelliseen suorituskykyyn suurin osa informaationmenetyksistä tapahtuu verkkokalvolla fotonien pyydystämisessä ja verkkokalvon signaalinkäsittelyssä. Käyttäytyminen sen sijaan on huomattavan lähellä tilannetta, jossa aivot lukevat verkkokalvon lähettämää signaalia lähes täydellisesti.

Väitöskirjassani näytän kahdella selkärankaisella, kuinka näkösuoritus pääsee useassa tehtävässä erittäin lähelle fysikaalisten reunaehtojen määräämiä raja-arvoja. Suorituskyky riippuu kuitenkin kontekstista ja käyttäytymistehtävän merkityksestä eläimelle sekä aivojen sen hetkisestä tilasta.

CONTENTS

LIST OF ABBREVIATIONS AND SYMBOLS

A	absorbance
A_c	collecting area for rod at its peak wavelength
A_{pupil}	pupil area, mm²
A_{retina}	retinal projection area
A1	retinal
A2	3,4-didehydroretinal
AANAT	aralkylamine N-acetyltransferase
AMPA	α-amino-3-hydroxy-5-methyl-4-isoxazolepropionic acid
ATP	adenosine triphosphate
ADP	Adenosine diphosphate
AII	AII amacrine cell
BMAL1	(Aryl hydrocarbon receptor nuclear translocator-like) transcription factor
BS	blue-sensitive
c	speed of light; 299 792 458 m s^{-1}
c	concentration
cAMP	cyclic adenosine monophosphate
Ca^{2+}	calcium
CNG	cyclic-nucleotide-gated channel
cGMP	cyclic guanosine monophosphate
CLOCK	(Circadian Locomotor Output Cycles Kaput) transcription factor
CRY	cryptochrome circadian protein
CV	coefficient of variation
D	distance, mm
d	diameter, mm
$\Delta\varphi$	inter-receptor angle
$\Delta\rho$	angular width, or acceptance angle
DNA	deoxyribonucleic acid
dLGN	dorsal lateral geniculate nucleus
DLP	Digital Light Processing
E	energy per photon, J $photon^{-1}$
ϵ	molar extinction coefficient
ε	optical density per unit distance
ERG	electroretinogram
F	photon flux density, photons μm^{-2} s^{-1}
f	focal length
Φ	flux of photons, s^{-1}
F_{cornea}	corneal photon flux, photons μm^{-2} s^{-1}
FWHM	full-width at half-maximum
γ	quantum efficiency of photoactivation
G* or Gα-GTP	activated G-protein
G-protein	guanosine nucleotide-binding protein
GABA	γ-aminobutyric acid
GC	guanylate cyclase
GCAP	guanylate-cyclase-activating protein
GDP	guanosine diphosphate
GS	green-sensitive
GTP	guanosine triphosphate
h	Planck's constant; 6.626×10^{-34} Js
IGL	intergeniculate leaflet
IPL	inner plexiform layer
ipRGC	intrinsically photosensitive ganglion cell
I_o	incident light
I_t	transmitted light
LWS	long-wavelength-sensitive
L	length
N	nodal point
OD	optical density
OPL	outer plexiform layer
OPN	olivary pretectal nucleus
OS	outer segment
P	power, J s^{-1}
PDE	phosphodiesterase
PDE*	activated phosphodiesterase
PER	Period –protein complex
r	radius, mm
R*	activated rhodopsin
R* rod^{-1} s^{-1}	photoisomerizations per rod per second
RBC	rod bipolar cell
RGC	retinal ganglion cell
RHT	retinohypothalamic tract
$R_{\lambda max}$	relative absorption factor
ROS	rod outer segment
RPE	retinal pigment epithelium
RS	red-sensitive
σ^2	variance
SC	superior colliculus
SCN	suprachiasmatic nucleus
SNR	signal-to-noise ratio
SWS	short-wavelength-sensitive
τ	transmittance
TRP	transient receptor potential
Ub	ubiquitylation
UV	ultraviolet
θ	visual angle, degrees

In the text, gene names are written in *italics*. Protein names are written in Roman.

LIST OF FIGURES

Figures are authors own, unless otherwise mentioned.

LIST OF ORIGINAL PUBLICATIONS

This thesis is based on the following publications:

I Yovanovich, C.A.M., **Koskela, S.M.**, Nevala, N., Kondrashev, S.L., Kelber, A., and Donner, K. (2017). The dual rod system of amphibians supports colour discrimination at the absolute visual threshold. Philosophical Transactions of the Royal Society B: Biological Sciences. *372*, 20160066.

II **Koskela, S.**, Turunen, T., and Ala-Laurila, P. (2020). Mice reach higher visual sensitivity at night by using a more efficient behavioral strategy. Current Biology. *30*, 42–53.e4.

III Westö, J., Martyniuk, N., **Koskela, S.**, Turunen, T., Pentikäinen, S. & Ala-Laurila, P. (2020). Visually-guided behavior in mice at starlight reaches the limit set by the retinal OFF pathway for detecting light decrements. (*in preparation*).

The publications are referred to in the text by their roman numerals.

AUTHOR'S CONTRIBUTION

I The author designed and set up the phototaxis experiments together with C.A.M.Y. and K.D., collected the animals together with N.N. and analyzed the data together with K.D. She also participated in writing and revising of the manuscript.

II The author designed the experiments together with P.A.–L., performed all the experiments and analyzed the data together with T.T. and P.A.–L. The author wrote the first draft of the manuscript and created all the figures together with T.T. and P.A.–L. and participated in writing and revising the final manuscript.

III The author participated in setting-up the behavioural experiments, in the design of the experiments, in the collection and analysis of the ganglion cell, behavioural, and pupil data. The author also participated in creating of the manuscript figures and writing of the manuscript.

1 INTRODUCTION

Animal behavior depends on information acquired by sensory systems. The more accurate information the animal obtains, the better equipped it is to adjust its behavior to meet the demands of the variable environment (Dall et al., 2005). Physical limits and biological trade-offs constrain the acquisition and use of sensory information. Throughout the visual system, we find compromises and optimizations at the crossroads of several competing goals. On an evolutionary time scale, natural selection works to find compromises that increase fitness in any given niche. During the life history of the individual, adaptation mechanisms acting on different time scales serve similar purposes.

Vision at night is often operating near its physical limit, as photons are so sparse that only a few photoreceptors among thousands absorbs a photon within their integration time (Kiani et al., 2020). Further, the quantal fluctuations of light and neural noise in the retina and the brain limit the detection of light signals, leading to a compelling trade-off between sensitivity and reliability. The challenge for vision, as for all senses, at the sensitivity limit lies in discriminating weak signals from noise. Remarkably, reliable visually guided behavior may be driven by only a handful of photons, reflecting the striking capacity of the neural circuits of the retina and the brain to process weak signals and reject noise.

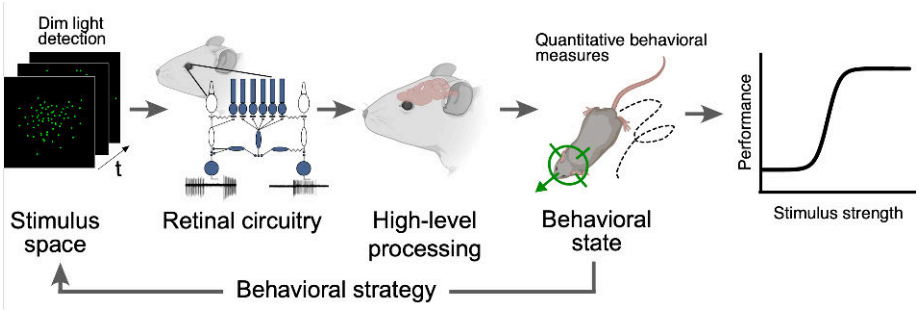

Figure 1 **Integrative research from photon distribution to neural circuitry to behavioural performance.** Studying signal/noise discrimination at several levels of the visual system, from single retinal cells to behavioural performance, using controlled stimuli and quantitative methods reveals general principles of signal processing and noise handling by neural circuits. Figure partly created with BioRender.com.

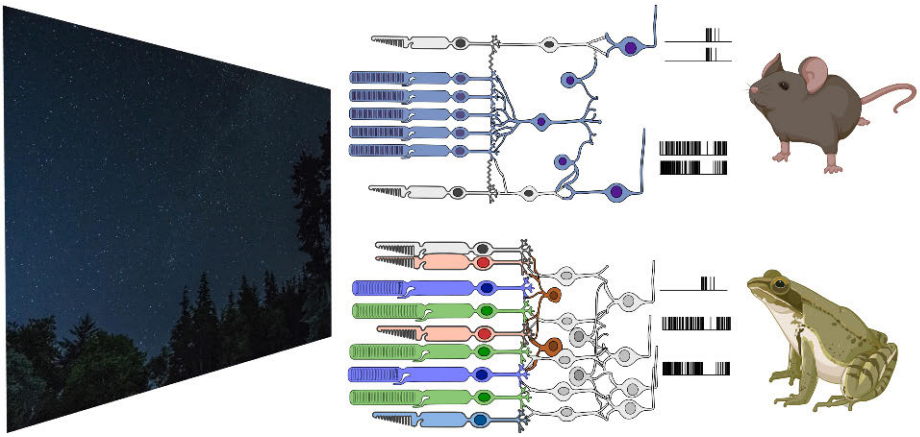

Figure 2 **Sparse signal detection in the mouse and frog visual systems.** The aim of this thesis is to study limits of visual performance at low light levels from single retinal neurons to behavioural performance in two vertebrate species, mouse and frog. The retinal circuitry processing signal at scotopic light levels in mice is well known (rod bipolar pathway, blue). Unlike other vertebrates, amphibians possess two classes of rod photoreceptors (blue-sensitive and green-sensitive) for dim light vision, besides red-sensitive and blue-sensitive cones. Unfortunately, the frog inner retinal circuitry (grey) is not known well enough to allow a more detailed description. Figure partly created with BioRender.com.

As expressed by Peter Sterling, "where actual performance approaches "ideal" performance calculated from physical limits, there is a genuine opportunity to address the "why" of a design" (Sterling, 2004). The "why" comprises the entire information chain from the sensory receptors through several levels of neural processing to the actual behavior (Figure 1). Why is it important to invest vital resources in the processing of this information? To paraphrase a famous quote by Theodosius Dobzhansky, nothing in neuroscience makes sense except in the light of behavior. The "behavior" of neural circuits is not the same as the behavior of the animal. "Ideal" performance at some neural stage is biologically meaningful only if the information is needed for guiding similarly ideal animal performance.

When evolution works to improve performance, it does so by tinkering, not by designing (Jacob, 1977). Thus "an animal's solution reflects a unique nervous system with adaptive limitations, biases, and distortions" (Wehner, 1987). Therefore, it is crucial not to limit investigations to a single species. In this thesis I study the limits of visual performance at low light levels in two vertebrate species, frog and mouse, and analyze the physical, physiological and behavioral factors affecting the limits (Figure 2). I show how remarkably close to ultimate performance limits set by physics visually guided behavior can get in certain tasks. On the other hand, I show how different performance may be in similar tasks in somewhat different situations, indicating how strongly the use of sensory information depends on behavioral context, relevance of the task and state of the brain.

2 REVIEW OF THE LITERATURE

The first part of the literature review concerns the limits of vision in dim light, both physical and physiological. The second part discusses how vertebrate evolution has dealt with these limits when responding to differing needs dictated by the lifestyles of different species, using the visual systems of mouse (*Mus musculus*) and frog (*Rana temporaria*) as examples.

2.1 THE LIMITS OF SCOTOPIC VISION

2.1.1 PHYSICAL AND MOLECULAR LIMITS

2.1.1.1 Nature of light

Any light sensing system from photoreceptors to man-made electronics must overcome the elemental physical limits that stem from the nature of light itself. Light is electromagnetic radiation that propagates through space. It is described either as a wave or as a flux of discrete energy quanta, photons, depending on the situation. Associated with both characterizations are properties that set ultimate limits to the use of light information, but it is mainly the particle nature of light that sets the ultimate limit for vision in dim light.

In a dark forest at night or underground in a cave, vision faces the challenge of capturing enough photons for a reliable signal. Photons are scattered and reflected even before they reach the photoreceptors. Already at starlight intensities, photons are spread so sparsely that vision relies on the absorption of single photons in a few rod photoreceptors among thousands. As already discovered in the 1940's in a set of famous experiments, rod photoreceptors of the human eye must be able to respond to single photons to enable the absolute sensitivity of human vision (Hecht et al., 1942). For an ideal, noiseless photodetector, a single photon would be enough. But it turns out there's more to it: from the quantal nature of light follows that the arrival of photons is governed by Poisson statistics, meaning that photons arrive to the detector stochastically, like raindrops from the sky. Hence nominally constant light produces a time-varying rate of photons: for example, a light source producing an average of six photons in 1 s will sometimes send five or less, sometimes seven or more photons. This inherent variation, or noise, in the arrival and absorption of photons sets the absolute limit for the performance of any detector. The effect is well demonstrated in an illustration of how precisely an increment or decrement pattern is depicted on a photoreceptor grid based on different numbers of randomly arriving photons (Figure 3; Pirenne, 1967).

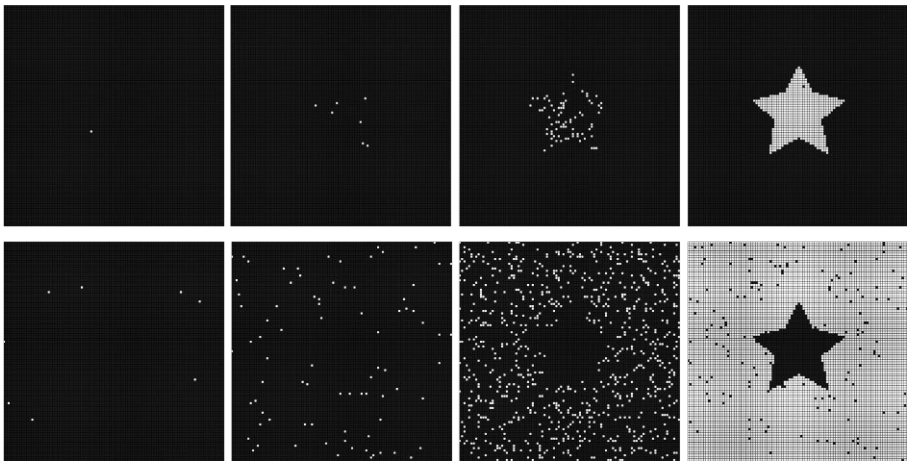

Figure 3 **The effect of photon shot noise on the resolution of images based on positive and negative contrast.** At the lowest light level (1x) only a few photoreceptors are absorbing a photon and the image is indistinguishable. Even at ten times higher light level (10x) the shapes of the white increment and the dark decrement remain disguised. When increasing the light intensity another 10-fold (100x), the star appears but still with a considerable amount of uncertainty. We need to increase the light levels yet another ten times to get a well-resolved image.

In natural scenes which present a palette of multiple contrasts, this photon 'shot noise' has an even more degrading effect than for the simple binary black-or-white image (Figure 4). The quantum fluctuations will limit the finest contrast that can be discriminated at any given light level. This is clearly explained by Poisson statistics. A key property of Poisson statistics is that the variance of the event count is equal to the mean. Thus, the standard deviation of absorbing the mean of N photons is √N. In other words, if we say that N photons (signal) are absorbed within a certain integration time, the shot noise associated with the sample is √N. The ratio of signal to noise, SNR, reduces to the square root of the signal

$$SNR = \frac{N}{\sqrt{N}} = \sqrt{N}. \qquad (1)$$

This is the famous Rose–de Vries or square-root law demonstrating how the SNR, and thus contrast discrimination, improves as the square root of the photon catch. This explains why, even though Poisson fluctuations are present at all light levels, their impact increases dramatically when the light levels decrease.

The second important physical limitation to consider here is the differing photon energies (E) associated with different wavelengths of light, described by the equation:

$$E = \frac{hc}{\lambda}, \qquad (2)$$

where h is Planck's constant (6.6 x 10^{-34}), c the speed of light (ca. 3 x 10^{8} m/s in air) and λ the wavelength of light. Only a narrow wavelength band is visible to the human eye, roughly 380-720 nm corresponding to a frequency range of ca. 790-420 THz, with no sharp cut-off. The limits are determined by the limitations of the primary molecules which absorb the photon energy and transduce this event into a chemical signal in the photoreceptor cell (see 2.1.1.2 below).

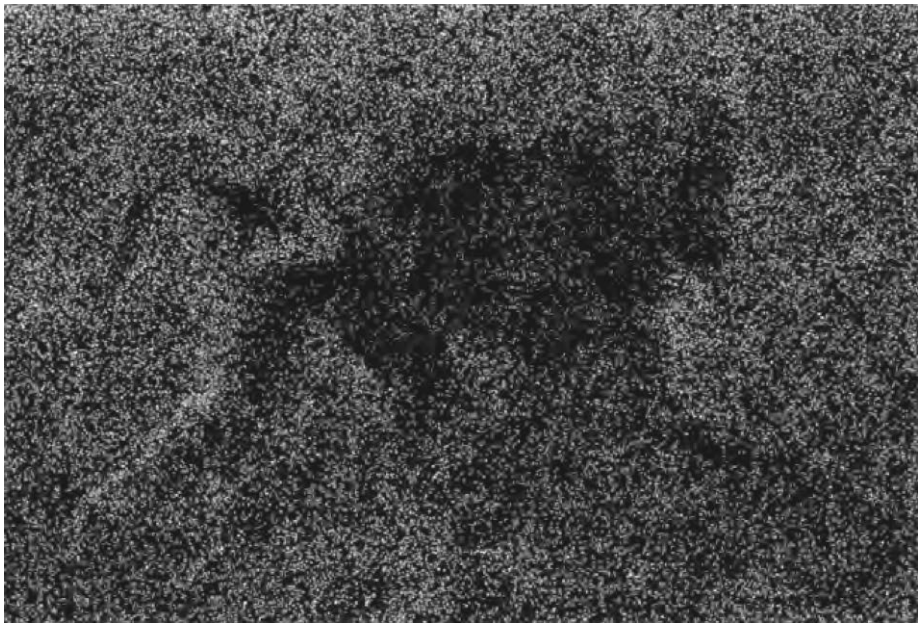

Figure 4 **A baboon in starlight.** Each dot denotes one photon absorption. Photons are captured randomly with probabilities described by Poisson statistics and thus the SNR of the image would improve with the square root of the number of photons (eqn. 1). Reprinted from Sterling (2004) with permission from MIT Press.

2.1.1.2 Limits set by the properties of biomolecules

Eukaryotes developed light sensitive molecules – known as visual pigments or 'type 2' rhodopsins – to catch photons and translate the photon's energy into a chemical signal roughly 700 million years ago. Similar molecules ('type 1' rhodopsins) had been developed both for catching energy and sensing light by archaeans a couple of billion years ago, but the evolutionary relationship to visual pigments is unclear. The properties of these ancient molecules set constraints on vision that can be regarded as equally fundamental as the purely physical limitations. On a general level, this is because the basic properties of proteins determine life as we know it. More specifically, once this particular protein-ligand -pair had been selected as the source of all true vision, evolution could not reverse and invent anything more competitive. In a similar manner to rhodopsin, all the biomolecules in the phototransduction cascade and in the downstream circuitries can set theoretical limits to vision (see e.g. discussion in Kiani et al., 2020) but here I shall focus on the properties of rhodopsin for two reasons: first, because of its unique position at the very input to the visual system, second, because of the exceptionally detailed functional understanding of this protein.

Phototransduction The protein-ligand -pair in visual pigment molecules consists of a protein called opsin to which the ligand, chromophore, is covalently bound. Opsins are all similar in structure with 7 transmembrane α-helical segments and belong to the family of G-protein-coupled receptors or GPCRs, the largest and most diverse class of transmembrane receptors (Palczewski et al., 2000; Luo et al., 2008). In most GPCRs binding of a ligand causes a conformational change which in turn activates an associated G-protein. G-proteins (belonging again to a bigger class of GTPases) are internal cell messengers with a variety of signaling routes. Opsins are special GPCRs because their covalently bound ligand, the chromophore, acts as an antagonist locking the molecule in its inactive state. The chromophore is the primary light-absorbing part of the visual pigment molecule, with a long chain of alternating double and single bonds. Altogether four different chromophores are known in the animal kingdom, of which the most common is a vitamin A1 aldehyde, knowns as 11-cis-retinal or simply, retinal (Cronin et al., 2014). The second chromophore that occurs in vertebrates, mainly in amphibians and fish, is an A2-derivative, 11-*cis*-3,4-didehydroretinal (or 3-dehydroretinal).

Phototransduction begins when a photon hits the visual pigment molecule (Figure 5) (reviewed in e.g. Burns and Lamb 2004; Fu and Yau, 2007; Luo et al., 2008). The bond between the 11th and 12th carbon atoms in the chromophore reacts to the photon's energy by changing from the kinked *cis*- to the straight *trans*-configuration. This isomerization forces the surrounding opsin protein to go through a number of very fast conformational changes to the more long-lasting active state (R* or metarhodopsin II) and coupling it to the G-protein (often called transducin in vertebrates). Consequently, a series of biochemical events is initiated resulting in the closure of sodium channels

and hyperpolarization of the photoreceptor cell. Thus, the physical energy of the photon absorbed in one molecule has been transduced into a chemical signal involving thousands of molecules and finally into a voltage-change of the photoreceptor cell (see Figure 5 for details). Because the initial reaction requires only one photon and because of the impressive amplification factor of the phototransduction cascade, the dark-adapted rod photoreceptors are in fact capable of signaling the absorption of single photons. This remarkable capability was in fact discovered first in invertebrate photoreceptors more than 60 years ago (Yeandle, 1958; Fuortes & Yeandle 1964, reviewed in e.g. Warrant 2017). Compared to vertebrate rod responses, these so called 'bumps' are however more variable, causing more transducer noise.

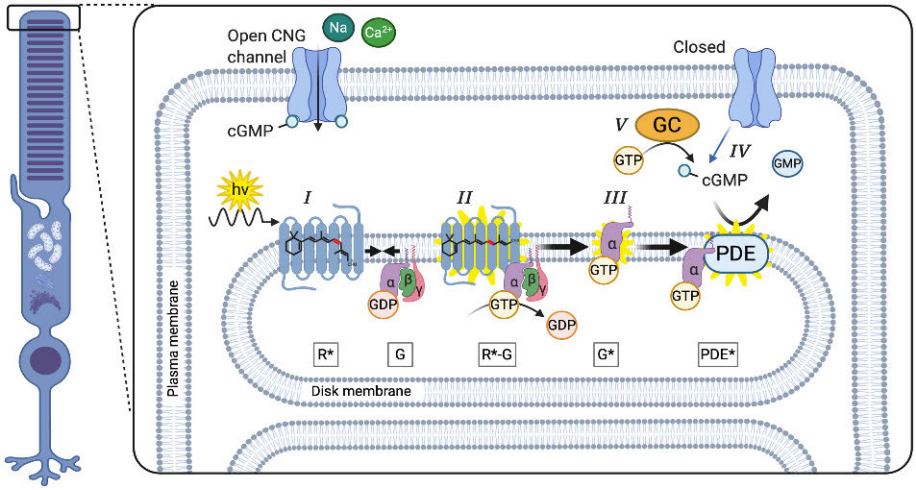

Figure 5 **Phototransduction in the rod outer segment.** In darkness, the cyclic-nucleotide-gated (CNG) channels are open and a steady-state current through them depolarizes the photoreceptor. I) The CNG-gated channels are hetero-tetrameric, relatively non-specific cation channels, which require the binding of at least three cyclic nucleotide molecules to be open. When a photon hits the visual pigment located on the disk membrane in the rod outer segment, the energy of the photon isomerizes the chromophore from 11-*cis*-retinal to all-*trans*-retinal (R*). II) The activated visual pigment molecule (R*) in turn activates the G-protein so that the α-subunit of the G-protein switches guanosine triphosphate (GTP) to guanosine diphosphate (GDP). III) The activated G-protein (Gα-GTP or G*) encounters and activates the phosphodiesterase (PDE to PDE*), which catalyzes the hydrolysis of cyclic monophosphate (cGMP). IV) The drop in the cGMP concentration leads to the closure of the CNG-channels and results in a hyperpolarization of the membrane potential of the rod and decrease in the intracellular Ca^{2+}. V) The cGMP levels are restored by guanylate cyclase (GC) synthesizing cGMP from GTP in a calcium-dependent manner. See text for references. Figure created with BioRender.com.

Thermal noise Photons in starlight are sparse, and even in daylight the chances of two photons hitting the same rhodopsin molecule so that both contribute to excitation are close to zero. The visual pigments should be able to catch photons efficiently and be activated by the energy of single photons, yet minimize the tendency to be activated by thermal energy alone. Randomly occurring thermal or spontaneous activations of the rhodopsin molecule trigger the same amplification cascade as photoactivations and the cell's responses to the two cannot be distinguished. Therefore, they constitute an irreducible internal noise obscuring the detection of real photons (reviewed in Donner, 2020). For example, the thermal stability of the mouse rod pigment is such that at 37 °C a molecule is spontaneously activated on average once in a few hundreds of years (Burns et al., 2002). Nonetheless, as a single rod packs hundreds of millions of rhodopsin molecules into its outer segment membranes to achieve high photon catch (e.g. typically 10^7 in mammalian rods to 10^9 in amphibian rods, estimation based on rod dimensions from Carter-Dawson and LaVail, 1979; Donner et al., 1990b). This means that even with the high degree of thermal stability there will be 20-30 spontaneous events within the integration time and area of a large mouse retinal ganglion cell (RGC) (see e.g. paper II of this thesis). It is obvious that the internal noise caused by the thermal isomerizations sets a theoretical limit to visual sensitivity. To which extent this limit can be reached in distinct visual computations at the lowest light levels remains to be seen (Field et al., 2019; Kiani et al., 2020).

The quantum efficiency, the probability that the absorption of a photon initiates photoactivation of the visual pigment molecule, of 0.67 is a rare constant in the animal kingdom implying that it reached some functional maximum during evolution (Dartnall, 1968). Indeed, compared to other photochemical events this is a high efficiency. The fact that the quantum efficiency of the rhodopsin molecule is at least two times higher than that of the 11-*cis*-retinal protonated Schiff base not bound to the opsin indicates how much the protein binding site optimizes the photoisomerization event (Freedman et al., 1986; Birge et al., 1988).

Spectral sensitivity The second important property of visual pigments is how well they can utilize the light spectrum available. Spectral sensitivity describes the relative probabilities of the visual pigment to be activated by different wavelengths of electromagnetic radiation (Cronin et al., 2014). Visual pigments are always maximally sensitive to a certain wavelength, so that the absorption probability is highest for photons corresponding to that wavelength, and absorption probabilities fall off monotonically towards shorter and longer wavelengths. The differing spectral absorbances of visual pigments also enable color vision: The ability to distinguish colors is based on the analysis of wavelength distributions based on comparison of signals from at least two visual pigments with different spectral sensitivities.

The wavelength of maximum absorption (λ_{max}) varies between 360–630nm (Shichida and Imai, 1998), being limited by the energy content of the photons. For one, proteins are destroyed by high-energy photons of very short-wavelength radiation (<360nm, UV-radiation, X-rays) whereas the low-energy photons of very long-wavelength radiation (>630 nm, infrared, microwaves) fail to excite them. Furthermore, if the visual pigment is sensitive to moderately long wavelengths with low photon energies (near infra-red), they become susceptible to activation by thermal energy alone (Barlow, 1957; Ala-Laurila et al., 2004a; Ala-Laurila et al., 2004b; Luo et al., 2011). The predicted high noise for pigments with λ_{max} in infra-red also explains why they do not apparently exist in nature (Luo et al., 2011). This can also be a reason why the longest wavelength absorbing pigments, in combination of the use of A2-chromophore, are restricted to ectothermic animals (such as frogs and fish).

For maximal advantage, the spectral sensitivity of the pigments should be tuned and matched to the available spectrum in each animal's photic environment. This is called spectral tuning and three mechanisms control it. First, changing the amino acid residues of the opsin in the binding-pocket of the chromophore that interact with the chromophore's light absorbing properties and thus shift its ability to absorb certain wavelengths (Kito et al., 1968). These point mutations in the opsin's amino acid sequence (termed 'opsin shift') allow organisms to adapt to their environment on evolutionary time scales. The second mechanism changes the chromophore from A1 to A2: the addition of a double bond between 3rd and 4th carbons in the A2-chromophore shifts the absorbance spectrum to longer wavelengths and broadens it (e.g. Dartnall and Lythgoe, 1965). The chromophore-switch can happen on a physiological timescale and, for example, many fishes and amphibians modulate their spectral sensitivity seasonally or when moving from one light environment to another during their ontogeny. The third mechanism of spectral tuning happens via chloride ion binding to a specific high-affinity chloride-binding site in the opsin and shifts the λ_{max} to longer wavelengths in long-wavelength sensitive cone pigments (Crescitelli, 1972; Wang et al., 1993; Zak et al., 2001). However, removing chloride from chloride-tuned pigments seems to abolish their function in phototransduction (Zak et al., 2001).

Shifting spectral sensitivity will inevitably affect thermal noise since the two are closely associated. The opsin shift adjusts λ_{max} by reducing or increasing the activation energy of the pigment (again, by how the amino acid residues interact with the chromophore). The activation energy refers to the minimum energy required for the electronic excitation of a molecule from its ground state to the first electronically excited state. An increase in activation energy will shift the spectral sensitivity to shorter wavelengths and a decrease will shift to longer wavelengths. A low activation energy will imply a high probability for the pigment to be activated by thermal energy alone. Thus, there is a clear correlation between spectral sensitivity and rates of

spontaneous, randomly occurring pigment activations (Ala-Laurila et al., 2004b; Luo et al., 2011). However, this spectral-thermal association is not so tight as not to include some exceptions. For example, the bullfrog (*Lithobates catesbeianus*, formerly *Rana catesbeiana*) and cane toad (*Rhinella marina,* formerly *Bufo marinus*) have nearly exactly the same λ_{max} in their rods (502 and 503 nm respectively) but the thermal event rate is one order of magnitude lower in the bullfrog (Baylor et al., 1980; Donner et al., 1990a, reviewed in Donner, 2020). Similarly, the rods of cane toad and mouse have nearly the same λ_{max} (ca. 500 nm) but differ in thermal activation rates by more than one order of magnitude (Luo et al., 2011). Thus, it seems likely that the spectral and thermal properties of rod pigments can, and have been, manipulated independently of each other to some extent during evolution (Donner, 2020). Cone pigments display a similar correlation between λ_{max} and thermal noise as do rod pigments, but on a 2-3 orders of magnitude higher overall level of thermal activation rates. The molecular basis of this generic difference is now being unraveled at the level of single amino acid substitutions (e.g. Kojima et al., 2017). Expressed mathematically, these substitutions control the pre-exponential factor in Arrhenius-type equations relating reaction kinetics to activation energy and temperature. Similar molecular differences could underlie the large differences between the rod pigments that do not differ in λ_{max} (see above).

Temperature Temperature affects the molecular reactions in the phototransduction cascade in many ways. Firstly, the rate of spontaneous isomerizations depends on the temperature, with the frequency rising at higher temperatures (ca. 3–4 fold per 10°C) (Baylor et al., 1980; Matthews, 1984; Sampath and Baylor, 2002). This temperature dependence with the fact that high activation energies of rhodopsins are high (e.g. (Cooper, 1979; Gozem et al., 2012) is best reconciled by a model observing the multiple vibrational modes of a complex molecule (Hinshelwood, 1933; Ala-Laurila et al., 2004b). Thermal activation is supported by internal energy present in a large number of vibrational modes of a molecule composed of many atoms (such as the rhodopsin or even the chromophore), which fundamentally changes the fraction of particles with energy exceeding a certain limit (e.g. the activation energy) compared with classical Boltzmann statistics. Secondly, temperature increases diffusion speed in aqueous solutions, affecting the kinetics of phototransduction and thus the speed of vision. Compared to salamander studied in room temperature, mammalian body temperature doubles the rate at which the R* encounters and activates the G-protein as well as the rate at which the G-protein activates the phosphodiesterase (Sterling, 2004).

Pigment differences Pigment properties also impact the temporal tuning of dark-adapted vision. Pigments with high rates of thermal activation (e.g. cone pigments, especially in long-wavelength sensitive cones) keep the

photoreceptor light-adapted even in darkness leading to decreased sensitivity but also to faster kinetics (Kefalov et al., 2003; Fu et al., 2008). Compared to rod opsins, the cone opsins also have a higher tendency to dissociate into opsin and chromophore in darkness, probably to enable faster pigment regeneration (Shichida et al., 1994; Kefalov et al., 2005; Ala-Laurila et al., 2009). But this lowered rigidity of the pigment leads to a small fraction of cone opsin being without chromophore even in the dark and contributes to the cone's lower sensitivity (Kefalov et al., 2005). Downstream, cones and rods have different isoforms of all the central transduction molecules (Ingram et al., 2016), which together determine their different set points for the trade-off of sensitivity versus speed and regeneration.

2.1.2 PHYSIOLOGICAL CONSTRAINTS

Vision is not just about maximizing photon catch to increase sensitivity. An organism interested only in monitoring the illuminance levels for the purpose of circadian rhythms or light-avoidance responses does not need any other structures than one or two photoreceptors with visual pigment and a signaling mechanism (and prokaryotes can achieve this with type 1 rhodopsin signaling in a single cell). This kind of sense is referred as non-visual photoreception. To achieve image-forming vision, an animal needs eyes capable for spatial vision and the nervous system to support the increased information flow. Several constraints emerge for such true vision.

2.1.2.1 Emergent constraints and optimizations

The first inherent constraint in any eye design comes from the unavoidable trade-off between resolution and sensitivity (Figure 6). Summing photons across space, time and wavelengths will increase the absolute sensitivity to light detection in purely linear imaging systems, but with the cost of losing finer spatial, temporal or chromatic detail of the visual environment.

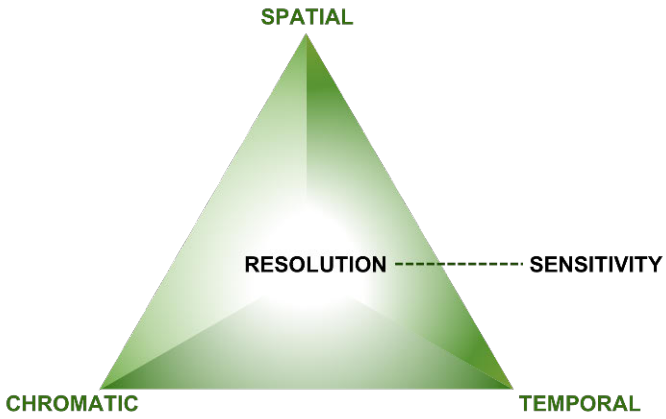

Figure 6 **Trade-off between resolution and sensitivity.** Dividing the photons absorbed into packages in the spatial, temporal or chromatic dimension will improve resolution in that dimension but with the cost of decreasing absolute sensitivity.

Spatial resolution vs. sensitivity Optical spatial resolution is the precision by which the eye splits up light coming from certain direction. It is a combination of the quality of the image provided by the optics and the fineness of photoreceptor mosaics which include both the size of the photoreceptors and their spacing. The upper limit for spatial resolution is determined by the wave nature of light (Cronin et al., 2014). Firstly, in too narrow photoreceptors the light "leaks" outside to the adjacent photoreceptors. This in turn also determines the focal length of the eye. Secondly, the sharpness of the retinal image is limited by diffraction, defining for a certain pupil size a point-spread function, i.e. the retinal light distribution due to a point source. For example, in the human fovea, the image of a point source effectively covers some 30 cones when the pupil is maximally constricted (and thus aberrations due to imperfect optics are minimized).

Thirdly, to some extent the spatial acuity will be set by the sampling density of a relevant population of ganglion cells from which the brain receives its information for a certain task. Ganglion cells as well as the second and third-order neurons of the brain sum the signal over many photoreceptors (convergence) so that the spatial resolution taken as static "grain" (or "pixelization") decreases downstream. Functionally, however, there are two factors to consider. First, in low light sufficient spatial (as well as temporal) summation is a prerequisite for achieving useful signal-to-noise ratios. Secondly, with point-spread functions covering several tens of photoreceptors and images in constant motion on the retina, spatial resolution is generally set by statistical analysis of a spatio-temporal pattern in the brain and bears only an indirect relation to the grain of the cell mosaics.

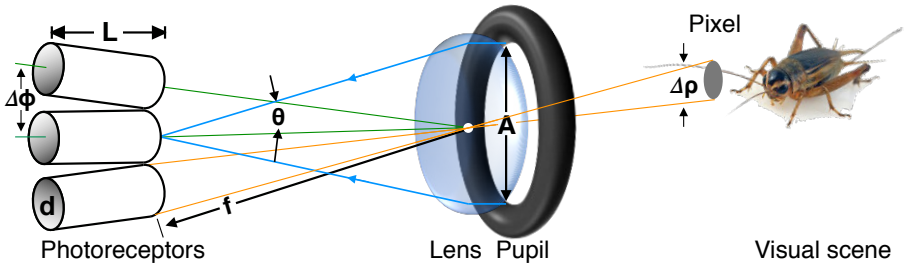

Figure 7 **A schematic of an eye viewing a visual scene.** An array of photoreceptors, each with length *L* and diameter d, and with the inter-receptor angle $\Delta\varphi$ receives a focused beam of light with the angular half-width θ through the aperture of the pupil with diameter *A*. Each photoreceptor has a small receptive field, with the angular width of $\Delta\rho$ (also known as the acceptance angle), sampling only a small part (or a 'pixel') of the visual scene. The focal length *f* of the eye is the distance between the optical nodal point *N* (in this figure located in the center of the lens) and the focal plane at the tips of the photoreceptors. Redrawn from Cronin et al. (2014).

The trade-off between sensitivity and spatial resolution is readily seen in Figure 7. Each photoreceptor captures light from certain direction, defining in a single "pixel" of the image. An eye striving for higher resolution should decrease the pixel size by minimizing the diameter of the receptor as well as pack the photoreceptor mosaic as densely as possible (specified by their interreceptor angle, $\Delta\phi$). But consequently, the photon sample collected by each photoreceptor as well as the reliability of that sample (as a consequence of photon shot noise) will unavoidably decline.

Increasing sensitivity The concentration of visual pigment in the membrane layers of the photoreceptors is roughly a constant and to increase the probability of catching arriving photons, the photoreceptor can only add more membrane layers. It would seem that to maximize sensitivity adding more and more membrane and thus increasing the photoreceptor length would be optimal. But there are good reasons why photoreceptors are a certain length. *Absorbance* (*A,* also called *optical density*) is a dimensionless number describing the amount of light transmitted by a substance at a given wavelength, and it is defined as the base 10 logarithm of the incident light (I_o) divided by the transmitted light (I_t):

$$A = log_{10}(\frac{I_0}{I_t}) \qquad (3)$$

Absorbance can also be described as:

$$A = \epsilon cL \qquad (4)$$

where ϵ is the molar extinction coefficient (an intrinsic molecular property, for rhodopsin at its λ_{max} about 42 000 liters cm^{-3} $mole^{-1}$, Fein and Szuts, 1982), c the concentration in moles per liter and L the path length in centimeters. A more useful measure, when thinking how the photoreceptor with increasing length absorbs light, is a*bsorptance,* which gives the fraction of incident light that is absorbed with a given absorbance:

$$Absorptance = 1 - \frac{I_t}{I_0} = 1 - 10^{-A} = 1 - 10^{-\epsilon cL} \qquad (5)$$

The relationship between length and absorptance is logarithmic rather than linear because with increasing the path length there is less light left to absorb: if the first μm absorbs 90 % of the light (A = 1), for the next 1 μm there is only 10 % of the incident light left to absorb and so on (Land and Nilsson, 2012; Cronin et al., 2014). Thus, increasing receptor length infinitely will not increase photon catch beyond a certain maximum. Only when the pigment solution is infinitely dilute and the path length infinitely short, does absorptance equal absorbance.

Another consequence of eqn. (5) is that with increasing path, the absorptance spectrum becomes increasingly broader (termed *self-screening*; for large L values, $10^{-\epsilon cL}$ approaches zero for a broad range of wavelengths around λ_{max}) (Warrant and Nilsson, 1998; Cronin et al., 2014). In other words, visual pigment early in the light path absorbs most of the light close to the wavelength of peak absorption and the remaining pigment absorbs more of the remaining light, further away from the peak, broadening the spectral sensitivity of the receptor as a whole. The longer the photoreceptor, the more photons it will absorb but the broadening of the absorptance spectrum can potentially degrade the discrimination of different wavelengths (Cronin et al., 2014).

Temporal resolution vs. sensitivity Another trade-off related to the size of the photoreceptors lies between sensitivity and temporal resolution. First, in smaller compartments the diffusion distances are short and a high concentration of reactants can be reached in a few milliseconds. Second, the absolute amount of effector molecules to be modulated is smaller. For example, the photocurrent in vertebrate photoreceptors is generated by closing the cGMP-gated cation channels and thus depends on the intracellular concentration of cGMP (Burns and Lamb 2004). The enzyme that hydrolyses cGMP, phosphodiesterase (PDE), is among the fastest enzymes with its catalytic activity approaching the diffusion limit of how fast cGMP can reach it (Leskov et al., 2000). Thus, the process can be accelerated by decreasing diffusion distances and reducing the cytoplasmic volume to reduce the amount of cGMP. For example, the mammalian rod's cytoplasmic volume is only 4 % of that of the salamander rod, raising the transduction speed 25-fold (Sterling, 2004). For the same reasons, smaller compartments in principle allow faster termination of responses.

2.1.2.2 Neural noise

Sensory signals are fundamentally noisy, i.e. contain random variability. The biological system made of protein circuits that transduce, process and interpret the signals inevitably add more variation to the signal. In the visual system the photon shot noise arising from the randomness of photon arrivals and absorption sets the ultimate physical limits for visual information. However, these limits are never quite reached as the intrinsic noise sources, within photoreceptors and later in the signaling cascade, degrade the signal-to-noise ratio further. Several retinal noise sources set theoretical limits for visual computations and ultimately for behavioral visual detection, although it is not clear which source of noise is most critical in various distinct visual computations (Field et al., 2005; Field et al., 2019; Kiani et al., 2020). The limiting factors also depend on the species in question and the state of adaptation. But as it turns out, evolution has minimized the noise sources as well as optimized the neural circuitry function so that the behavioral sensitivity gets remarkably close to the physical limit.

In photoreceptor transduction, two major forms of noise degrade the signal produced by photon absorption: discrete and continuous noise (Baylor et al., 1980). The thermal or discrete noise arises from the spontaneous thermal activations of visual pigment molecules, as discussed in the previous chapters. The discrete noise, consisting of events identical to light-evoked responses to single photons, cannot be filtered out by any means without loss of some of the real single-photon signals. These events are remarkably rare, though, especially in visual pigments evolved for dim-light vision (cf. section 2.1.1.2 above). In rod photoreceptors they occur only every 1–3 minutes (depending on species and temperature), which is remarkably little considering that every receptor has millions of pigment molecules (Liebman et al., 1987). Thus, the average life time of a single molecule is on the order of several hundreds of years (Baylor et al., 1980; Baylor et al., 1984; Burns et al., 2002; Field et al., 2019). Nonetheless, as the downstream circuitry pools from thousands of rods, even the low levels of noise can degrade visual sensitivity considerably. The effect is greatest near the absolute visual threshold, where only a few rods out 10 000 contain a real, photon-induced signal while the rest contribute only noise.

The continuous noise is produced by the spontaneous activation of the phosphodiesterase (PDE) molecules, which catalyze the hydrolysis of cyclic GMP molecules (Rieke and Baylor, 1996), leading to a fluctuation in cGMP. The single events constituting the continuous noise have smaller amplitude than the discrete (pigment-generated) events but, as the name implies, this noise dominates the photosensitive current in darkness by being present continuously (Field et al., 2005). In mammals and especially mouse, the two components are generally more difficult to discriminate than in amphibians with respect to both amplitude and frequency composition, and occasional large continuous noise deviations may resemble the single-photon response (Baylor et al., 1984; Field et al., 2005; Field et al., 2019; Kiani et al., 2020).

The smaller the amplitude of these fluctuations, the higher the SNR of the single-photon responses (Field and Sampath, 2017). However, the amount of continuous noise is inherently linked to the kinetics and amplitude of the single-photon response and its recovery to baseline (Field and Sampath, 2017). This is because the basal turnover of the cGMP, i.e. the drop in concentration and subsequent returning to dark level, is set by the rate of spontaneous PDE activity via the Ca^{2+}-dependence of guanylyl cyclase activity (Rieke and Baylor, 1996; Field and Sampath, 2017). Hence, decreasing the spontaneous PDE activity would decrease the basal turnover of cGMP in darkness and ultimately lead to slowing of the single-photon response. Here lies yet another trade-off, between the detection sensitivity and temporal resolution which have been balanced in the phototransduction.

The dark noise components discussed above are "additive", not related to variability in the transduction of a photoisomerization into an electrical response. However, there is variability in the single-photon response amplitude that is not accounted for by these two forms of intrinsic noise, but due to variation in phototransduction ("transduction noise"), although this is fairly tightly controlled. If rhodopsin activation and deactivation were unimolecular stochastic processes, the coefficient of variation (CV) should typically be ~1 (Field and Rieke, 2002b). However, the observed CV is only ~0.3. This is because the rhodopsin deactivation is a multi-step shut-off mechanism with a series of phosphorylation events at the rhodopsin's C-terminus by rhodopsin kinase, followed by binding of arrestin (Field and Rieke, 2002b). This delays most of the response variability to the falling phase of the response, leaving the rising phase (essentially tuned to be as fast as possible) and the peak highly reproducible. As the rising phase largely drives the most time-sensitive downstream neural computations, this is a great optimization.

It is not clear how much other noise sources, for example synaptic noise in retina and cortex and noise in spike generation, contribute near absolute threshold. Synaptic noise in retina results from statistical fluctuations in the neurotransmitter vesicle release, for example, glutamate release in the first synapse of the rod pathway. Nevertheless, the remarkable behavioral performance at the visual threshold requires that all the noise sources downstream from rods are small (Field et al., 2005). This is evident from comparisons between rod noise and the total noise and losses of signals limiting behavior, since most of the limiting noise can be attributed to a combination of photon shot noise and to noise in rod responses (Kiani et al., 2020).

Exactly which intrinsic noise source limits vision at its absolute threshold has been the subject of vigorous research and discussion ever since it was realized that the photon shot noise alone is not sufficient to describe the statistics of human light detection near the behavioral threshold (Barlow, 1956). In the first experiments of human visual threshold the variability of the test subjects' responses to a given light intensity was assumed to arise solely

from the Poisson fluctuations in the number of absorbed photons, leaving no room for biological noise (Hecht et al., 1942; Van Der Velden, 1946). According to this view, a threshold number of photons was required for the subjects to report having seen a flash, and only the Poisson fluctuations in the given intensity cause the threshold sometimes to be reached and on other occasions to be missed. However, already almost a century before this Gustav Fechner had introduced the idea that intrinsic "background light" in the eye ("Augenschwartz" or "Eigengrau") could limit visual sensitivity (Fechner, 1860). Further, Autrum (1943) suggested that the spontaneous activation of rhodopsin molecules would produce such an irreducible light-like background activity. Barlow (1956) gave this notion the more specific formulation that it is the noise (randomness) of the thermal activations that must set a theoretical limit to light detection (absolute limit). This also helped to explain why the subjects in the Hecht et al. (1942) experiments sometimes reported seeing a flash when no flash was given. These false-positive responses are not expected from a purely Poisson-limited photon detector.

Studies in amphibians supported Barlow's idea that the performance limit of visually guided behavior is set by the thermal noise. Aho et al. (1988; 1993a) demonstrated that the absolute behavioral threshold of toads is consistent with predictions based on the rate of dark events recorded in toad rods, and that the absolute threshold of frogs as well as frog retinal ganglion cells rose with warming as qualitatively expected from the temperature dependence of the rate of such events. However, as the temperature manipulation can alter several noise sources in the retina, this temperature correlation did not conclusively prove that the discrete noise was the limiting noise source. In addition, as Barlow (1988) points out that the precise dependence between behavioral threshold and rates of thermal events in the target area as reported in Aho et al. (1988) deviates from what would be expected from the simplest dark-event-rate-limited models. Species differences are also highly likely since the retinal circuitries differ between amphibians and mammals. In mice, there is a thresholding nonlinearity between the rod and rod bipolar cell, which - at the cost of losing real single-photon events - filters out much of the rod noise (Field and Rieke, 2002a) and a second thresholding nonlinearity operating at the last synapse of the ON (but not the OFF pathway) primary rod pathway (Ala-Laurila and Rieke, 2014). Continuous noise but also small rod responses are rejected and only sufficiently large responses are transmitted to the bipolar cell. In amphibian retina, on the other hand, the rods are strongly electrically coupled so that the single photon response in one rod is spread as a low-amplitude signal to dozens of its neighbors (Fain, 1975; reviewed in Donner and Yovanovich, 2020). For the rod signal thresholding to be effective in these conditions, it must separate signal and noise before such averaging, making this strategy futile in the amphibian retina. Thus, the limiting noise source depends on the number of rods being pooled and whether they are pooled linearly or nonlinearly. Also, the relative amplitude of dark noise in mouse is slightly higher than in primates with the SNR of a single-photon response

estimated to be 3 in mouse while in primates it is 6 (Baylor et al., 1984; Field and Rieke, 2002a; Field et al., 2005). Nevertheless, recent modeling work in primates suggests that both continuous and pigment noise could constrain vision in darkness but in distinct ways. The absolute detection is suggested to be limited by pigment noise, whereas the temporal resolution seems to be limited by continuous noise with some contribution from photon shot noise (Field et al., 2019). However, these modeling results remain to be tested against experimental work.

In primate cones, the pigment-derived noise has much less effect and the limiting noise comes from the fluctuations in cyclic GMP level and channel noise (depending on the state of adaptation) (Angueyra and Rieke, 2013).

2.1.2.3 Energy and neural investment

Information is metabolically expensive. The more reliable and the more relevant information a sensory system can extract from the environment, the more accurate decision making and motor control it can potentially facilitate, but, the more energetically costly the sensory structure becomes (Niven and Laughlin, 2008). Thus, sensory systems emerge as a compromise between minimizing energy consumption and acquiring reliable, relevant information.

The brain and the nervous system are famously costly with, for example, the human brain taking up 20% of our daily energy budget despite representing only 2% of the body mass (Kety, 1957; Herculano-Houzel, 2011). The retina is not only an embryological projection of the forebrain but like the rest of the brain, it processes vast amounts of information: the human retina, for example, was estimated to transmit 10 megabits per second to the brain (Koch et al., 2006; Sterling and Laughlin, 2015). It comes as no surprise that the retina shares the high metabolic demands of central nervous system, and in fact might be the most demanding (Ames et al., 1992; Ames, 1992; Wong-Riley, 2010; Country, 2017). This is exemplified by the regressive evolution of vision in animals living in darkness, underground or in caves. For example, the Mexican tetra (*Astyanax mexicanus*) has different populations, apart from the surface-living population, independently evolved to live in dark caves with the most divergent being eyeless and its optic tectum reduced to only half of the surface-living fish. The energetic cost of vision in this species was estimated as 5–15 % of their resting metabolism (Moran et al., 2015). Consequently, partial or complete elimination of the visual system in the cave environment saves considerable amount of energy and neural investment, demonstrating how energy acts as a selective pressure on the evolution of sensory systems.

The greatest expense of information processing in neural circuits comes from the restoration of ion movements generated by action potentials, postsynaptic currents and neurotransmitter uptake (Ames et al., 1992; Attwell and Laughlin, 2001). The Na^+/K^+ -ATPase, or sodium-potassium pump, exports three Na^+ ions and imports two K^+ ions for each ATP molecule that is

converted to ADP and thus keeps these ions in thermodynamic disequilibrium. Many symporters and antiporters are coupled to the Na^+/K^+ -ATPase linking its energy consumption to numerous other ion movements, for example Ca^{2+}, Cl^- and HCO_3^-. In the vertebrate retina, Na^+/K^+ -ATPase accounts of about half of the total energy budget in the dark, mostly consumed by the dark current (41 %) generated in the photoreceptors (Ames et al., 1992). Because rods and cones hyperpolarize in response to light, their highest energy intake is in the dark. Apart from the Na^+/K^+ -ATPase action, energy in the retina is required for rapid turnover of the cGMP molecules with high-energy phosphate bonds (13%), presynaptic calcium influx, for transmitter recycling and for action potentials in the RGCs (Ames et al., 1992; Attwell and Laughlin, 2001; Country, 2017).

The high metabolic and oxygen demands of the retina, especially in the photoreceptor layer, set specific constraints on how the tissue should be organized (Country, 2017; Damsgaard et al., 2019). The metabolic cost requires high vascularization but at the same time the retina needs to remain as thin and transparent as possible for the best light capturing properties. Blood vessels anywhere proximal to the photoreceptors will interfere with the light path. In fact, many vertebrates like rabbits and guinea pigs have avascular retinas and the blood supply happens only via diffusion from the choroid (the vascularized tissue behind the photoreceptors, away from the light path). Primates have solved the issue by adding vascularization to the peripheral inner retina while the fovea stays avascular, supporting high visual acuity of that region. Mice, on the other hand, do not have a fovea and the vascularization continues throughout the inner retina, possibly contributing to their visual acuity being poorer than in primates (Prusky et al., 2000; Country, 2017; Dyballa et al., 2018). The fact that retina needs to remain thin also limits the cellular volume of the retinal circuits (Sterling, 2004).

Generally, spikes are expensive, so from an energetic perspective sparse coding is more efficient. In the spiking neurons energy consumption is high during rest due to maintaining the resting potential, but even higher during signaling because ATP is required for synaptic transmission and for the restoration of ion balances after signaling (Attwell and Laughlin, 2001; Sengupta et al., 2010). Maximum firing rates increase proportionally to the axon diameter i.e. higher spike rates require myelinated and thicker axons as well as larger axon terminals to support the extra active zones to transfer information synaptically at higher rates (Balasubramanian and Sterling, 2009; Perge et al., 2009). But the mitochondrial volumes rise as the diameter squared. Thus, to double the information rate in a neuron requires more than doubling the space and the energy capacity. This is another example of the "law of diminishing returns" and is proposed to be one reason for the parallel processing in the retina: splitting the information over many thin, low-rate fibers in the optic nerve saves energy and space compared to a few thick, high-rate fibers (Balasubramanian and Sterling, 2009). Sparse codes are also more informative, because for any given spike time precision information rate

increases sublinearly with spike rate (Rieke et al., 1997). Consequently, as spike rate rises, information content per spike decreases, which is observed also experimentally (Koch et al., 2006; Balasubramanian and Sterling, 2009). The lower limit of axon diameter is set by the channel noise. Below 0.5 μm diameter axons have such low numbers of ion channels that the spontaneous, stochastic channel fluctuations cause variations in spike timing that are sufficient to degrade the message such that these axons become unreliable (Faisal and Laughlin, 2007).

The graded potentials of photoreceptors and bipolar cells use at least as much energy as the action potentials of ganglion cells, but it seems that far more information can be transmitted per second with the analogue signaling (Laughlin et al., 1998; Niven and Laughlin, 2008). Computing via chemistry (analog signals) is beneficial because the irreducibly small circuits save space and materials (i.e., it is wireless) (Sterling and Laughlin, 2015). A downside is that the graded potentials degrade over long distances becoming unreliable so they can only be used for local signaling.

To save energy and space, the retina should reduce redundancy and not transmit information which is not needed. For example, it has been suggested that because natural images contain more negative contrasts than positive contrast, the OFF-ganglion cells, which respond by depolarization to light decrements, are more numerous than ON cells (Balasubramanian and Sterling, 2009). Similarly, the spatial modulation transfer function of daylight vision attenuates low spatial frequencies, which occur with high power in natural scenes (decreasing redundancy). Each species' retina is thus thought to have evolved to match the visual statistics of their environment and lifestyle.

2.2 EVOLUTIONARY AND PHYSIOLOGICAL ACCOMMODATION TO THE CONSTRAINTS

The vertebrate retina evolved to the duplex, three-layered tissue common to all clades of jawed vertebrates more than 500 million years ago. Nothing in biology makes sense except in the light of evolution, and evolution is driven by maximizing fitness. The performance of the eye including the retina has an impact on fitness only through behavior and thus eye evolution must be seen in the context of the evolution of visually guided behaviors of different species. By definition, eyes of any extant species are good enough for the species-specific behaviors that allow the survival and reproduction of the individuals. To the extent that performance approaches some physical-theoretical optimum, this tells something interesting about the biology of the animal.

2.2.1 FROM PHOTONS TO BEHAVIOR IN FROGS AND MICE

2.2.1.1 The vertebrate retina

The vertebrate retina is a highly organized layer of brain tissue computing the first stages of visual processing. It has five major neuronal cell classes in addition to glial cells. Most of the retina's computational power resides in the two synaptic layers where the processes of the different cell types interact: the outer and inner plexiform layers (OPL and IPL). Two types of photoreceptor cells, rods and cones, catch part of the stream of incoming photons translating the absorption events into graded changes of the membrane potential via the phototransduction cascade. The ribbon synapses of the photoreceptors release glutamate constantly in darkness and reduce the amount of glutamate release in response to light. Photoreceptors synapse in the outer plexiform layer on two cell classes: horizontal cells and bipolar cells. The horizontal cells are laterally connecting interneurons that provide feedback and feedforward inhibition to photoreceptor terminals as well as feedforward inputs to bipolar cell dendrites creating a local gain control circuitry (and in some cases colour-opponency) in the outer retina (Peichl et al., 1998). The synaptic input from the photoreceptors drives bipolar cells which integrate the signal from photoreceptors and connect the outer plexiform layer with the inner plexiform layer. Bipolar cells are also the first to create parallel processing channels of the visual signal with 14 types now known in mouse (Masland, 2012; Behrens et al., 2016; Greene et al., 2016). They may either depolarize (ON-bipolars) or hyperpolarize (OFF-bipolars) in response to the light-induced decrease in glutamate release from photoreceptors (Werblin and Dowling, 1969). Recent evidence shows that this separation of ON and OFF pathways in the vertebrate retina is evolutionary ancient, and may date back 500 million years (Ellis et al., 2020). The bipolar cells project to the inner retina and use ribbon synapses to release glutamate to ganglion cells and amacrine cells. Amacrine cells are the interneurons of the inner plexiform regulating and further processing the signal in synaptic microcircuits. Finally, the RGCs integrate information over many bipolar and amacrine cells and translate the signal into action potentials which are send to the brain via the optic nerve.

Each of the cell classes comprises multiple cell types and each of these types is regularly spaced across the retinal surface covering it evenly (Masland, 2012). However, each cell type is evenly spaced only with respect to other cells of the same type, while their spacing in relation to other types is random and independent. Not only are the cell bodies regularly spaced creating a mosaic but even the dendrites arrange themselves not to overlap too much, fitting together at their edges. This phenomenon is called tiling and it ensures that all types survey the visual scene efficiently.

Another hallmark of retinal processing common to all vertebrates is the center-surround organization of the receptive fields of bipolar cells and ganglion cells. The center-surround receptive field is an area in the visual

space where presentation of a stimulus in the receptive field center excites the cell whereas the same stimulus on the surround area, outside the center, suppresses the center response or produces a response of opposite polarity (for review, see e.g. Masland, 2012; Wienbar and Schwartz, 2018).

Most of the studies on visual processing were originally done on cats and amphibians, but many of the discovered underlying principles seem to generalize well to other vertebrates as well (e.g. what is described above). But the detailed anatomical and functional properties of individual retinal circuits are known in only a few species and most knowledge comes from the mouse retina.

2.2.1.2 Photoreceptors

Photoreceptors come in many different plans across the animal phyla but they can be divided into two main classes depending on the structure used for packing the large amounts of membrane required for containing millions of visual pigment molecules (based on cilia and microvilli, respectively). This also correlates with the division into two opsin families. In many invertebrate photoreceptors the plasma membrane expansion for visual pigment is arranged to rhabdoms, which consist of microvilli extending straight from the cell body. Vertebrate photoreceptors are derived from ciliated epidermal cells and the visual pigment is localized in stacks of membrane. One of the biggest functional differences between the two types stems from the opsin-classes they use: the phototransduction pathway of the rhabdomeric or R-opsins leads to the opening of TRP (transient receptor potential) cation channels whereas the ciliary or C-opsins act to hydrolyze cGMP, leading to the closure of the cyclic nucleotide gated cation channels (Shichida and Matsuyama, 2009). Thus, light has opposing actions in the two receptor motifs, depolarizing the rhabdomeric receptors and hyperpolarizing the ciliary receptors.

In the vertebrate retina the ciliary photoreceptors are further divided into rods and cones based on their structure and the light regime they work in. In rods, the membrane expansions are sealed off the plasma membrane to form discrete discs inside the outer segment. Cones retain folded membranes continuous with the plasma membrane. Above a certain illumination level, cones mediate what is known as photopic (daylight) vision, and below this range, the retina switches to rods to enable dim light (scotopic) vision. Mesopic vision operates at light levels between the two extremes, relying to both rod and cone systems. The differences between rods and cones relate to these light regimes. Vertebrate retinas typically have two or more cone types, structurally similar within species but containing different opsins and giving basis for color vision. The defining feature of rods is their ability to signal the absorption of single photons with remarkable reliability and high signal-to-noise ratio under dark-adapted conditions (Hecht et al., 1942; Baylor et al., 1979; Field et al., 2005). Genetic studies indicate that all cone opsins emerged before the rod pigment evolved (Shichida and Matsuyama, 2009). From

comparative and anatomical studies, it is also clear that the rod photoreceptors developed from the cones. For example, in mammals the whole rod circuitry "piggybacks" the cone circuitry.

Mammalian versus amphibian photoreceptors The typical rods contain basically the same pigment, rhodopsin (Rh1), absorbing maximally at ca. 500 nm meaning that they are green-sensitive and appear reddish under microscope (and thus called "red rods"). In the mouse retina, much like in most mammalian retinas, these rods outnumber the cones by about 20 to one (Sterling, 2004) and they have a specific circuitry dedicated to transmitting rod signals at scotopic light levels. This always involves pooling of signals from many rods. In primates, rods are missing in the fovea, which enables high visual acuity relying on the faster and spectrally different cones, whose signals are transmitted through the retina without pooling. The anuran retina is also rod dominated, at least in the few species that have been investigated (all are nocturnal or crepuscular, reviewed in Donner and Yovanovich, 2020).

Unlike the other vertebrates, most anurans (frogs and toads) and some urodeles (salamanders and newts) have, additionally to the typical rods found in most other vertebrates, a rod-like receptor called "green rod" (because they appear greenish under microscope) (Denton and Wyllie, 1955; Govardovskii and Reuter, 2014). These are blue-sensitive (absorbance peak at ca. 430 nm) and thought to be modified cones (Figure 8). They constitute about 6–14 % of all rods (Denton and Wyllie, 1955). The pigment is a cone opsin (SWS1 or SWS2 depending on species) with fast regeneration characteristics after bleaching but the morphology is rod-like, thus increasing photon-catch and slower responses (increasing temporal summation) (Hisatomi et al., 1999; Ala-Laurila et al., 2006).

For a cone pigment, the anuran version of the SWS2 pigment contained in the blue-sensitive rods is thermally well stabilized (Ma et al., 2001; Kojima et al., 2017). A single amino acid mutation (threonine in position 47) gives this pigment a rhodopsin-like (Rh1) stability. The same SWS2 found in urodelan blue-sensitive rods lacks the mutation and these pigments have as high thermal isomerization rates found in the blue-sensitive cone pigments present in cones (Kojima et al., 2017). However, the exact thermal stability of the anuran SWS2 is still controversial, with the measurements ranging from four times higher thermal event rate than that of rhodopsin (Matthews, 1984; Yanagawa et al., 2015) to 100 times lower event rate (Luo et al., 2011).

Beside the two rod types, frogs have single and double cones (reviewed in Donner and Yovanovich, 2020). In many species the single cones consist of at least one red-sensitive type, usually with LWS pigments ($\lambda_{max} \approx 565$ nm, (Koskelainen et al., 1994; Chang and Harris, 1998). Another single cone spectral type, the blue-sensitive cones, were not found until much later, probably because of their low numbers (Hárosi, 1982; Koskelainen et al., 1994). Interestingly, at least in the bullfrog (*Lithobates catesbeianus*), the pigment in the blue-sensitive cones is SWS1 with spectral absorbance (λ_{max}

~430 nm) virtually indistinguishable from the SWS2 of the blue-sensitive rods (Koskelainen et al., 1994; Hisatomi et al., 1998). Usually, when both pigments are present, the SWS1 pigments are UV/violet-sensitive and SWS2 blue-sensitive (Yokoyama, 2000). In urodeles, the SWS2 is found in both blue-sensitive rods and cones (Ma et al., 2001).

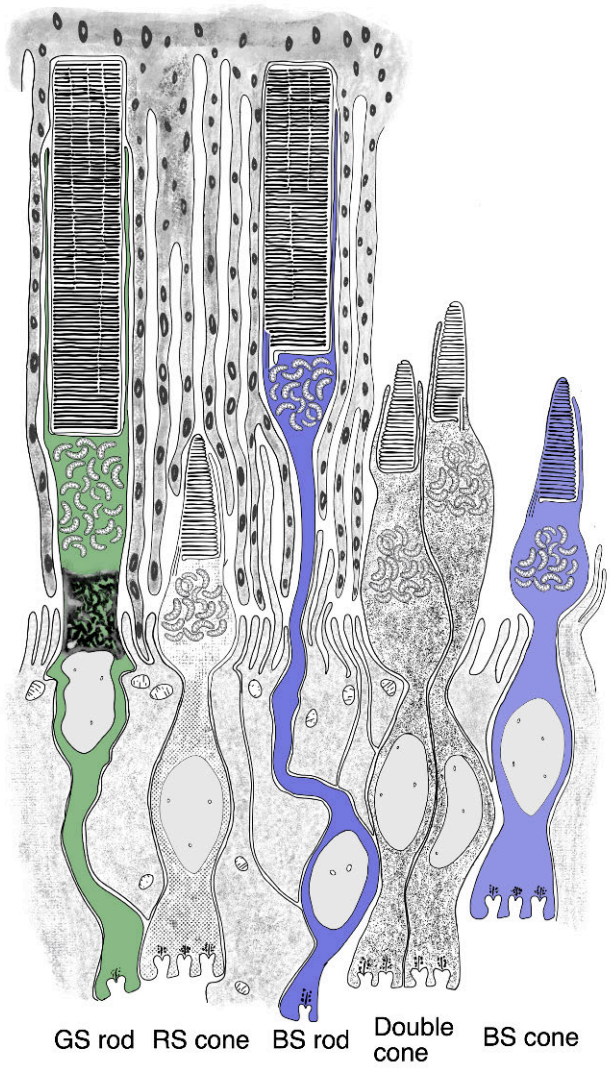

Figure 8 **Frog photoreceptors.** Frogs and toads have two classes of rod photoreceptors: green- (GS) and blue-sensitive (BS). Beside these two rod types, frogs possess red- (RS) and blue-sensitive (BS) cones and additionally, so-called double-cones, of which the principal component has the same absorbance peak as the RS cones. See text for references. Redrawn from Nilsson (1964).

The double cones consist of a principal component and an accessory component. The principal component has the same absorbance peak as the red-sensitive single cones (Liebman and Entine, 1968). The accessory member has been reported to be green-sensitive in some studies, while others have not verified this (Liebman and Entine, 1968; Hárosi, 1982; Koskelainen et al., 1994). None of the expected green-cone opsins (typically Rh2 in birds and fish) have been found in amphibians (Yokoyama, 2000; Bowmaker, 2008; Lamb, 2013). However, some early studies speculated that the accessory member could contain the green-sensitive rod rhodopsin (Rh1) pigment which would fit in with descriptions of the development of the double cones. Saxén (1954) found that the accessory member had rod-like features and speculated that the double cones are formed as a fusion of rods and cones (Saxén, 1953; Saxén, 1954; Crescitelli, 1972). However, this has not been followed up since. The red-sensitive single cones and the principal component of the double cones also contain colorless oil droplets, which serve to increase the photon catch (Liebman and Entine, 1968; Hailman, 1976; Röhlich and Szél, 2000; Siddiqi et al., 2004; Wilby and Roberts, 2017).

Chromophore switching is another interesting feature of the amphibian retina not found in mammals. Most adult anurans are terrestrial and use A1-vitamin based chromophore in their visual pigments while the tadpoles of many species are aquatic using A2 or combination of A1 and A2 (e.g. *R. temporaria* and *Lithobates pipiens*) (Crescitelli, 1958; Muntz and Reuter, 1966; Liebman and Entine, 1968; Reuter, 1969; Crescitelli, 1972). The shift to dominance of A1 pigments in *Rana temporaria* happens at the same stage of development as the emergence of fore-limbs (Reuter, 1969). This could be an adaptation for the photic environment, as the red-shift in the pigment caused by the A2 chromophore would seem to give a benefit mainly in the habitats of the tadpoles, e.g., murky, reddish freshwater ponds (Reuter, 1969). The African clawed frog, *Xenopus laevis*, which is aquatic throughout its lifecycle, has mostly A2 (with small amount of A1) as adult (Wald, 1955; Crescitelli, 1972). However, the photic environment cannot be the sole explanation, as the Bufonids never use A2, even when occupying the same ponds as the frogs (Muntz and Reuter, 1966; Crescitelli, 1972; Donner and Yovanovich, 2020).

The ratio and the timing of the switch in the Ranidae also varies, associated with light regime and possibly temperature (Muntz and Reuter, 1966; Reuter et al., 1971; Makino et al., 1983). For example, the bullfrog uses A2 pigments not only in the tadpole phase but in varying degrees throughout its life. In adult bullfrog the retina can contain 30–40% of A2-pigment, all of it segregated to the dorsal part (Reuter et al., 1971). On the other hand, there are environmental effects on the A1/A2 ratio throughout life. Makino et al. (1983) found a seasonal cycle in the amount of A2-pigment throughout the year with highest amounts from January to June. This variation might be linked to temperature, because the amount A2-based pigment also increased when the average temperature became lower than 20 °C and decreased when the temperature exceeded 20 °C. In Ranidae the A2/A1 proportions can also

depend on the amount of light: if the tadpoles are kept in darkness, the amount of A2-pigment decreases over a period of several weeks (Bridges, 1974). The process is reversible over several light-dark cycles but the effect of light is the most dramatic: exposing the tadpoles to bright light returned their retinae almost purely A2-based pigment in 24–48 hours. Since the A2 chromophore not only red-shifts the pigment but also makes it thermally less stable, the evidence is consistent with the hypothesis that A2 is decreased in conditions where thermal pigment noise threatens to significantly limit visual sensitivity, i.e. in high temperature and/or low light (cf. chapter 2.1.1.2 above).

The A1/A2 chromophore switch could in part explain why the thermal event rate of the bullfrog green-sensitive rods is lower than that of cane toad rods despite their λ_{max} being almost exactly the same. As the bullfrog uses the A2 chromophore during its larval stages (and in the dorsal retina even as an adult), it is possible that the pigment evolved to limit noise when combined to the A2 chromophore (Donner and Yovanovich, 2020; Donner, 2020). This would then result in the unusually stable rhodopsin in the A1-form during the adulthood of the frog. The evidence from tiger salamander larvae supports this, as they use almost purely 100% A2-pigments. When the A2 is artificially replaced by A1, the pigment's thermal event rate decreased as low as in the bullfrog opsin with A1 chromophore (they have the same λ_{max} of 502 nm) (Ala-Laurila et al., 2007; Donner, 2020).

Another clear difference in the mammalian outer retina to the amphibian one is that mammalian rods are slender and densely packed. However, this does not increase spatial resolution, as one could assume, because signals are always pooled from many rods. The advantages are firstly, less noise-producing pigment in one cell, and secondly, shorter diffusion distances, which enables faster response rise as discussed already in chapter 2.1.2.1 *Emergent constraints and optimizations*. The amphibian photoreceptors are also much more electrically coupled compared to the mouse photoreceptors (Fain, 1975).

Mice have green and UV light sensitive cones (named M- and S-cones respectively, for medium and short wavelength-sensitive) as well as cones that co-expresses both pigments (Röhlich et al., 1994; Szél et al., 1994). Interestingly, a pronounced dorsoventral gradient exists in the opsin expression across the retina. The "true" S-cones are sparse (~5 %) and homogenously distributed across the whole retina, but the proportion of M-cones co-expressing S-opsin increases towards the ventral edge of the retina so that the retina can be divided roughly into three functional regions: dorsal retina contains M-cones with very little S-opsin co-expression, interspersed with "true" S-cones, a narrow, transitional central zone where the S/M opsin co-expression increases and the predominantly UV-sensitive ventral retina where S opsin dominates (Baden et al., 2013). This effectively makes the upper visual field strongly UV-sensitive (Tan et al., 2015). Furthermore, this asymmetry is accompanied by a shift in contrast sensitivity (Baden et al., 2013). The strongly S-opsin co-expressing MS-cones in the ventral retina

respond with larger amplitudes to dark contrast compared with light contrast of the same magnitude, whereas the dorsal, dominantly M-opsin expressing (green-sensitive) cones respond to light and dark flashes with equal and opposite gain. This effectively makes the ventral retina, which surveys the upper visual field, i.e. the sky, preferentially tuned to dark objects against UV-background.

2.2.1.3 Retinal circuitry

The retina contains many functionally overlapping circuits processing in parallel the light distribution falling on it. The starting point for all circuits is the same: photoreceptors form a single sheet of regularly spaced cells that sample the dynamic photon flux falling on it. With few exceptions, each cone contacts each of the different types of bipolar cells creating parallel information channels – a central principle of retinal signal processing (Masland, 2012). Each bipolar cell contacts all the cone terminals within the reach of its dendritic arbor. This means that by tuning the cone-to-bipolar synapse, each of the bipolar cells can transmit a different parsing of the cone's output. For example, the ON and OFF channels are created in the first synapse by the expression of different glutamate receptors. ON bipolar cells, which have their axon terminals in the inner half of the inner plexiform layer, express a metabotropic receptor called mGluR6. Glutamate binding to these receptors leads, via a transduction chain, to closing of the cation channel TRPM1. As photoreceptors are depolarized in dark releasing glutamate constantly, the ON-bipolar cells are hyperpolarized. The transduction machinery coupled to the mGluR6 receptor is thus sign-inverting. When light causes the photoreceptors to reduce their glutamate release, the cation channels in ON-bipolars can open and the cells will depolarize. OFF-bipolar cells on the other hand, with axon terminals located in the outer half of the inner plexiform layer, express ionotropic AMPA and kainate receptors. These receptors are cation channels opened by glutamate, and when photoreceptors are hyperpolarized by light reducing their glutamate release, the OFF-bipolar cells are also hyperpolarized. The OFF-bipolar synapses are thus sign-conserving. Another example of the divergence of signals into parallel channels is the difference between transient and sustained bipolar cells, which arises from the expression of rapidly and slowly inactivating glutamate receptors (Awatramani and Slaughter, 2000; DeVries, 2000). These two complementary pairs alone create four distinct types of cone bipolar cells: ON sustained, OFF sustained, ON transient and OFF transient.

The output of the different bipolar cells (13 types of cone bipolar cells in mouse) is further modulated by amacrine cells and relayed to the brain by the retinal ganglion cells. The selective connectivity of the multiple bipolar, amacrine and ganglion cell types, together with the intrinsic properties of the ganglion cells, make each ganglion cell responsive to specific visual features. The circuitries and numbers of cell types are currently best known in mouse.

Of the amacrine cells, sixty-three types have been molecularly identified to date in mouse (Yan et al., 2020). The total number of distinct retinal ganglion cell types in mouse currently is ca. 40, identified both functionally (Baden et al., 2016), morphologically (Bae et al., 2018) and molecularly (Rheaume et al., 2018).

It has been postulated that the "the dumber the animal, the smarter the retina" meaning that an animal with larger cortex processes more visual information on the cortex, whereas less cortically sophisticated animals rely more heavily on retinal processing (Johnston and Lagnado, 2012; Baden et al., 2020). This idea is somewhat supported by the midget pathway of primates, which is one of the simplest known retinal circuits. Especially in the fovea, which provides up to ~50% of input to primary visual cortex, this pathway conveys the signal directly from the receptors to the ganglion cells via bipolar cells and with fewer inner retinal inhibitory connections, which are the trademark of more complex retinal circuits (Wässle et al., 1989; Sinha et al., 2017; Bringmann et al., 2018). Mice, however, don't seem to have such a simple circuitry as the midget pathway, but instead a greater mix of different types of circuitries (Baden et al., 2016; Baden et al., 2020). To this date there is less of distinct ganglion cell types identified in primates, 17 in total, although some rarer types might still be missing (Masri et al., 2019; Peng et al., 2019). Furthermore, even though the midget and parasol cells dominate the primate fovea (accounting for over 80% of the ganglion cell types), these types account for only 50% in the peripheral retina. Thus, it is likely that in the primate peripheral retina the ganglion cell diversity is as great as that reported in nonprimate retinas (Masri et al., 2019).

The idea that the specificity coding by the retinal ganglion cells is a feature of "dumber animals" originally stemmed from studies on amphibian retina. Thus, specificity coding was thought as a specialization of the ectothermic retina whereas in mammals feature extraction was studied and found in the visual cortex (Hubel and Wiesel, 1959; Hubel and Wiesel, 1962; Johnston and Lagnado, 2012). As the mouse took over the neuroscience field with the idea that a mammal is closer to humans and because of the genetic tools available (Huberman and Niell, 2011), the anuran retinal research slowed down and not many advances have been made in the past 20 years (Donner and Yovanovich, 2020). Thus, compared to mouse, less is known about the details of the amphibian retinal circuitry, even though many of the fundamental discoveries about retinal design and function were originally made using frogs and toads. The general plan follows the vertebrate retinal design, but the distinct cell types are not as well characterized. Ramón y Cajal (1894) described eleven morphological classes of retinal ganglion cells in *Rana temporaria* (Grüsser and Grüsser-Cornehls, 1976). In the 1980's altogether eight morphological types were found by histological studies (Frank and Hollyfield, 1987; Kock et al., 1989). Physiologists found similar numbers of functional classes from the 1930's to 1970's. Firstly Hartline (Hartline, 1938) described three kinds of receptive fields: ON, OFF and ON/OFF and Barlow (1953) described the

organization of the receptive fields of ON/OFF cells, comprising an excitatory center and an inhibitory surround. Building on this, the famous paper "What the frog's eye tells the frog's brain" by Lettvin et al. (1959) described the feature detector ganglion cells of the anuran retina, the first description of the aforementioned specificity coding. They included, for example, the 'sustained contrast detector' (or class 1 unit) which generates sustained output whenever an edge is present in the field. A second type, the famous "bug detector" (officially called 'net convexity detector' or class 2 unit), responds to moving small dark object crossing the field with the idea that these neurons provide the brain with the information that drives the tracking and capture of small moving prey. The other three functional units that Lettvin and colleagues described were the moving edge detectors (class 3), net-dimming detectors (class 4) and dark detectors (class 5) (Lettvin et al., 1959; Maturana et al., 1960; Grüsser and Grüsser-Cornehls, 1976). Later the class 0 was added which consists of the ON-cells described by Hartline (1938). Each class has distinct morphologies and projections patters (Grüsser and Grüsser-Cornehls, 1976). Additionally, several electrophysiological studies have described functional types that do not fit into the Lettvin-Maturana classes (Bäckström and Reuter, 1975; Witpaard and Keurs, 1975; Donner and Grönholm, 1984).

The dominant signal flow in amphibian retina seems to be through amacrine cells to ganglion cells with fewer direct contacts from bipolar cells to ganglion cells, in contrast to mammalian retina. The evidence comes from electron microscope studies showing that in the frog inner plexiform layer most of the ribbon synapses (i.e. bipolar cell synapses) have synaptic vesicles in the postsynaptic terminal and only a small portion have ribosomes and no vesicles (Dowling 1968, 1970). In primates this ratio is reversed (Dowling, 1976). Ganglion cell dendrites usually do not contain vesicles but ribosomes, while amacrine cells have vesicles but no ribosomes (Dowling et al., 1966). Thus, amphibian ganglion cells seem to be driven largely by the amacrine cells.

A clear functional difference compared with mammalian ganglion cells is the more extensive multiplexing of information by the amphibian retinal ganglion cells. A single anuran ganglion cell can convey ON-OFF, luminosity and chromatic contrast information through distinct temporal response patterns (Yang et al., 1983; Donner and Grönholm, 1984; Maximov et al., 1985; Donner et al., 1998; Donner and Yovanovich, 2020). Multiplexing in mammalian ganglion cells is not as well known, although Wienbar and Schwartz (2018) argue that even with over 40 different RGC types there must be significant amount of multiplexing to send all the required visual information for higher order processing in the optic nerve. With moving stimuli, it is known both from salamander and mouse retina that the same RGC can report both smooth motion of an object across its receptive field center as well as a sudden reversal of the movement direction of an object distant from the receptive field center (Schwartz et al., 2007).

Circuitry in dim light The rod signals in mammalian retina may reach the ganglion cells through three pathways: the rod bipolar pathway, the rod-cone pathway and the rod-OFF pathway (reviewed by Bloomfield and Dacheux, 2001; Field et al., 2005) (Figure 9). The primary route for rod signals operating at light levels near the absolute threshold is the rod bipolar pathway, a unique feature of the mammalian retina (Field et al., 2005; Murphy and Rieke, 2006). In this pathway the light responses from rods are passed to rod bipolar cells, a depolarizing or ON-type bipolar cell and the only bipolar cell receiving input from rods, conveying the signals to the inner plexiform layer (IPL). The distinct feature of the rod bipolar cell is that it does not make direct contacts to ganglion cells (Kolb and Famiglietti, 1974; Kolb, 1979; Nelson and Connaughton, 2020). Instead, it synapses to several electrically coupled AII amacrine cells. The AII amacrines in turn form inhibitory glycinergic connections with OFF cone bipolar terminals, but are also electrically coupled through gap-junctions to ON cone bipolar cells. Thus, the AII amacrines separate the rod OFF and ON input into different channels. The OFF and ON cone bipolar cells then transmit the rod signals respectively to OFF- or ON-ganglion cells.

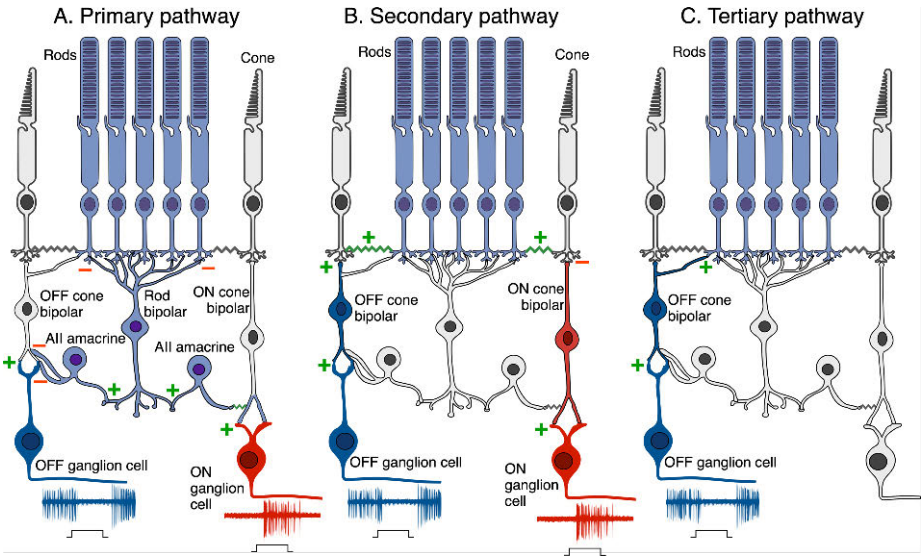

Figure 9 **Rod pathways in the mammalian retina.** A) In the primary (rod-bipolar pathway) rod signals are routed to rod bipolar cells (ON-type bipolar), which in turn synapses with the AII amacrine cells. AII amacrines make inhibitory glycinergic synapses to OFF-cone bipolar cells but are also electrically coupled to ON-cone bipolars. These cone bipolars transmit the signals to retinal ganglion cells. B) In the secondary pathway (rod-cone pathway), rod signals spread to cones via gap junctions. Cones relay the signals to ganglion cells through cone bipolars. C) In the tertiary pathway (rod-OFF pathway), rod signals reach OFF-ganglion cells via direct synaptic contacts that the rods make with OFF-cone bipolars. Plus and minus signs represent sign-conserving and sign-inverting synapses. See text for references. Figure created partly with Biorender.com.

In the secondary pathway (the rod-cone coupling pathway), rod signals are fed via gap junctions directly to cones and mediated via the cone circuitry (Bloomfield and Dacheux, 2001). In the third pathway rods synapse directly on OFF cone bipolar cells. Additionally, recent work also shows that rod input reaches cones via horizontal cells, creating a rod-cone spectral opponency (Joesch and Meister, 2016). A major challenge for vision is adapting to the vast range of illumination changes, as even the lower range from scotopic (starlight) conditions to the mesopic conditions of dusk or dawn spans 5 orders of magnitude (Grimes et al., 2018). The long-standing hypothesis has been that the different rod pathways function in these different conditions, matching their amplification and filtering properties to each light level. To some extent this seems to be the case in rodents (Soucy et al., 1998; Trexler et al., 2001; Deans et al., 2002; Grimes et al., 2018). But interestingly, the rod signals in primate retina use almost exclusively the rod bipolar pathway from the absolute threshold to light levels where rods start to saturate (~300 R*/rod/s in primates) (Grimes et al., 2018). Cone and rod signals also seem to be mixed more in rodent retina, as the rod bipolar cells can make contacts with cones (Behrens et al., 2016) and can even convey cone signals (Pang et al., 2010; Szikra et al., 2014).

Less is known about amphibian retinal circuitry in dim light and much needs to be deduced without direct evidence. First, the mammalian rod bipolar cells were described in dog retina by Cajal already in 1894 whereas in amphibians neither Cajal nor anyone after him has not found rod bipolar cells (Ramón y Cajal, 1894). Thus, it is a reasonable assumption that amphibians do not have a dedicated rod pathway. Secondly, in salamanders the same bipolar cells contact both rods and cones, suggesting that this might be the case in anurans as well (Lasansky, 1973; Hensley et al., 1993). Thirdly, in Xenopus the chromatic bipolar cells are driven under photopic conditions by cones but the same cells under mesopic conditions also get rod input (Yang et al., 1983).

2.2.1.4 Downstream pathways

Mouse The retinal ganglion cells in mammals send their projections to multiple sites in the cortex as well as other visual centers. In mice there are over 50 retino-recipient brain areas (Morin and Studholme, 2014; Martersteck et al., 2017; Wienbar and Schwartz, 2018) (Figure 10). The broadest functional division is between image-forming and non-image forming pathways. The main image-forming pathway, the thalamo-cortical pathway, underlies conscious vision, whereas the non-image forming circuits operate below the level of consciousness and support other functions such as circadian control, or e.g. image stabilization or control of pupil size.

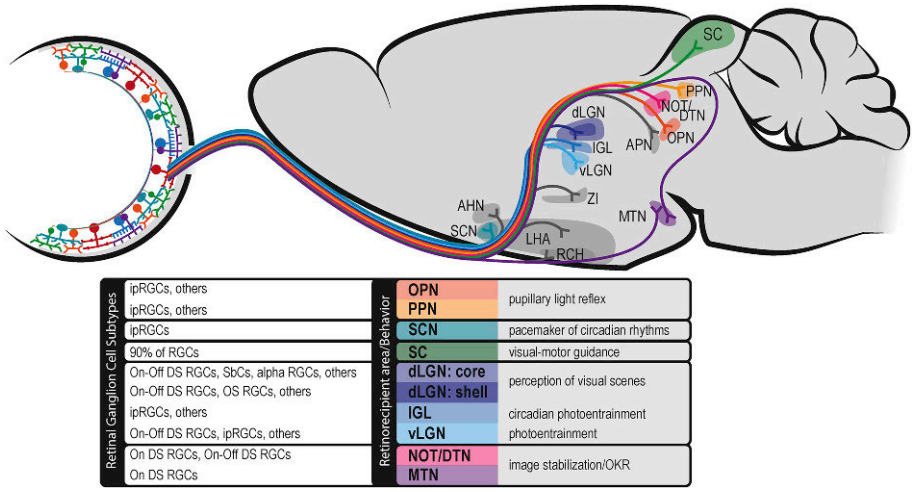

Figure 10 **A subset of the retinal projections to rodent brain targets.** The most well studied brain regions are colored and listed with their known RGC inputs and behavioral functions. Less known regions are shown in gray. Abbreviations: AHN: anterior hypothalamic nucleus, APN: anterior pretectal nucleus, IGL: intergeniculate leaflet, LGN: lateral geniculate nucleus, LHA: lateral hypothalamic area, MTN: medial terminal nucleus, NOT/DTN: nucleus of the optic tract/dorsal tegmental nucleus, OPN: olivary pretectal nucleus, PPN: pedunculopontine pucleus, RCH: retrochiasmatic area, SC: superior colliculus, SCN: suprachiasmatic nucleus. Reprinted from Wienbar and Schwartz (2018) with permission from Elsevier.

Of the multiple pathways, the primary visual pathway (also called the retinogeniculostriate pathway) from the retina to the dorsal lateral geniculate nucleus (dLGN) in the thalamus (in diencephalon) and further on to the primary visual cortex (V1) is the most studied. The dLGN is a key center transmitting information to V1. Most of the rodent dLGN neurons have circularly symmetric receptive fields (Piscopo et al., 2013) and are believed perform linear summation, similar to primates (Grubb and Thompson, 2003; Denman and Contreras, 2016; Román Rosón et al., 2019). However, mouse dLGN also has neurons performing more complex computations, e.g. orientation-selective and direction selective cells (Piscopo et al., 2013). It is still unclear how much of the information arises directly from the different ganglion cell types and how much the dLGN neurons integrate and compute themselves. Recent evidence shows that majority of the functional RGC types (75%) project to the dLGN and, accordingly with the rich input, dLGN maintains a high degree of functional diversity (Román Rosón et al., 2019).

In primates, each dLGN is layered into four parvocellular and two magnocellular layers with alternating ipsi- and contralateral input and interspersed koniocellular layers. The mouse, however, lacks this cytoarchitectural lamination (Seabrook et al., 2017), but does have some crude functional division in the dLGN, for example, the direction sensitive RGCs project to the LGN shell whereas the alpha RGCs project to the core regions

(Huberman et al., 2008; Piscopo et al., 2013; reviewed by Kerschensteiner and Guido, 2017; Seabrook et al., 2017) (see also Figure 10).

Of the non-image forming pathways the retinohypothalamic pathway is one of most important. The intrinsically photosensitive retinal ganglion cells (ipRGCs) project to the core of the suprachiasmatic nucleus (SCN) as glutamatergic innervation (Abrahamson and Moore, 2001). The major function of this pathway is providing external light input for the circadian master clock residing in the SCN. The main behavioral outputs of this pathway include the entrainment of the intrinsic circadian clock, regulation of hormone rhythms and sleep cycles.

A second major non-image forming target for the ganglion cell axons is the pretectum, lying between the thalamus and the midbrain (Purves et al., 2012). This is called retino-pretectal pathway and it is crucial for the pupillary light reflex. Third, the superior colliculus (SC) in the midbrain is a major visual center, corresponding to the tectum opticum that is the main visual brain center of the frog and other "lower" vertebrates. It receives input directly from the retina as well as from the visual cortex. The main task of the superior colliculus is to direct head and eye movements to particular locations in visual space. Its importance in mouse is shown by the fact that up to 90% of all RGCs project to this brain center (Ellis et al., 2016). In contrast, only ~10% of the primate RGCs project to the SC (Perry and Cowey, 1984). Also 80% of the retinogeniculate inputs are collaterals of axons that also innervate the superior colliculus (Huberman et al., 2008; Ellis et al., 2016).

Other early targets of visual input in the mammalian brain include the pulvinar, or lateral posterior nucleus (LP) in rodents, which relays information about the sensorimotor mismatches between self-generated and externally generated visual flow to cortex (Roth et al., 2016; Seabrook et al., 2017). It receives direct input from the deepest portion of superficial superior colliculus (Gale and Murphy, 2014). In primates the LP/pulvinar has been implicated in modulating attention (Saalmann et al., 2012). In mouse the comparable recordings are lacking, but would be interesting.

Neighboring points in the visual field are mapped onto adjacent neurons in the retina and the spatial order of these retinotopic maps is kept in early brain target areas as orderly representations of visual space. Each eye has its specific target areas giving rise to ocular maps. In primates and carnivores there is a strict division in the decussation of RGC axons so that information from the left half of the visual world, originating both in the right temporal retina and in the left nasal retina, is mapped in the right half of the brain and vice versa. But rodent eyes are positioned more laterally and as a consequence, each eye has a large monocular field of view while the binocular field is only 40° (Saalmann et al., 2012). Thus, the ocular maps in rodents are quite different, without a strict line of decussation, and the RGCs from throughout the retina project to the contralateral hemisphere. The small portion of RGCs that project ipsilaterally (5%) are distributed among the contralaterally projecting

RGCs within the ventrotemporal retina (Dräger and Olsen, 1980; Seabrook et al., 2017).

Anurans The frog may be considered as a model of vertebrate visual organization before the evolution of the telencephalon (Ingle, 1976). Most of what is known about the optic pathways in frog comes from recordings of the optic tract fiber terminals in the superficial neuropil of the optic tectum (also called tectum opticum or optic lobe) residing in the midbrain, the homologue of the mammalian superior colliculus (Figure 11). Like in all non-mammalian vertebrates this is the main visual center of the anuran brain, to which the RGCs project contralaterally (Scalia, 1976). The four RGC classes described by Lettvin and colleagues (Lettvin et al., 1959; Maturana et al., 1960) terminate in different layers of the tectum. The most superficial layers have class 1 and 2 neurons (responding preferentially to edges and small objects moving across the visual field) which together are believed to be part of the prey-detection visual system (Barlow, 1953; Lettvin et al., 1959; Ingle, 1976). The next layer contains ON-OFF fibers ('changing contrast detectors') and the fourth layer contains OFF-fibers ('dimming detectors').

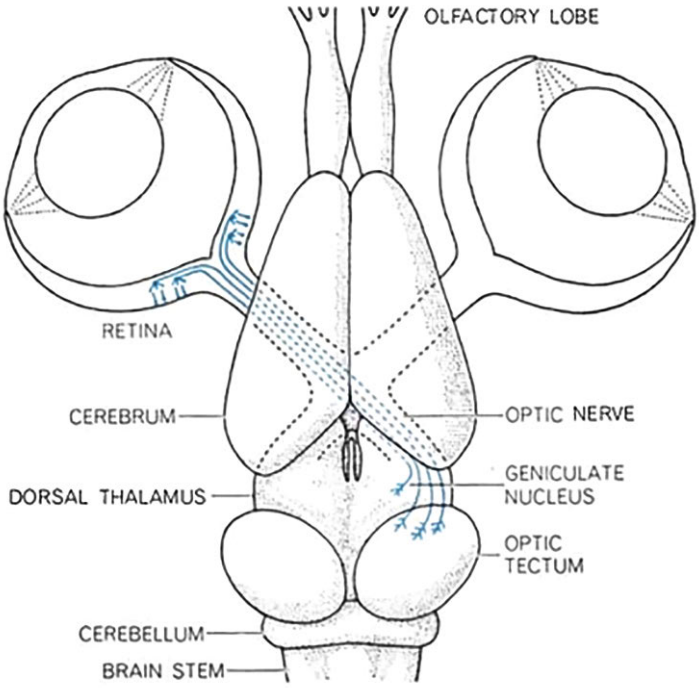

Figure 11 **Main visual pathways of frog.** The frog retinal ganglion cells project to the optic tectum and, to some extent, to the geniculate nucleus in the dorsal thalamus. Reprinted from Muntz (1964) with permission from Bungi Tagawa's estate. Credit: Bungi Tagawa.

In parallel to the tectal projections, the retina projects to the diencephalon, particularly to the thalamic regions (lateral geniculate nucleus and nucleus of Bellonci, which is found in teleost and amphibians). Interestingly, the projections to the tectum and to diencephalon are functionally entirely different (Muntz, 1962b). The projections to the tectum are the class 1–4 neurons as described above whereas the diencephalic projections contain only ON-fibers, seemingly identical to the 'sustained ON' retinal ganglion cells described by Hartline (Hartline, 1938). Muntz (1962b) found that these axon terminals respond without exception most strongly to blue (450–480 nm) light than any other color. Maximov et al. (1985) showed that the nucleus of Bellonci has a true blue vs. long-wavelength opponency system such that the cells respond with long discharges to a shift of balance in favor of the blue channel (whether by increased excitation of the blue channel or decreased excitation of the red channel), and by short-latency bursts to the opposite shift. The tectum, however, seems to respond only in achromatic way. This blue-sensitive diencephalic system could mediate the positive phototaxis response, as at photopic light levels frogs are known to prefer blue light (Muntz, 1962a; Muntz, 1963; Hailman and Jaeger, 1974).

Additionally, amphibians have retinal projections to the pretectal region like in mammals Scalia 1976). Another retinal target is the basal optic nucleus, which is a small cluster of cells in the midbrain and has been implicated in the optokinetic response of frogs (Lázár, 1972; Scalia, 1976).

2.2.2 NEURAL SUMMATION AND THRESHOLDING

For sensory detection, "it is not the difficulty of amplifying weak signals that limits the sensitivity, but the difficulty of distinguishing a weak signal from the background of spurious signals, or "noise"" (Barlow, 1956). In other words, amplification is beneficial only when the signal can be amplified more effectively than the noise. Neural summation and thresholding are circuitry level strategies to improve visual detection when the signal is low and noise relatively high. Unlike hardwired adaptations in the eye design or retinal morphology, neural adaptations can be matched to the current illumination and distribution of contrast in the visual scene.

The signal can be summed in space and time not only on the photoreceptor level (as described in Emergent constraints and optimizations) but also by downstream summation. Spatial summation acts through convergence, pooling signals across many adjacent input neurons. Signal reliability is increased, if the signal is correlated in the adjacent units. Signal amplitude increases proportionally to the number of (weighted) units, while noise that is uncorrelated between the input units will increase much less (Hemilä et al., 1998). In a similar manner, the signal may be summed temporally over a certain neural integration time. The signal-to-noise level increases to the extent that the signal is correlated but the noise uncorrelated over the summation or integration time.

Mammalian night vision, relying on the rod bipolar pathway, employs both of these strategies. Rods converge to rod bipolar cells in higher number to increase spatial pooling downstream, whereas, especially in the areas of high visual acuity (area centralis), cones connect to bipolar cells one-to-one. Rods have slower response kinetics than cones, making their integration time longer so that they sum more photons giving a more reliable response to sparse photons (the same goes for dark-adapted photoreceptors vs. light-adapted ones). But because of the inevitable tradeoff between sensitivity and resolution, neural summation has its drawbacks. Increasing spatial summation leads to reduced resolution in space and loss of spatial detail. Likewise, increased temporal summation results in decreased temporal resolution and motion blur. The extent of neural summation is therefore expected to be matched to the visual needs and lifestyle of each species. Nocturnal species employ enhanced spatial summation, as in the rod-dominated retina of mouse or increased temporal summation as e.g. in the toad retina, whose integration time can be over 2 s at 15 ^{o}C (Aho et al., 1993b).

Interestingly, at higher light intensities, where there is no need to increase the signal-to-noise ratio to enhance detection, spatial summation can function to shorten visual latency (Donner, 1989). This is because the early part of the ganglion spike response relies on the early rising phase of the photoreceptor response, which scales linearly with the number of absorbed photons. Summing such photoreceptor responses linearly gives a signal that retains the shape of the photoreceptor response but reaches threshold at an earlier time point. Doubling the spatial summation area has the same effect on the early rise of the response as doubling the light intensity. This of course is crucial for surviving, since the response speed to the presence of predators or prey is a matter of life and death.

Besides neural summation, another circuitry level strategy that may improve signal-to-noise ratio at low light levels is adding a thresholding nonlinearity. Theoretically, linear filtering can remove some noise with temporal frequencies not associated with the single photon response (Bialek, 1987; Bialek and Owen, 1990; Pahlberg and Sampath, 2011). Indeed, in the amphibian retina a presynaptic mechanism causes the synaptic transmission between rods and bipolar cells to preferentially transmit temporal frequencies near 2 Hz (Armstrong-Gold and Rieke, 2003). At least at some conditions (depending on temperature and light level), this may be ideal since temporal frequencies below 1 Hz are slower than the single photon response and frequencies above 4 Hz are dominated by noise. But linear filtering cannot be the dominant noise removal mechanism because noise and signal in rods (both originating in the phototransduction cascade) are largely composed of the same frequencies, and linear filtering will act on both. Clearly, nonlinear mechanisms are necessary.

As discussed in the chapter Neural noise, the first synapse in the mouse rod bipolar pathway has a nonlinearity that filters out most of the noise originating in rod phototransduction (Field and Rieke, 2002a). This nonlinearity operates

on signals from individual rods. It separates signals in rods that have absorbed a photon from noise generated by the same rod as well as others. The presence of this nonlinearity is shown by comparing recordings from rods and rod bipolar cells: while the rod response grows linearly with increasing flash strength, the responses of rod bipolar cells grow supralinearly. This is because the synapse between rods and rod bipolar cells have a threshold that eliminates small rod responses. The mechanism acts through a saturation of the metabotropic glutamate receptor (mGluR6) (Sampath and Rieke, 2004). Glutamate bound to this receptor closes ion channels in the rod bipolar cell. In darkness, the rate of glutamate release from rods is enough to keep nearly all ion channels closed in the rod bipolar cell dendrites. Small fluctuations in the release, as in small single-photon responses or discrete noise events, are not sufficient to change the activity of the mGluR6 receptor significantly and the channels do not open. Surprisingly, the saturation is positioned so that more than half of the single photon responses are eliminated (Field and Rieke, 2002a). This may be related to the low probability of photon absorption in each rod near visual threshold (Kiani et al., 2020). At 0.001 R* per rod there is a 99.9% probability that the rod is producing noise and not a real single photon response. Thus, the threshold in the mouse rod bipolar pathway might be strongly biased towards avoiding false positives: eliminating noise and retaining only large single-photon responses. The relative amplitude of continuous dark noise in mouse is slightly higher than for example in primates, which motivates more stringent thresholding.

A second threshold in the mammalian rod bipolar pathway has been found between the ON-cone bipolar cell and the ON-ganglion cell (Ala-Laurila and Rieke, 2014). This downstream threshold operates at light levels ca. 1000 times lower than the one between rods and rod bipolar cells and removes much of the noise introduced in rods and in the retinal circuit preceding ganglion cells: most single single-photon responses as well as dark events originating from thermal pigment activations. The threshold is placed such that it acts on a collected input from 500-1000 rods. For a signal to pass this threshold, at least two single photon responses (or discrete noise events) are required to occur in this collection of rods, within <200 ms of each other. It is present only in the ON-pathway, increasing the reliability of the ON-ganglion cells, which indeed produce little or no spiking in darkness, effectively removing all rod noise (reviewed by Takeshita et al., 2017). The OFF pathway does not have this nonlinearity, and the responses of OFF-ganglion cells depend nearly linearly on the flash strength. The nonlinearity also makes the ON-pathway slightly less sensitive, as all single photon events are eliminated.

A crucial difference between mammals and amphibians in their strategies for dealing with weak signals and noise at low light levels is the substantial electrical coupling of the amphibian rods (Fain, 1975). The strong coupling enables a single photon event in one amphibian rod to leak to several neighboring rods. These simultaneous mini-events are not distinguishable in the synapse between each rod and bipolar cell, but are summed later at the

bipolar, or at the latest the ganglion cell level, reconstituting the true single photon event (Copenhagen et al., 1990; reviewed in Donner and Yovanovich, 2020). Because the single photon events are shared between a large number of neighboring rods, thresholding in single synapses between rods and rod bipolar cells such as in mouse would be quite futile in amphibian retina. A high threshold is likely applied at the ganglion cell level, preceded by noise-dependent gain adjustment, such that most noise is rejected before spike generation, yet the linear scaling of (small) supra-threshold signals is retained at the ganglion cell output (Copenhagen et al., 1990; Donner et al., 1990a; Donner and Yovanovich, 2020) (see also Donner & Yovanovich 2020 figure 3B).

2.2.3 EVOLUTIONARY HISTORY AND LIFESTYLE

Sensory systems have ultimately evolved to acquire and process information crucial for survival and fitness. The environment has practically an infinite amount of information carried by numerous forms of energy: electromagnetic radiation as light and heat, volatile molecules and molecules in solution, sound waves, mechanical contact, magnetic fields and gravity. Organisms have evolved sensors to collect information from all these sources but the sensors differ greatly in their cost. It depends on the animal's choice of lifestyle in which sensors it should invest the most. For example, the animal's choice of time of day for foraging (day/night/crepuscular) decides whether fine spatial vision is more beneficial than acute hearing or echolocation. As is evident throughout this thesis, the fittest optimizations depend on the lifestyle of the animal and reflect compromises that promote survival in a given niche.

2.2.3.1 Evolutionary history

The living amphibians are representatives of the first vertebrates that moved to land about 400 million years ago. They are a widely diverse group, of some 8000 species known (almost 200 new species being described still yearly according to AmphibiaWeb, 2020) (Wells, 2007). The major amphibian groups are very different from each other: frogs and toads (order Anura) are specialized for jumping and have large heads and eyes. Salamanders and newts (order Urodela) are more elongate with a long tail and roughly equal sized limbs. Caecilians (order Gymnophiona) have snakelike bodies lacking legs and greatly reduced eyes, as they are specialized to life underground. All amphibians need water to reproduce, as their eggs lack hard shell and will dry easily. The typical lifecycle of an amphibian starts with larval stage that lasts a few months, followed by a metamorphic period.

Anurans (meaning 'tailless') is the biggest order with 88% of amphibians (7244 species, 6.8.2020 AmphibiaWeb, 2020). They share shortened bodies, extremely large hind legs and large heads and eyes. However, they are also

morphologically diverse group occupying varying habitats from ponds and streams to tropical rainforests, grasslands and hot desserts. Some are strictly aquatic while others are specialized to terrestrial or arboreal life. Visual science has concentrated mainly on a few species in the family Ranidae and Bufonidae. Ranidae are mostly semiaquatic or terrestrial while Bufonidae are terrestrial. The main mode of locomotion in anurans is jumping, and other modes are modifications of jumping, like hopping, walking and burrowing. Nearly all frogs are either insectivorous or carnivorous as adults, generalist feeders on a variety of insects, other invertebrates or small vertebrates. The frog tongues have the same basic morphological structure but vary in anatomical detail and in the degree of protrusion. Most of the modern lineages have a muscular tongue, which is attached in front, with a free posterior flap that can be projected by flipping it forward out of the mouth. This mode of tongue protraction is called inertial elongation, and it allows the frog to capture prey at some distance without moving its head toward the prey.

Mammals diverged from the shared tetrapod history with amphibians about 350 million years ago when the first amniotes (mammals and reptiles including birds) appeared (Campbell et al., 2005). The recent evolutionary history of the mouse (~ 10 ka) is comparable to some of the most important domestic animals with respect to the huge human impact. The shared history of house mice and humans dates back millennia, ever since mice spread from their origin in northern India and found a new habitat in the cereal stores of the first farmers (Berry, 2012). The house mouse is found all over the world, from tropical islands to deserts and from sea level to mountains, often but not always, in contact with humans.

The *Mus musculus* is a polytypic species composed of five subspecies (including *musculus, domesticus, castaneous, gentilulus, molossius)* (reviewed in Auffray and Britton-Davidian, 2012). Apart from these, it has chromosomal races due to centric fusions and other chromosomal rearrangements. It is thought that *M. musculus* and its ancestors thrived on temperate dry, grassy lands (steppe climate) somewhere on the Indo-Pak continent and neighboring Afghanistan and Iran areas (reviewed in (Bonhomme and Searle, 2012)). This terrain, with its mountain barriers and intervening lowlands, is highly dissected and would have advanced segregation of gene pools each time climatic conditions allowed natural migration of the species into new territory. The initial, major differentiation of the different present-day subspecies possibly started two major interglacial periods ago, somewhere south of the Himalayas (where still the greatest genetic diversity of the house mouse exists). The association with humans and the consequent dispersal all over the world is more recent, starting about 12 000 years ago in the area of the Fertile Crescent, as suggested by mitochondrial DNA studies. Nowadays, the house mouse is one of the most widespread mammals, thriving in diversified habitats. The inherited variation is the basis of differences between inbred strains, but these strains carry only a fraction of the variation found in wild mice. The history of the modern

laboratory mouse dates back to 1907 when C.C. Little started breeding mouse colonies to study the inheritance of coat color (the resulting Jackson Laboratory is now a world center of mouse research).

2.2.3.2 Visual behaviors

The superiority of vision lies in its being a 'remote' spatial sense, providing instant, potentially high-resolution spatial information about the surroundings without any direct contact. The model animals of this thesis, the mouse and the frog, critically depend on vision in many tasks. The mouse does not rely on vision to the same extent as many other mammals, including primates, but in the frog, vision is by far the most important sense. Importantly in the present context, both are crepuscular or nocturnal species, meaning that they are active and forage preferentially in low-light conditions. Both are predators as well as preyed upon, giving rise to approach and avoidance behaviors in response to specific visual cues. The escape and freezing reactions in response to visual threat rely purely on vision, with a sweeping dark stimulus generally causing a mouse to freeze while an enlarging disc imitating an approaching predator causes the mouse most often to flee (Yilmaz and Meister, 2013; De Franceschi et al., 2016). Which reaction is triggered, depends not only on the stimulus statistics but on the internal state of the mouse (Salay et al., 2018). Likewise, frogs have predator avoidance behaviors (e.g. avoidance jumping, side-stepping or ducking) and an approaching stimulus makes them flee, especially expanding dark stimuli (reviewed in Ingle, 1976). Frog prey capture relies entirely on vision. Mice are capable of capturing prey relying on their hearing alone, but efficient prey capture depends on vision as measured by accuracy and capture rate (Hoy et al., 2016).

Another interesting visually-guided behavior of frogs is their orientation towards light or phototaxis when enclosed in a dark container. This experimentally useful innate behavior is probably an escape response. The chromatic sensitivity in the frog phototaxis has been known since the 1960's when Muntz performed a set of experiments describing the frog's preference towards blue light and later demonstrated in several species of frogs and toads (Muntz, 1962a; Muntz, 1962b; Jaeger and Hailman, 1973; Hailman and Jaeger, 1974). Muntz found that adding green light to blue, while this increased the photon catch in the BS photoreceptors, actually reduced the blue preference (Muntz, 1962a). Thus, he concluded that the blue preference resulted from a true wavelength discrimination and not from the photoreceptors being more sensitive to blue than green wavelengths. The hypothesis for why frogs would prefer the blue wavelengths is that the frogs interpret the blue light as coming from the sky. Hailman and Jaeger (1974) suggested that a frog waiting for a flying insect might benefit from facing the sky in order to obtain high-contrast background against which to visualize the prey item.

Besides feeding and escaping, mate choice is one of the life-important behaviors where frogs depend on vision. Here, color vision is important. When the mating season starts in the spring, the throat of *Rana temporaria* males turns blue while the females are yellow or reddish. The males have been shown to prefer red and yellow female dummies to blue ones (Kondrashev et al., 1976; Kondrashev, 1976). How much mice use vision in social contexts is not known, but certainly olfaction and hearing play greater roles as mice are known to communicate primarily with chemosensory signals and ultrasonic vocalizations (Musolf and Penn, 2012; Stopka et al., 2012). Mice are capable of making short/middle-wavelength discriminations in a behavioral task, but the use of color vision in natural conditions remains the subject of speculation (Denman et al., 2018; Szatko et al., 2020).

2.2.3.3 Matched filtering

A key concept in how the sensory systems have evolved to their specific niche and environment is matched filtering. The term matched filtering was first introduced in neuroethology by Rüdiger Wehner (1987), generalizing from the common usage in electrical engineering. The basic idea is that animals have evolved to match their response range to the stimulus range beneficial for their survival and reproduction, and suppress or even reject irrelevant stimuli. Wehner described spatial orientation tasks, like the desert ant using sky's polarization pattern for navigation, arguing that already the spatial design of the receptor layer at the periphery of the sensory system solves the particular navigational problem its facing, adapting approximations and simple tricks rather than intricate algorithms. This severely limits the information available to the brain, but frees energy and space to perform more complex computations needed to extract the required information for the task.

For the visual system this means that each animal's vision is pre-adapted or tuned by evolution to the spectral, temporal and spatial statistics of their visual environment. One of Wehner's examples is provided by the topography differences in the photoreceptor and ganglion cell layers. The visual streak may be seen as a matched filter in ground-living animals, inhabiting a predominantly horizontally oriented environment, whereas species living in cluttered environments, such as forests, tend to have a spot-like acute zone, 'area centralis'. A surface-feeding fish striped panchax (*Aplocheilus lineatus*) has in fact *two* visual streaks, one for the horizon above the water surface, and one below it, and positioned such that the optically split visual world is reunited neurally (Munk, 1970; Wehner, 1987). A spectral matched filter can be seen in the visual pigment absorption maxima of deep-sea fish, that are more blue-shifted than fresh-water or surface-living species and as such matched to the light in the environment where the only light available is the narrow-band blue light and blue bioluminescence. Matched filtering can sometimes be seen very directly in behavioral responses, as the avoidance responses of mice and frog described above. Colour may be one important

variable defining the matched filter. Short wavelengths seem to have a specific meaning in frog phototaxis, as frogs preferentially jump towards blue stimulus at photopic light intensities (Muntz, 1962a; Muntz, 1962b; Hailman and Jaeger, 1974). Similarly, the attractiveness of certain wavelengths during mating season in anurans serves a reproductive matched filter.

The choice of activity period affects the available stimulus range and thus matched filters for nocturnal and diurnal animals differ. For example, the diurnal ground squirrel, which forages solely at daytime, has only cones, while the crepuscular frog, in addition to cones, has even two kinds of rods, enabling extraction of wavelength information also in dim light. Natural images benefit from increasing light even in the range of daytime illumination, as contrasts are generally low (Laughlin, 1981; Sterling, 2004). Especially the important objects tend to blend in, as both predators and prey want to be inconspicuous. As discussed already, intensity at any given point in the retina varies temporally according to the Poisson statistics and thus, photon shot sets a theoretical limit to the contrast detection at any given light level (see Equation 1). But the higher the acuity, the smaller is the photon number in each "pixel". The higher the speed, the smaller is the photon number in each "frame". Once again, we face the trade-off between sensitivity and resolution. The lifestyle of mammals is to be fast, so they cannot depend on extended temporal integration to increase the photon numbers. Daylight has enough photons for fine spatial detail at an integration time of 100 ms, but the excess is not large and definitely limited at even slightly dimmer conditions (Sterling, 2004).

Inextricably linked to neural matched filtering is the notion of efficient coding proposed early on by Attneave (1954) and Barlow (1961) based on information theory (reviewed by Simoncelli and Olshausen, 2001). Barlow suggested that the peripheral sensory neurons (using the retina as the example) should reduce the statistical redundancy in the sensory input. Natural images are statistically redundant and neurons should get rid of this redundancy and pass on "only what is news" (Barlow, 1961). In an experimental test of this idea, Srinivasan et al. (1982) measured how the visual system of a fly deals with this correlation. They measured the autocorrelation of natural scenes and calculated the inhibition between neighboring photoreceptors required to cancel out these correlations. They then compared the predicted inhibitory surrounds to the actual measured surround fields in the fly and showed that these matched really well, thus demonstrating the efficient coding strategy (or predictive coding as the authors called it). In an elegant study on efficient coding of contrast information, Laughlin (1981) showed that the function relating contrast to the membrane potential of the fly's large monopolar neurons transforms the probability distribution of contrasts found in the natural environment into a uniform distribution of membrane potential. This implies optimal use of the signaling range of the neuron. Obviously, however, all considerations of efficient coding must be informed by (biological) hypotheses on *what* information is most relevant to the animal and should be retained.

2.2.3.4 Behavioral state

A fundamental complication for matched filtering and efficient coding is that the environment is not fixed. Neither is the animal and its nervous system. The effects of general illumination have already been mentioned, but the statistics of the retinal image from a fixed scene is subject to fast changes regardless of illumination. For example, when the animal moves, the natural images on the retina shift toward higher spatiotemporal frequencies. On the other hand, what information is "relevant" changes on longer time scales, e.g. with reproductive cycles. Thus, it is an enormously interesting question how the matched filters can change in accordance with the behavioral state.

That brain state affects the neural response patterns has been known ever since the first recordings from the mammalian brain by Richard Caton (1887), and already David Hubel (1959) discovered that the firing rate in the visual cortex of awake, unrestrained cats was modulated by the cat's level of arousal. These findings have now been advanced by the more sophisticated recording techniques on awake animals performing behavioral tasks. The transitions between sleep and wakefulness and the different sleep-stages are well-characterized, but new studies have started to resolve different brain states within the wakefulness period and their effect on sensory processing (reviewed in McGinley et al., 2015b).

In fact, it is established that behavior can shape sensory processing in multiple ways, ranging from modulation of responsiveness, or sharpening of tuning, to a dynamic change of response properties or functional connectivity. McGinley and coworkers project the ways in which behavioral state can modulate basic sensory processing to five dimensions: 1) response magnitude, 2) signal-to-noise-ratio, 3) precise timing, 4) variability, and 5) how this variability is correlated across cells (noise correlations) (McGinley et al., 2015b). Effects of arousal level have been particularly extensively studied, and locomotion is often used as an experimentally convenient, quantifiable behavioral state character. In many species heightened arousal state and/or locomotion directly influence cortical visual processing (reviewed by Maimon, 2011; McGinley et al., 2015b; Cardin, 2019; McCormick et al., 2020). For example, the central visual neurons of the fruit fly extract a different temporal range of signals when the fly is moving versus when it stationary (Chiappe et al., 2010; Maimon et al., 2010; Tuthill et al., 2014; Strother et al., 2018). Even when the fly is walking, the visual cells are modulated by nonvisual signals from leg-driven movements (Fujiwara et al., 2017). Similar results have been observed in mouse V1, where neurons carry signals associated with running speed, even in darkness, probably contributing to computations of self-motion (Saleem et al., 2013). Locomotion shapes visual physiology by altering response gain and stimulus selectivity both in mammals and flies (reviewed by Maimon, 2011; Busse et al., 2017). For example, Niell and Stryker (2010) recorded mice running on an air-supported Styrofoam ball and discovered that when the mouse transitions from standing to running, the visually evoked responses in V1 are more than two-fold stronger. Furthermore, mice perform

better at visual tasks during locomotion than during quiescence, as movement decreases trial-by-trial response variability of subthreshold membrane potentials of V1 neurons (Bennett et al., 2013). Both locomotion and arousal without locomotion decrease noise correlations in the neural population (Erisken et al., 2014; Vinck et al., 2015; Dadarlat and Stryker, 2017).

Pupil size is another widely used quantifiable marker of behavioral state, used already in the 60's in humans to record the levels of interest, emotional state and mental activity (Hess and Polt, 1960; Hess and Polt, 1964; Kahneman and Beatty, 1966). Even Charles Darwin mentioned pupil dilation as indicator of emotional state (Darwin, 1986). Human and animal studies have demonstrated that arousal, attention, and emotions such as fear, anxiety and stress are correlated with pupillary changes (after correcting for effects of luminance and depth accommodation) (reviewed McGinley et al., 2015b). Recent studies have reported that large pupil dilations occur at the time of locomotion and whisking in mice, and demonstrated a relationship between exploratory behavior, pupil size and low-frequency oscillations in membrane potential or local field potential (LFP) in visual, somatosensory and auditory cortical areas (Reimer et al. 2014, McGinley et al. 2015, Vinck et al. 2015). As pupil dilation was found to be associated with increases in cortical activation and suppression of low frequency rhythms even in the absence of movement, pupil size has been proposed as a relatively independent measure of the level of arousal (Murphy et al., 2014; Reimer et al., 2014; Salay et al., 2018; Shimaoka et al., 2018; Liang et al., 2020; Salkoff et al., 2020; Schröder et al., 2020). However, states of arousal measured by pupil dilation and by locomotion activity differ in their cortical correlates (Vinck et al. 2015). Locomotion and whisking require arousal but arousal does not necessitate movement. Thus, exploratory behavior appears to be a sub-state of a more general state of heightened arousal (McGinley et al., 2015b). The relationship could be more complex, as recent theories suggest that the arousal control system infiltrates the autonomic and somatomotor control networks to coordinate changes associated with sleep, s so that one primary function of sleep is to suppress motor activity (Liu and Dan, 2019).

All this evidence is building up to a view in which arousal potentially promotes perceptual performance through enhanced sensory encoding (Cardin, 2019). Behavioral state-dependent control of sensory processing may allow the cortex to flexibly switch between modes optimized for detection of conspicuous objects and discrimination between more complex cues (Cardin, 2019). For example, a resting animal would mainly need to detect predators fast and easily, while a foraging animal would need to discriminate between different food items as well as social and environmental cues. In zebrafish larvae, for example, hunger not only modulates the behavioral decision whether to approach or avoid an object (risk-prone behavior), but tunes the responses of visual neurons in the tectum to small visual stimuli (Filosa et al. 2016). In blowflies, nutritional status alters the temporal frequency tuning of motion-vision neurons (Longden et al. 2014).

Modulations associated with behavioral state are not necessarily restricted to the cortex. Interestingly, recently the output of retinal ganglion cells to the superior colliculus as well as the thalamus has been reported to depend on the animal's level of arousal (Liang et al., 2020; Schröder et al., 2020).

2.2.4 CIRCADIAN RHYTHMS

One fundamental factor regulating the behavioral state of an animal is its circadian rhythm. Earth's rotation around its axis provides a regular, dynamic pattern of environmental variation. To predict the changes in the solar day, virtually all living organisms have developed an endogenous, biological clock. Circadian clocks are ancient and phylogenetically widespread, having possibly first evolved 3–4 billion years ago in cyanobacteria, either for optimizing the conditions for photosynthesis or to avoid ultraviolet radiation (Dunlap, 1999; Johnson and Golden, 1999). The power of circadian rhythms is that they let the organism regulate physiology and adapt predictively instead of passively responding to the environmental changes. Thus, they also manage the sleep-wake cycle so that the animal forages at the optimal time (a temporal niche to which the species has evolutionarily adapted) while avoiding predation and saving energy and resources during rest.

Circadian rhythms have three characteristics defining them. Firstly, they free-run with a period of approximately 24h in constant conditions. Secondly, they synchronize, or entrain, to the environmental cycle, so that the phase of the intrinsic rhythm matches that of the environmental cycle. Light is the principal signal synchronizing the circadian clock, although in the absence of light other cues (called zeitgebers, "time givers") can also set the circadian clock (e.g. food availability, social interaction (Kolker and Turek, 2001). Thirdly, circadian rhythms are temperature compensated, meaning that the free-running rhythm is not affected by moderate changes in ambient temperature (although temperature cycles can also act as a zeitgeber).

2.2.4.1 Circadian clocks and ipRGCs

Circadian clocks seem to be a product of convergent evolution, with the specific components of the clock being divergent across the lifeforms, but sharing a common network motif of a negative feedback loop with a delay (Dunlap, 1999; Takahashi, 2017). In mammals, the core clock is a transcriptional autoregulatory feedback loop of key clock components, mainly the CLOCK and BMAL1 transcription factors (Figure 12) (reviewed by e.g. Dunlap, 1999; Reppert and Weaver, 2002; Takahashi, 2017). The mammalian circadian clock is a hierarchy of peripheral pacemakers (called slave clocks or oscillators) scattered in all tissues and governed by one central master clock, which synchronizes and entrains them to the environmental cycle. The peripheral clocks are found in just about every tissue and, for example, nearly

half (43%) of all mouse genes have a circadian rhythm somewhere in the body (Zhang et al., 2014). The master clock is comprised of approximately 20 000 'clock cells' residing in the suprachiasmatic nucleus (SCN) of the hypothalamus (Reppert and Weaver, 2002).

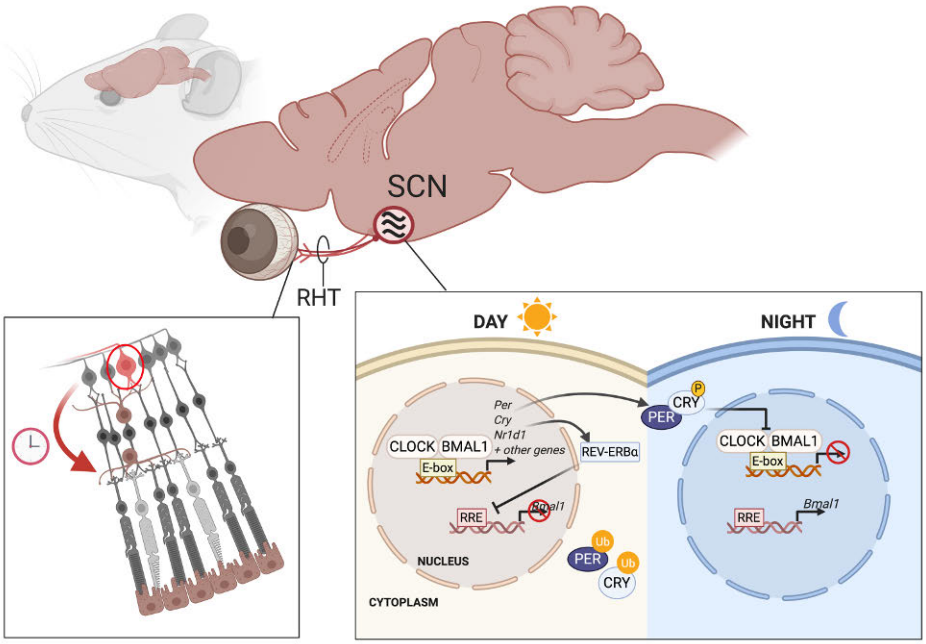

Figure 12 **Retinohypothalamic tract and the core molecular clock machinery.** The mammalian master clock resides in the suprachiasmatic nucleus (SCN) of the hypothalamus. It receives input about the environmental light conditions from the intrinsically photosensitive retinal ganglion cells (ipRGCs) of the retina via specialized projections. Of these, the retinohypothalamic tract (RHT) provides the most substantial input. Inset (left): The ipRGCs (red, circled) express melanopsin and are capable of phototransduction, signaling the presence of light over long term. In addition, the retina itself contains a circadian clock regulating retinal functions. Inset (right): The core clock mechanism consists of activators CLOCK and its heterodimeric partner BMAL1. These transcription factors form a complex that binds to the regulatory elements (E-boxes or enhancer boxes, short regulatory elements in the eukaryotic promoters) of clock genes encoding repressor proteins PER and CRY (mammals have several copies of these, encoded by genes *Per1, Per2, Per3, Cry1* and i). In mice, CLOCK-BMAL1 activation happens during the day leading to accumulation of PER and CRY during the late afternoon or evening. PER and CRY interact with each other as well as with a kinase, and subsequently translocate at night to the nucleus, where they interact with the CLOCK-BMAL1 to repress their own transcription. This forms the negative feedback loop. PER and CRY have relatively short half-lives, and they are shortly ubiquitylated and degraded. A positive feedback loop is formed as the CLOCK-BMAL1 complex activates the nuclear receptors REV-ERBα and REV-ERBβ (encoded by genes *Nr1d1* and *Nr1d2*). These accumulate, translocate to the nucleus and bind to the Bmal1 promoter inhibiting its activity and BMAL1 levels fall. As PER and CRY inhibit the CLOCK/BMAL1 complex, they also inhibit the transcription of REV-ERBα leading to de-repression or activation of Bmal1 transcription. P, phosphorylation; RRE, REV-ERB/ROR response elements; Ub, ubiquitylation. See text for references. Figure created with BioRender.com.

Light is the most powerful signal for the circadian clock and the major input to the SCN comes from the retina through the retinohypothalamic tract. As the intrinsic period of the clock is not exactly 24h, it needs the extrinsic sensory input or will otherwise drift out of phase with the environmental cycle. Bilateral removal of eyes abolishes all responses to light, including photoentrainment, and so it was long thought that the same photoreceptors responsible for pattern vision mediate also the non-image forming, circadian vision (Freedman et al., 1999; Berson, 2003; Lucas, 2013). However, because rodless and coneless mice, as well as blind people, were still capable to photoentrain, and light suppressed their melatonin levels, another system seemed to be responsible of the circadian entrainment (Foster et al., 1991; Czeisler et al., 1995). Only about 20 years ago this was confirmed, as the intrinsically photosensitive retinal ganglion cells (ipRGCs) were found (Berson et al., 2002; Hattar et al., 2002), reviewed in (Berson, 2003; Do and Yau, 2010; Lucas, 2013). These retinal ganglion cells express a visual pigment called melanopsin (belonging to the class of rhabdomeric visual pigments, based on r-opsins, used by most invertebrates) and respond to light by depolarization through a G-protein cascade. Thus, they are directly photosensitive and capable of phototransduction. Initially, ipRGCs were thought to be a homogeneous population but since then they have been shown to have a surprising diversity in their morphological and electrophysiological characteristics. Now six types (called M1-M6) are known with diverse functions (reviewed in Schmidt et al., 2011; Do, 2019)). Moreover, the subpopulations of ipRGCs innervate dozens of other brain regions besides the SCN, for example, the olivary pretectal nucleus (OPN, responsible for pupil constriction) and the dLGN and intergeniculate leaflet (IGL, a center for circadian entrainment and responsible for integrating photic and non-photic circadian cues) (Gooley et al., 2003; Hannibal and Fahrenkrug, 2004; Hattar et al., 2006). Not surprisingly, ipRGCs evoke a range of physiological responses to light besides photoentrainment. These non-image forming functions include the pupillary light reflex, suppression of pineal melatonin production and sleep regulation (Gamlin et al., 2007; Altimus et al., 2008; LeGates et al., 2012; Keenan et al., 2016). In recent years, more evidence has come to light that melanopsin is capable for rudimentary pattern vision in the absence of rods and cones, and that the ipRGCs (particularly the 'non-M1' types) are contributing to the image-forming pattern vision as well (reviewed in Sonoda and Schmidt, 2016; Do, 2019). On the other hand, the 'traditional' photoreceptors also contribute to the non-image forming vision, with cone photoreception playing a minor role while rods are the predominant photoreceptors besides ipRGCs in photoentrainment (Altimus et al., 2010).

M1 ipRGCS are postsynaptic to dopaminergic amacrine cells (and also drive them reciprocally (Zhang et al., 2008), which release both dopamine and GABA (Contini and Raviola, 2003; Vugler et al., 2007; Do and Yau, 2010). Dopamine has diverse effects in the retina, and thus ipRGCs could regulate retinal physiology. This could connect the ipRGCs to the retinal circadian

clock, and vice versa. Melanopsin expression in ipRGCs has diurnal variation (Chaurasia et al., 2005; Hannibal et al., 2005) and ipRGCs themselves express the core clock proteins (Liu et al., 2012).

2.2.4.2 Circadian retina

Interestingly, the retina is not only conveying the information of light/dark cycles to the master clock, but retinal cells also contain the molecular components of the clock and support a retinal rhythm independent of the master clock. The first evidence of the retinal clock was found in amphibians, as the retinal arylalkylamine N-acetyltransferase activity (AANAT, a key enzyme in melatonin synthesis) was found to have a circadian rhythm in the *Xenopus laevis* eyecups *in vitro* (Besharse and Iuvone, 1983). In mammals, studies on hamsters indicated that mammalian retina has an endogenous circadian rhythm and suggested it uses the same molecular machinery as the SCN clock (Grace et al., 1996; Tosini and Menaker, 1996; Tosini and Menaker, 1998). Since then, circadian rhythms in melatonin synthesis or gene expression have been shown in isolated bird, fish and reptile retinas (Tosini and Menaker, 1998; Kaneko et al., 2006; Steele et al., 2006; Tosini et al., 2014) and numerous studies have found clock gene expression in the retinal cells (e.g. Witkovsky et al., 2003; Ruan et al., 2006; Tosini et al., 2007a; Liu et al., 2012). The main question left seems to be whether all the clock genes are expressed in most cell types or in specific populations. In amphibian and avian retinas, there is strong evidence that the photoreceptors express the core clock components and are capable of generating circadian rhythms in isolation from other cell types (Cahill and Besharse, 1993; Zhu et al., 2000; Hayasaka et al., 2002; Ivanova and Iuvone, 2003a; Ivanova and Iuvone, 2003b). The circadian organization of mammalian retina seems to be more complex, as melatonin is synthesized rhythmically in the photoreceptors, but clock gene expression is more concentrated in cells of the inner retina, thus raising the possibility that the inner retina drives the rhythms in the photoreceptors (Gekakis et al., 1998; Ruan et al., 2006; Tosini et al., 2007a; Sandu et al., 2011; Liu et al., 2012; McMahon et al., 2014). Tosini et al. (2007a; 2007b) suggested that the mammalian retina has at least two independent circadian systems, one in photoreceptor layer and one in inner retina. Liu et al. (2012) proposed an even more intricate system, where core clock genes are expressed heterogeneously in multiple cell types, so that different cell types express various amounts of clock proteins with different rhythmicity.

The primary output signals of the retinal clock are the neurohormones melatonin and dopamine, respectively considered as signals of night and day (McMahon et al., 2014; Tosini et al., 2014). They are mutual antagonists, inhibiting each other. As melatonin production is acutely suppressed by dopamine during the light phase and melatonin quickly cleared away from circulation, the time and duration of the melatonin peak accurately reflect the environmental night period (Cardinali and Pévet, 1998; Tosini et al., 2012).

The synthesis and utilization of dopamine follow a diurnal cycle, but most studies have failed to show an actual circadian dopamine rhythm (Melamed et al., 1984; Wirz-Justice et al., 1984; Nir et al., 2000; Pozdeyev and Lavrikova, 2000). This might be because it is dependent on melatonin, so that in constant darkness melatonin drives the dopamine rhythms (Doyle et al., 2002; Ribelayga et al., 2004). Both hormones have diverse effects on retinal function.

Multiple aspects of retinal physiology and morphology are under the control of the endogenous retinal clock (reviewed in e.g. Tosini et al., 2014; Ko, 2018). Among the first discovered, was the rod outer segment disc shedding, which is a continuous process but the rate is circadian, with bursts occurring at dawn (LaVail, 1976; LaVail, 1980; Grace et al., 1996). In amphibians and teleost fish, contraction or elongation of photoreceptor inner segments (known as retinomotor movements) are controlled by ambient illumination as well as the circadian cycle (Burnside and Ackland, 1984; Dearry and Barlow, 1987; McCormack and McDonnell, 1994). Also, the strength of electrical coupling between rods and cones is higher during the night and low in daylight due to the effect of light or circadian release of dopamine, while the amplitude of single-photon response is reduced at night (Ribelayga et al., 2008; Jin et al., 2015; Jin et al., 2020). Other circadian rhythms found in retina include, for example, opsin expression (Pierce et al., 1993; von Schantz et al., 1999; Dalal et al., 2003), the affinity of CNGCs to cGMP (Ko et al., 2001), synaptic ribbon number and ultrastructure (Adly et al., 1999).

Electroretinography (ERG) is a noninvasive, widely used method to record changes in the field potential across the eye. Diurnal or circadian rhythms in the ERG waveform have been shown in many species, usually involving a larger b-wave amplitude at night in photopic (but not scotopic) ERG (humans: e.g. Birch et al., 1984; Hankins et al., 1998; Lavoie et al., 2010; mice: e.g. Barnard et al., 2006; Cameron et al., 2008; Baba et al., 2009; Cameron and Lucas, 2009; Sengupta et al., 2011; birds: Manglapus et al., 1999; Peters and Cassone, 2005; lizards: Shaw et al., 1993; Miranda-Anaya et al., 2002; fish: Dearry and Barlow, 1987; Li and Dowling, 2000; amphibians: Wiechmann et al., 2003). Many studies have linked the rhythm to melatonin, dopamine or both (e.g. Wiechmann et al., 2003; Baba et al., 2009; Lavoie et al., 2010; Sengupta et al., 2011). The circadian rhythmicity in the ERG likely depends on the intrinsic retinal clock as shown first in a study where one eye of a rabbit was sutured to occlude light input (White and Hock, 1992). The decrease in ERG amplitude happened in the unpatched eye always ~30 min after subjective dawn, but in the sutured eye this amplitude drop occurred earlier and earlier as the days progressed, corresponding to the free-running circadian rhythm. Furthermore, the circadian rhythmicity in the photopic ERG is lost in retina-specific *Bmal1* knock-out mice (Storch et al., 2007), further supporting the view that retinal clocks are the timekeepers of the retina. Only the cone-isolated photopic ERG has markedly larger responses at

night, and the dark-adapted ERG has circadian rhythm only at flash intensities high enough to stimulate also cones (e.g. Barnard et al., 2006; Cameron et al., 2008; Sengupta et al., 2011). However, ERG cannot reveal changes in the pattern of action potentials generated by RGCs, which transmit the signals to the brain. Thus, even though circadian changes in the photoreceptor or outer retinal level are established, it is unclear to what extent they translate to functional effects in the image-forming vision on the level of retinal computations, and ultimately, behavior.

Circadian or diurnal studies of the RGC responses or visually guided behavior have remained scarce. Recently, Hong et al. (2018) measured the mouse single RGC responses *in vivo* using a chronical retinal implant. They found circadian modulation in the firing rates of the directionally selective ganglion cells at mesopic light levels, with a firing rate during the day phase on average 77% higher than during the night phase. Also the rat M4 type of the ipRGCs (also known as the ON-sustained alpha RGCs in mice) has higher firing rates during the day (Pack et al., 2015). Psychophysical studies on humans have shown a slightly increased sensitivity to dim light stimuli at night (Bassi and Powers, 1986) and diurnal variation in the scotopic and mesopic luminance sensitivities (O'Keefe and Baker, 1987; Tassi et al., 2000). In mice, Balkema et al. (2001) reported the highest sensitivity in the early morning, 2 hours after light onset, in a decrement detection task under background light.

3 AIMS

A fundamental challenge for vision, as for all senses, lies in separating the weakest signals from the neural noise originating within the sensory system. In this thesis, I study signal/noise discrimination at several levels of the visual system, from single retinal cells to behavioural performance. The general aim was to measure the limits of scotopic visual performance in two vertebrate model species (frog and mouse) and analyze the physical, physiological and behavioral factors affecting the limits.

In Paper I, the aim was to determine the sensitivity limit of amphibian color vision at scotopic light levels in three different behaviors. The specific questions were:

1. Does the dual rod system of the amphibian retina support color discrimination at scotopic light levels?
2. What is the absolute behavioral threshold of color discrimination in the common frog? How close is it to theoretical limits set by rates of photoisomerizations and thermal noise in the two spectrally different rod types?
3. How does the use of color information in frogs and toads differ between behavioral tasks?

Paper II studies the dependence of the absolute visual sensitivity on the circadian rhythm in mice, especially against the background of known circadian rhythms in the retina. The specific questions in this paper were:

4. Does the sensitivity limit of visually guided behavior in a light detection task change between day and night?
5. Do the responses of the most sensitive retinal outputs change between day and night?
6. Which neural mechanisms underlie changes in performance between day and night?

Paper III studies the absolute limits of decrement detection in mice. The ultimate limit for detecting the weakest light increments has been discussed and studied for decades, with recent important insights regarding the limiting mechanisms in mice (Smeds et al., 2019; paper II of this thesis). An equally fascinating question, much less studied but of equal importance for visual performance, is the sensitivity limit for detecting the weakest light decrements. The specific questions of Paper III were:

7. What is the absolute threshold of decrement detection in mice as measured by a visually guided behavior?
8. What is the absolute threshold of decrement detection by the most sensitive ON and OFF retinal ganglion cells in the mouse retina?
9. What neural mechanisms allow and limit decrement detection from the retina to behavior?

4 MATERIALS AND METHODS

4.1 ANIMALS AND HOUSING CONDITIONS

4.1.1 FROGS AND TOADS (I)

The breeding couples of Asiatic toads *Bufo gargarizans* used for the behavioral mate choice experiments in Paper I were collected at Popov Island (Peter the Great Bay, Sea of Japan) during their migration to the breeding pond. Only males (n = 10) were used for the experiments that lasted 9 days. The animals were kept in a dark room at 5–8 °C in plastic vessels with wet soil, each housing one breeding pair. For the experiments the animals were transferred to another vessel with small amount of water and adapted for 1h at 20–22 °C and luminance 2–9 cd m^{-2}.

For the prey-catching experiments common toads (*Bufo bufo*, n = 5) and common frogs (*Rana temporaria,* n = 3) were collected at Lund University's biological station in Skåne, Sweden. The animals were kept in glass terraria at 20 °C under 12 h/12h light/dark photoperiod with access to water. They were fed crickets and mealworms three times a week.

The *Rana temporaria* used for the phototaxis experiments were captured in April in the wild in southern Finland with the permission of the Centre of Uusimaa for Economic Development, Transport and the Environment (ELY-Center). The animal experiments were approved by the Animal Ethics Committee of the Regional State Administrative Agency of Southern Finland. The frogs (7 females and 10 males) were kept in basins at 16 °C under 12 h/12h light/dark photoperiod with access to water. The basins were covered for the frogs to receive only dim light. They were force-fed with chicken liver and fish food every day after experiments. The testing was done during the light period but the animals were always dark adapted for at least 2 hours before the testing. The testing room temperature was kept constant at 18 °C.

4.1.2 MICE (II, III)

Mice (C57BL/6J; Charles River Laboratories, Sulzfeld, Germany and CBA/CaJ; Jackson Laboratory, Bar Harbor, ME, USA) used in Papers II and III were housed in 12 h/12h light/dark cycle with free access to water and food. The mice for Paper II were kept in two rooms with different light/dark cycles: lights were on from 06:00 to 18:00 in the room designed for the "day group" and from 20:00 to 08:00 in the room designed for the "night group'. The lighting of both rooms was monitored with a data-logging lux meter (model HHLM112SD, Omega Engineering Inc). The animals were always acclimated to their respective light cycles at least for 20 days. All animal procedures were

performed according to the protocols approved by the Regional State Administration Agency of for Southern Finland. Details of the sample sizes and sexes of the used animals can be found in Papers II and III.

4.2 BEHAVIORAL METHODS

4.2.1 BEHAVIORAL EXPERIMENTS ON ANURANS (I)

To determine the lowest light levels where anurans can discriminate colors, we used three different behavioral experiments described briefly below. The further details for each experiment can be found in Paper I and its supplementary material.

Mate choice experiments Breeding males of the genus *Bufo* show characteristic sexual behavior even in the laboratory conditions during the mating season. Exploiting this behavior in the mate choice experiments, male toads were presented a female model with differential spectral compositions under different illumination conditions. The experiments were designed to differentially stimulate the color channels of the amphibian retina (blue, green and red), where the spectral characteristics of the three channels are assumed to be like the visual pigments of, respectively, the blue-sensitive rods or cones, the rhodopsin rods, and the red-sensitive cones, with no commitment to the exact photoreceptor type underlying the responses. The goal was to determine at which light intensities the differential stimulation of the different channels stops contributing to mate choice. The female models consisted of stationary paper discs printed in selected colors, and the male toad had to choose between two differentially colored models. An animal was considered to have made a choice when it approached one of the stimuli and grasped it with its forelegs. The pairing of the stimuli was done based on different computed excitation rates for each of the color channels and the stimuli were grouped into three different groups based on relative excitation rates for the red and blue channels. The experimental arena was a rectangle with 20 cm high walls covered with white paper. The diffuse illumination was provided by the light of a stabilized halogen source (24 v, 150 W) that reflected from a screen covered with white filter paper (Whatman). Neutral density glass filters (GOST USSR (State-standard) 9411-75) were added in front of the light source to achieve different illumination levels. The motivation of the toads faded at light intensities several orders of magnitude higher than the absolute visual threshold, and the lowest intensities (0.1 cd/m^2 or 80 000 R*/rod/s) were still above cone thresholds (Orlov and Maximov, 1982).

Prey-catching experiments The prey-catching experiments were based on the visual motion detection of anurans when they hunt prey. A set of green and blue stimulus pairs were designed to control especially for brightness cues, meaning that the same stimuli were used for achromatic brightness comparison as well. Brightness was calculated as the quantum catches provided by each colored stimulus to different photoreceptors, with several combinations that covered all the possible brightness relationships for each of them. The prey dummies were printed in each stimulus color for a two-choice experiments. The arena was a Y-maze with one of the stimuli of a pair in each arm. Live mealworms were used as rewards and placed in hidden compartments underneath each of the stimuli. A fluorescent tube (Phillips Master TL5 HO 90 De Luxe 24 W/950) provided the illumination with neutral density filters (Lee filters, Hampshire, UK) used to achieve the different luminance levels. In each trial, both of the stimuli were simultaneously moved back and forth for ca. 3 cm to elicit the prey-hunting behavior. Pilot experiments showed that the animals had an innate preference for green stimuli, so choosing the "greener" stimulus was subsequently regarded as a "correct" choice. Thus, snapping at the green stimulus earned the animal a mealworm reward, while choosing the blue stimulus was not rewarded. Both frogs and toads were initially used in these experiments.

Phototaxis experiments A frog placed in a dark, closed container will interpret an illuminated area in the ceiling as an opening through which to escape and will jump towards it (Muntz, 1963; Aho et al., 1987; Aho et al., 1993b). This innate escape response was utilized in the phototaxis experiments that were especially designed to compare the sensitivity of the blue-sensitive and green-sensitive rods. Frogs have been reported to prefer the blue end of the spectrum in this task, enabling us to design a green vs. blue two-choice phototaxis experiment (Muntz, 1962a; Hailman and Jaeger, 1974). The testing chamber consisted of a bucket with four pairs of infrared emitter-detector pairs that recorded the jumps to four quadrants of the test chamber. Two lit windows (7cm diam.), one green and one blue, served as stimuli in diagonally opposite quadrants of the test chamber ceiling. The remaining two quadrants had "dark windows" meaning that they were not open. The colored stimuli were produced with Kodak Wratten 2 optical filters (no. 98, blue and no. 8, green; Eastman Kodak Company, USA). The relative transmittances of the two stimulus windows were adjusted so that both windows stimulated the green-sensitive rods equally, and the only difference should be that the blue window additionally stimulated the blue-sensitive rods. The photoisomerization rates from the blue window were slightly higher (ca. 30%) for the blue-sensitive rods than for the green-sensitive rods while the excitation from green window for the blue-sensitive rods was 20-fold lower. Thus, both windows stimulated the green-sensitive rods in equal amounts while only the blue window stimulated the blue-sensitive rods so that the only differential information comes through the blue-sensitive rods. The complete

testing arena had four identical test chambers, with one frog in each, placed in a square array and lit from above homogenously by a common light source (30 W halogen lamp driven by a stabilized current source). Neutral density filters were used to set the absolute illumination levels, like in the other two behavioral experiments.

4.2.2 BEHAVIORAL EXPERIMENTS ON MICE (II, III)

4.2.2.1 Black water maze (II)

As described in Paper II, the absolute visual thresholds of mice were assessed in a dim-spot detection task in a black six-armed water maze in darkness (see also Smeds et al., 2019). The mice were trained prior the testing to associate an escape ramp located in one of the six arms with a light spot. The training was done in dim ambient illumination using an easily detectable stimulus light intensity (ca. 200 000 R*/rod/s). The choice was defined as correct if the mouse entered the stimulus corridor before entering any other corridor. Once the mice reached a ca. 80% correct choice rate in the task, the testing began. In the testing, the stimulus intensity was gradually lowered until the mice could not locate it anymore. The testing was done in darkness using night-vision goggles (PVS- 7-1600, B.E. Meyers). The mice were always dark-adapted for at least 2 hours before the testing. The body and head positions of the mouse were monitored during the behavioral trials under IR illumination using a sensitive CCD camera (WAT- 902H2 ultimate, Watec; equipped with a 12VM412ASIR lens, Tamron) and an automated tracking system (Smeds et al., 2019). All experiments were recorded using an open-source video capture software.

The stimuli consisted of a circular plexi-diffusor window (40 mm diam.) located at the end of each corridor. The location of the stimulus light was pseudorandom across trials. The stimulus window was continuously illuminated by a green LED (peak at 515 nm) and narrow-band filtered with a 512-nm interference filter (~10-nm transmission bandwidth) during each experimental trial. The light intensity was set by neutral density filters and by controlling the current driving the LEDs. Light intensities were calibrated with an optometer (Models S470 & S450 with 268R sensor, UDT Instruments) at the level of the mouse cornea at the center of the maze. The spectral irradiances of stimuli were measured with a spectrometer (Jaz spectrometer, Ocean Optics).

4.2.2.2 Diurnal comparison (II)

To compare the behavioral absolute visual sensitivity of the mice between day and night, the mice (21 C57BL/6Jand 20 CBA/CaJ) were divided into two groups: one group was tested at their subjective day ("day group", at 3 hours from light onset, ZT3) and the other group at their subjective night ("night group", 3 hours from light offset ZT15). The CBA/CaJ mice were additionally tested at the time of their melatonin peak (ZT21, (Nakahara et al., 2003)). All mice were acclimated to their respective diurnal rhythms, and the adjustment was confirmed by monitoring running-wheel activity in their housing conditions. More details are provided in the Paper II.

4.2.2.3 Analysis of behavioral search strategy (II)

We estimated the behavioral strategy of the mice in the water maze task at day and night as described in Paper II. The mouse head- and body position as well as the head-direction in each frame was obtained using the automated video-tracking software. These were used to derive a set of quantitative features of the mouse behavior, for example: the length of the swimming path during each trial, the swimming speed, the angular velocity and how many times or how long the correct corridor was in the visual field of the mouse. The complete set of the features and their explanations are explained in Paper II.

To exclude the time after the moment when the mouse had detected the stimulus and was merely swimming towards it, we focused the analysis on the early part of each trial where the mouse was at the center of the maze looking for the stimulus. In this constrained area (corresponding to 50% of the area excluding corridors), we defined a choice as the mouse exiting the center region toward any corridor. The analysis was done in the intensity range corresponding to the greatest day–night difference in the fraction of correct choices for the C57BL/6J mice: 0.03–0.14 R*/rod/s. In all of the analyses, we assumed ± 100° field of view centered on the nose.

4.2.2.4 White water maze (III)

In Paper III we used a homogenously lit, white six-armed water maze to determine the behavioral limit of detecting light decrements in low background light levels. Mice were first trained to associate a visual stimulus with an escape ramp away from the water in bright illumination (ca. 70 000 R*/rod/s). The stimulus was a non-reflecting black spot (4 cm in diam., Weber contrast -97 % to -98%) mounted to a movable, white polyethene wall. The location of the stimulus wall was randomized across trials. Once the mice were performing the task of locating the stimulus corridor as their first choice 80% of the time, the testing began. In the testing the illumination was lowered until the mice could not locate the stimulus except randomly. The experiments were

monitored using IR light and a sensitive CCD camera (ACA1920-50gm, Basler).

At the end of the experimental series, the mice were re-tested at a high intensity to make sure that no significant changes had happened in their overall ability to perform the task (i.e. that the fraction of correct choices ≥ 80% of the trials at this high intensity). The mice were always dark adapted for a minimum of 2 hours before the experiments.

The maze was made of white polyethene and illuminated by an LED (peak at 515 nm) connected to a lens tube containing an interference filter (λ_{max} ~510 nm, FWHM ~10 nm), and neutral density filters (Thorlabs). The branches of a trifurcating fiber (Newport) originating at the end of the lens tube were placed symmetrically at 120-degree separation around the maze, and directed to project off a photographic reflector above the maze to yield uniform illumination. The maze was surrounded by white satin curtains. Convex lenses (N-BK7 plano-convex, Thorlabs) were attached to the three fiber ends to maximize the uniform illumination. The uniformity was tested regularly and was within 10% of the mean light level. Light intensity was set by neutral density filters and by controlling the current driving the LED. Background light intensity was measured horizontally at the level of the mouse cornea at the center of the maze with an optometer (UDT Instruments, Model S450) and the spectral irradiances of stimuli were measured with a spectrometer (Jaz spectrometer, Ocean Optics). The photoisomerization rates were then calculated based on the projection size of the dark stimulus spot on the retina and taking into account the pupil size of mice at each background intensity.

4.3 ELECTROPHYSIOLOGICAL EXPERIMENTS (II, III)

4.3.1 DIM LIGHT IN DARKNESS (II)

In Paper II we measured the sensitivity of retinal ganglion cells to dim light stimuli presented in darkness using flat mount preparations of mouse (CBA/CaJ and C57BL/6J) retina. The purpose was to investigate whether sensitivity would be different depending on the phase of the circadian cycle (day/night) when the retina was prepared and the experiment was conducted. The detailed description of the method can be found in the Paper II and in Smeds et al., 2019. The experiment timings were matched to the day/night testing times of the behavioral experiments, taking into account the previously reported melatonin synthesis cycle (Nakahara et al., 2003).

The mice were dark adapted for two hours before they were sacrificed by cervical dislocation. All procedures were done under IR light (>900 nm). The piece of retina was flattened on a poly-D-lysine-coated glass coverslip with the photoreceptor layer down and placed on a microscope. The preparation was perfused with oxygenated Ames medium (flow rate: ~8 ml/min) at 32 ± 1 °C. Spikes were recorded in cell-attached patch clamp configuration (loose patch).

The ON sustained, OFF sustained and OFF transient alpha cells were identified based on their large soma size and characteristic responses to light steps from darkness. The sensitivity of the cells was estimated by measuring their spiking activity in response to brief, spatially uniform flashes (20 ms, circular spot, diam. ~580 nm) of light from a blue LED (peak at 470 nm).

4.3.2 DECREMENTS (III)

In Paper III we recorded the sensitivity of retinal ON and OFF sustained alpha retinal ganglion cells to light decrements at dim background levels. The retinal flat mount preparation, spike recording and alpha ganglion cell identification were done as for the increment experiments in Paper II. The uniform background size was created with a DLP projector (912 x 1140 pixels; 1.8 µm/pixel on the retinal surface; 60 Hz frame rate; blue LED spectral peak ~450 nm; Texas Instruments, LightCrafter 4500). The decrement stimulus spots (circular, 0100 % contrast) from a background (square, 1000 x 1000 µm) were centered on the target cell's receptive field. Spots of various sizes (170–600 µm) and durations of the decrement (17–500 ms) were used to map the spatial and temporal characteristics of decrement sensitivity.

4.4 LIGHT CALIBRATIONS (I, II, III)

4.4.1 LIGHT MEASUREMENTS

The spectrum of the light source in each experimental setup was measured with a spectrometer (Jaz spectrometer, Ocean optics). The light intensities were calibrated with an optometer (Models S470 & S450 with 268R sensor, UDT Instruments), in the phototaxis experiments at the bottom of each testing chamber (Paper I) and in the water maze experiments at the center of the maze (Paper II, III).

In the behavioral decrement detection task in Paper III (4.2.2.4), the conversion to isomerizations rates per rod (R*/rod/s) required the amount of reflected light per wall area of the maze to be quantified. We did this by repeating the optometer measurements, as above, with and without the near-perfectly dark stimulus located at the back of the maze arm. The difference measured in this was very small, we therefore 3D-printed a cone that was mounted on top of the sensor to restrict the collecting angle, and thus make the relative difference larger. The difference was then taken to represent the amount of light reaching the same area as the stimulus on the retina.

Furthermore, it was crucial that the arena would be as homogeneously illuminated as possible. We measured the homogeneity several times during the experiment in the white water maze by placing a photodiode in the middle of the maze and measuring the reflected illumination from each wall. The

Weber contrast of the black stimulus was measured with a luminance meter (Konica Minolta LS-110).

4.4.2 PHOTOISOMERIZATION CALCULATIONS

The reported light intensities are expressed as rates of photoisomerizations per rod or per rod per second in all of the papers and they follow previously described procedures (Aho et al., 1993a; Naarendorp et al., 2010; Smeds et al., 2019). Here the principles are briefly summarized for easy reference and comparison between the original studies. The parameters used in Papers I-III are summarized in Table 1.

Behavioral measurements The power (in watts) of each light source was measured at the level of the cornea. The power measurements were converted into corneal photon flux densities for the stimulus light wavelength (measured with a spectrometer) as follows. Energy per photon E (joule photon^{-1}) can be calculated from equation (2) (chapter 2.1.1.1). Next, the flux of photons produced by the stimulus (s^{-1}) is determined by dividing the measured power of the stimulus (P, J s^{-1}) with the energy of photons:

$$\phi(\lambda) = \frac{P(\lambda)}{E(\lambda)} \tag{6}$$

The stimulus power P was measured in the water maze experiments at the center of the maze and in the phototaxis experiments at the bottom of each testing chamber (bucket). The corneal photon flux (ϕ) was further expressed as photon flux density $F_{\mathrm{cornea}}(\lambda)$ (photons μm^{-2} s^{-1}) by dividing it with the active area of the radiometric sensor (1 cm^2 in our case). To convert the F_{cornea} into the photon flux density at the level of the retina, we needed to estimate the pupil area (A_{pupil}) in each experimental condition, the size of the projected stimulus spot on the retinal surface (A_{retina}) and optical loss factors in the animal's eye. The pupil measurements are described below in section 4.4.3. For the A_{retina} in the mouse experiments we assumed that the mouse is looking at the stimulus in the middle of the maze, and computed the visual angle (θ, in degrees) from:

$$\theta = 2\left[\tan^{-1}\frac{r_{stimulus}}{D}\right] \tag{7}$$

where $r_{stimulus}$ is the radius of the stimulus window (20 mm) and D is the distance from the stimulus window to mouse eye (390 mm). We then approximated the mouse retina as a hemisphere with radius (r_{retina}) 1.7 mm and with the center corresponding to the posterior nodal point of the eye optics (Remtulla and Hallett, 1985; Lyubarsky et al., 2004). Thus, the diameter of projected stimulus spot on the retina ($d_{projection}$) can be calculated from:

$$d_{projection} = \frac{\theta}{180}\,\pi\, r_{retina} \qquad (8)$$

In the frog phototaxis experiments we instead used the posterior focal length (L) scaled down from the *Rana esculenta* model eye of Du Pont and De Groot (1976), when computing the $d_{projection,}$ as in Aho et al., 1987:

$$d_{projection} = \frac{L}{D}\ d_{stimulus} \qquad (9)$$

where D is the distance from the stimulus window to the frog's eye (260 mm) and $d_{stimulus}$ is the diameter of the stimulus window (70 mm). The posterior focal length, L, was estimated as by Aho et al., 1987 to be 4.5 mm. In both experiments, the area of the projection ($A_{projection}$) is calculated from:

$$A_{projection} = \pi\left(\frac{d_{projection}}{2}\right)^2 \qquad (10)$$

For the water maze experiments the numerical values were $d_{projection}$ = 0.17 mm and $A_{projection}$ = 0.0227 mm², and for the phototaxis experiments $d_{projection}$ = 1.21 mm and $A_{projection}$ = 1.13 mm².

The total photon flux density of the retinal image (F_{retina}, photons µm^{-2} s^{-1}) is then:

$$F_{retina}(\lambda) = \frac{F_{cornea}(\lambda)A_{pupil}}{A_{projection}}\tau_{media}(\lambda)\tau_{cornea}(\lambda) \qquad (11)$$

where $\tau_{media}(\lambda)$ is the light transmittance of the ocular media, $\tau_{cornea}(\lambda)$ the light transmittance through cornea and A_{pupil} the pupil area (see table 1 and 2). In the water maze experiments the rate of photoisomerizations per rod was estimated by multiplying F_{retina} by the collecting area for a rod at its peak wavelength (A_c) and by the relative absorption factor for mouse rod rhodopsin at the stimulus wavelengths 512 nm ($R_{\lambda max} = R_{512nm}$). Thus, light intensity (I, R*/rod/s) was calculated as:

$$I = \frac{F_{cornea}(\lambda)A_{pupil}}{A_{retina}}\tau_{media}(\lambda)\tau_{cornea}(\lambda)A_c(\lambda)R_{\lambda_{max}} \qquad (12)$$

The R_{512nm} was estimated to be 0.93 on the Govardovskii template (Govardovskii et al. 2000) when assuming the wavelength of maximum absorbance for mouse rhodopsin, λ_{max} = 497 nm (Toda et al. 1999). In papers II and III we used the collecting area for mouse rods of 0.63 µm² (Smeds et al., 2019, see below).

The stimulus light in the frog phototaxis experiment was not monochromatic as in the water maze, and thus we integrated over the absorptance spectrum calculated for frog rods with absorbance λ_{max} = 503 nm (Govardovskii et al., 2000). The absorptance spectrum was calculated from

the absorbance spectrum by the "self-screening" (expression from Koskelainen et al., 1994):

$$\alpha_{\lambda_{\max}} = \frac{1 - 10^{-OD\frac{A(\lambda)}{A(\lambda_{\max})}}}{1 - 10^{-OD}} \quad (13)$$

where *OD* is the rod optical density at peak wavelength (0.5 for *Rana temporaria*, Reuter, 1969) and $A(\lambda)$ is the absorbance spectrum from the Govardovskii et al. (2000) template normalized to 1 at λ_{max}. Instead of the collecting area of single rods, in the Paper I we based our calculations on the mean optical density of an isolated frog retina (OD_{retina}, 0.344 at λ_{max} = 503 nm, Donner et al. 1995) which gives the estimate of how many incident photons are absorbed. The estimate of the total number of photoisomerizations on the projected stimulus spot area in the frog retina for the green-sensitive rods ($I_{gs,total}$) is thus:

$$I_{GS,total} = F_{retina} * \alpha_{503nm} * (1 - 10^{-OD_{retina}}) * \gamma \quad (14)$$

This means that 55% of the photons of the peak wavelength are absorbed and given the quantum efficiency of photoactivation 0.66 (γ, Dartnall, 1968), 36% of these photons will cause a photoisomerization. This can be further expressed as R*/rod/s when divided with rod density (15 700 per mm², Hemilä and Reuter, 1981). As the OS length of the BS rods is 75% of that of the GS rods, their absorption is 87 % of the GS rod absorption ($\frac{1-10^{-0.016*32\mu m}}{1-10^{-0.016*43\mu m}} = 0.87$). The density of BS rods is 14% of the GS rod density (an average from Table 1 in Donner and Reuter, 1976).

Estimation of collecting area The collecting area is a construct devised to transform incident photon flux into numbers of isomerizations by multiplication with a constant having the unit of an area. It depends on several factors, such as the rhodopsin concentration in the rod outer segment, the absorption cross-section of an individual rhodopsin molecule, the outer segment diameter and length, and the probability that an absorbed photon isomerizes the rhodopsin (Rieke 2000). It also depends on the stimulus geometry but is a useful measure for a standard preparation. For axial stimulation, it can be estimated from the actual aperture of a rod while taking into account all factors that affect the effective light capturing properties (Cornwall et al., 2000; Lyubarsky et al., 2004; Naarendorp et al., 2010):

$$A_c = \pi \left(\frac{d_{rod}}{2}\right)^2 (1 - 10^{-\varepsilon * L_{rod}})\gamma \quad (15)$$

where d_{rod} and L_{rod} are the diameter and length of the rod outer segment, respectively, ε is the optical density per unit distance (0.0156/µm, Donner et al. 1990), and γ is the quantum efficiency of photoactivation (0.66, Dartnall, 1968).

The collecting area can be alternatively estimated directly from series of dim-flash responses, making use of the fact that for Poisson-distributed events the expected value of the variance is equal to the mean (as in Smeds et al., 2019). This method gives completely independent estimates of numbers of photoisomerizations produced by a flash of constant nominal intensity, which is also valuable for cross-checking with estimates based on photometry and cell properties. Thus, when repeating flashes producing on average $\overline{n}$ photoisomerizations, the variance in the number of photoisomerizations is equal to the mean $\overline{n}$. The single-photon response *r(t)* is unknown, but the measured ensemble response to repeated flashes is $\overline{R}(t) = \overline{n} \times r(t)$. Assuming that the variability in the responses is solely due to Poisson variability, the variance of the ensemble response is $\sigma^2 = \overline{n} \times r(t)^2$. By measuring the mean flash response $\overline{R}(t)$ and the ensemble variance of the flash response σ^2, the mean number of photoisomerization per flash can be estimated from $\overline{n} = \frac{\overline{R}(t)^2}{\sigma^2}$. The collecting area is then obtained by dividing the mean photoisomerization number $\overline{n}$ (R*/flash) by the mean number of photons (photons/μm²/flash) in the flash. This method was not directly used in this thesis, but paper II and III refer to the collecting area values obtained with this method in (Smeds et al., 2019).

Electrophysiological experiments The stimulus intensities in the electrophysiological experiments are given as photoisomerizations per rod (R*/rod). The calculation was otherwise the same as for water maze behavioral experiments, but in this case eye optics did not need to be considered.

Table 1. *Parameters used in the photoisomerization calculations for mouse and frog. GS = green-sensitive, BS = blue-sensitive.*

PARAMETER	MOUSE	FROG	REFERENCES
$\lambda_{max,}$ Peak absorbance wavelength	497 nm[a]	GS rods: 503 nm[b] BS rods: 434 nm[b]	[a]Toda et al., 1999 [b]Govardovskii et al., 2000
$\tau_{media,}$ Transmittance of ocular media	0.55[a]	1[b]	[a]Henriksson et al., 2010 [b]Govardovskii and Zueva, 1974
$\tau_{cornea,}$ Corneal transmittance	(Included in τ_{media})	0.91	Aho et al., 1987
L, Posterior focal length	-	4.48 mm	Aho et al., 1987
d_{rod}, Rod OS diameter	1.4 µm[a]	GS rods: 6.4 µm[b] BS rods: 6.4 µm[b]	[a]Carter-Dawson and LaVail, 1979 [b]Hemilä and Reuter, 1981
L_{rod}, Rod OS length	24 µm[a]	GS rods: 43 µm[b] BS rods: 32 µm[c]	[a]Carter-Dawson and LaVail, 1979 [b]Hemilä and Reuter, 1981 [c]75% of the GS rod, Nilsson, 1964
OD_{retina}, Optical density of retina at λ_{max} = 503 nm	-	0.344	Donner et al., 1995
A_c, Collecting area	0.63 µm^2 [a]	16.8 µm^2 [b]	[a]Smeds et al., 2019 [b]calculated Eqn. 15

4.4.3 PUPIL MEASUREMENTS

The pupil sizes of dark-adapted mice were determined in conditions corresponding to the behavioral experiments in darkness (Paper II) and in background light (Paper III). The IR LEDs of the experimental setup were turned on to allow the mouse pupils to be visualized. The mouse was held by its tail in the dry water maze and monitored with and IR-sensitive camera. The pupil areas were measured from single frames of the videos by tracking the border of the pupil in each frame.

Paper I used values reported in the literature for the frog and toad pupil sizes. Table 2 summarizes the pupil area values used in Papers I-III.

Table 2. *Table 2. Pupil areas (mean ± SEM) for mouse and frog in different experiment conditions.*

MEASUREMENT	CBA	C57	FROG	REFERENCE
Night: dark adapted	4.9 ± 0.1 mm^2	5.6 ± 0.1 mm^2	-	Paper II
Day: dark adapted	4.6 ± 0.1 mm^2[a]	5.1 ± 0.1 mm^2[a]	10 mm^2[b]	[a]Paper II [b]Aho et al. 1993
Dark-adapted (reference for measurement in background light)	6.4 ± 0.1 mm^2	-	-	Paper III
In background light (ca. 1100 photons/s/μm^2)	5.9 ± 0.2 mm^2	-	-	Paper III

5 RESULTS AND DISCUSSION

5.1 FROGS CAN DISCRIMINATE COLORS DOWN TO THE ABSOLUTE VISUAL THRESHOLD (I)

We found that the common frog is capable of color discrimination at light levels corresponding to their absolute light detection threshold, i.e. the frog can discriminate colors as soon as they start to see anything at all. Moreover, for detection of a persisting light target in darkness, the absolute threshold of humans is one log unit higher than the detection threshold of frogs and toads (Aho et al. 1988). At these light levels, the cone photoreceptors are not sensitive enough to respond and thus the frog color vision at low light levels depends on the two spectrally different types of rod photoreceptors. Calculations of SNR at the absolute threshold suggest that performance is close to an absolute physical limit set by the low rates of photoisomerizations. Even an upper-limit estimate of SNR, neglecting all intrinsic noise, is so low that the result owes its statistical significance to the very large number of jumps ("trials") in this type of experiments. This extremely sensitive wavelength discrimination was observed only in the phototaxis experiments. Intriguingly, when the overall light level decreased to scotopic intensities, the phototactic preference for blue reversed and the frogs started to prefer the green window instead, what prevails at higher light levels and is universally reported in the amphibian literature. Even more remarkably, the phototactic response to blue at the lowest intensities was aversive, such that frogs jumped less towards the blue window than the dark windows. One might speculate this could reflect the fact that blue-ON responses to very dim light are mediated by large-field, surround-type responses from pure OFF-center (class 4 cells, "dimming detectors"), maybe interpreted as "darker-than-dark" (Keating and Gaze, 1970; Donner and Grönholm, 1984).

Furthermore, it is surprising that the system performs color discrimination at the same light intensities where it starts detecting any light at all. As discussed in the Literature Review, dividing the photon catch into smaller packages that are subsequently compared, be it in the chromatic, spatial or temporal dimension, must in principle infringe on absolute light sensitivity (a trade-off that can be avoided only by investing in a parallel neural pathway summing all photons). This might not be mechanistically so enigmatic, when considering how highly nonlinear frog RGCs are (Donner et al. 1990, Donner & Yovanovich 2020): Their high threshold, while removing much of the noise, sacrifices some of the signal near the physical limit of photon detection. Thus, it is possible that there is already more photons available for the wavelength discrimination task at the light intensities where the system starts detecting any light. Speculation aside, our result highlights that wavelength

discrimination can be ecologically more important than just detecting as few photons as possible.

The color discrimination thresholds in the other two behavioral experiments did not reach low enough light levels to allow any conclusions about rod involvement. In the mate choice experiments, toads were presented with two female dummies between which they had to choose in different background light intensities. The goal was to determine at which light intensities the differential excitation rates of the color channels stops contributing to mate choice, without targeting the exact photoreceptor type underlying the responses. As described before, the male toads (*Bufo gargarizans*) preferred to approach female dummies that generated a stronger signal in the blue channel than in the red channel. We found that this was true even at previously untested lower light intensities. However, the motivation of the males to respond to the female dummy stopped several orders of magnitudes above the absolute visual threshold (threshold was ca. 0.3 cd m^{-2} or 8000 R*/rod/s). Thus, there was no indication of rod-based color vision. Interestingly, however, the "blue" color channel supported color discrimination down to lower light levels than the "red" color channel, consistent with the lower thermal noise in SWS compared with LWS cones. In the prey-catching behavior, we found that frogs used only brightness cues to make discriminations on the prey items, choosing always the darkest of the two prey items, and did not use the color information. The toads instead did utilize color information for the discrimination task but their threshold was at roughly 200 R*/rod/s (or 0.0004 cd m^{-2}), well above cone thresholds, although several log units lower than in the mate-choice. As the thresholds of toads were different in the mate-choice and prey-catching tasks, it suggests that the two behaviors are probably displayed at different illumination conditions.

A concluding remark when comparing the three behavioral experiments is that sensory thresholds can be context and task dependent, and tell more about the biological use of information for the specific behavioral response than about physical limits.

5.2 MICE AT NIGHT USE A MORE EFFICIENT SEARCH STRATEGY IN A LIGHT DETECTION TASK (II)

We found that mice have a significantly – more than 10-fold – higher behavioral performance level in a light detection task at night than at day. The difference between the day and night group performance was robust, and exemplified in the shape of their psychometric curves. However, contrary to previous hypotheses, the input from the retina to the brain, measured from the most sensitive mouse retinal ganglion cell types, did not differ between day and night. Instead we found that the mice utilized a more efficient behavioural strategy at night. This was exemplified by how the mice at night were sampling the visual cues a longer time and spent more time in the middle of the maze before making a decision. A surprising finding was that the night mice were able to maintain their higher performance level when tested subsequently during their day. This result is hard to explain even by the novel *in vivo* discoveries of the retinal output being modulated by arousal, since it would require a new kind of plasticity/learning on retinal level (Liang et al., 2020; Schröder et al., 2020). Hence, this kind of behavioral history-dependence supports the conclusion that a central rather than a retinal mechanism is in play.

The improvement in behavioral performance expected from more extensive sampling of the environment was computed based on a quantitative model mapping signals from the retinal projection of the stimulus window the ON-S RGC population code and ultimately to behavior (Smeds et al., 2019). While predicting part of the observed effect, the model failed to predict the entire behavioral day–night shift. Especially the striking change in the slopes of the frequency-of-seeing functions between day and night is not predictable by models that assume static higher-level processing throughout the circadian cycle. Only models making high-level readout mechanisms dependent on the behavioral or diurnal state would be able to reproduce the full magnitude of the slope change. Our dataset does not allow us to constrain such models in a meaningful way, as there remain too many free parameters. Validating such a model would require extensive recordings from the neural populations in the mouse brain centers involved in photon detection and decision-making, coupled to targeted (e.g. optogenetic) manipulations. The posterior parietal cortex is an obvious candidate, significant for action planning and decision making and receiving visual as well as other sensory input, but in fact multiple areas in rodent frontal cortex appear to play a role in decision making (reviewed in Carandini and Churchland, 2013).

The present results on day/night differences are not surprising in view of mounting evidence that sensory signal processing can vary vastly depending on the behavioral state of the animal. The nocturnal mouse is in a different state during its natural activity period at night compared with daytime. The water maze task is not a natural behavior for the mouse (unlike the phototactic jumping of frogs, for example), and perhaps such a cognitively challenging

task is easier to perform during the active phase. This idea is supported by our observation that the pupils are larger during the subjective night of the mice. Larger pupil size has been linked to heightened arousal in numerous studies (e.g. Reimer et al., 2014; McGinley et al., 2015a; Vinck et al., 2015; Salay et al., 2018, Clewett et al. 2020). Furthermore, arousal and attention have been found to strongly influence the processing and read-out of visual signals, as discussed in the literature review (Maimon, 2011; McGinley et al., 2015b; Cardin, 2019; McCormick et al., 2020). Likewise, the differences in the sampling strategies can emerge as a consequence of heightened arousal, when mice sample the visual world more attentively.

In conclusion, we hypothesize that diurnal changes in behavioral strategy are coupled with diurnal changes in the state of brain circuits reading out the retinal input and making decisions. Physical limits constrain the absolute sensitivity, but the behavioral state and behavioral strategy can substantially affect the behavioral output. It should be observed that the day-time behavioral performance in the present experiments was 10-fold off the physical limit.

5.3 LIMITS OF DECREMENT DETECTION (III)

This is the first measurement where behavioral decrement detection is correlated with ganglion cell measurements in matching conditions. Interestingly, we found that behavioral performance in decrement detection gets very near the limit set by the most sensitive OFF alpha ganglion cells. We also compared across the key neural levels (from rods to the most sensitive ON and OFF ganglion cells to behavior) decrement detection performance with ideal observer performance. We found that most of the losses occur in the retina, and the behavioral readout of signals from the population of sustained OFF alpha RGCs is close to the optimal. Recently, it was shown (Smeds et al., 2019) that behavioral readout of the weakest light increments is driven by the most sensitive ON RGCs in the mouse retina. Performance losses in this increment detection task happen also mainly in the retina. This lines up nicely with results presented here, considering that increment and decrement coding is driven by the primary rod pathway, which shares the same neural circuitry until the last synapse.

Finally, our theoretical analysis shows that a convergence of hundreds of rods is needed for even theoretically being able to encode increment and decrement stimuli at the lowest light levels. Interestingly, the split into ON and OFF outputs takes place at a level of convergence that just barely allows separation of these two distinct computations.

6 CONCLUSIONS

1. The presence of two spectrally different types of rods in amphibian retina enables them to make color discrimination even at the absolute visual threshold. Thus, frogs are dichromats at low light levels. However, the amphibian threshold for color discrimination is task- and context-dependent.
2. Visually guided behavior of mice in a light detection task in darkness reaches the highest sensitivity at night. However, the most sensitive and relevant retinal ganglion cells do not show diurnal changes in their sensitivity. Instead, the mice employ a more efficient search strategy at night than at day.
3. The behavioral performance of mice in decrement detection at the lowest light levels comes close to the limits set by the most sensitive (OFF) ganglion cells. The losses in this computation arise mainly in the retinal circuits.
4. Behavioral visual detection comes very close to the physical limits imposed by the quantum nature of light. This is demonstrated in both frog and mouse. However, in many tasks, sensory discrimination is not universally driven to absolute physical limits, but depends on evolutionary trade-offs and flexible brain states.

ACKNOWLEDGEMENTS

This thesis work was carried out at the University of Helsinki, in the Faculty of Biological and Environmental Sciences at the Division of Physiology and Neuroscience, which was later included in the Molecular Biology and Integrative Biosciences Programme. In part, the work also done at the Aalto University, in the Department of Neuroscience and Biomedical Engineering. For funding I wish to thank the Doctoral Programme of Brain and Mind, Doctoral School of Health Sciences, Academy of Finland, the Finnish Cultural Foundation, the Ella and Georg Ehrnrooth Foundation, the Oskar Öflunds Foundation and the Otto A. Malm Foundation. This thesis was done under the Doctoral Programme Brain & Mind, in the Doctoral School of Health Sciences.

Science is never a one-woman (or -man) operation and needs more than money and a place to do it. Numerous people deserve a huge thank you and hug (perhaps after the pandemic) for making this thesis possible.

First, a big thank you to my coauthors who have greatly contributed to this work and without whom this thesis would not exist. I'm also very grateful to the reviewers, Professors Tiffany Schmidt and Eric Warrant for taking the time to read my thesis on a tight schedule and for their invaluable comments. I also want to thank the Chief, Dr. Samer Hattar for agreeing to be my opponent in the public defense of my thesis. I am only sorry that because of the pandemic, he could not be here in person and enjoy the party in his honor.

I am grateful to Professor Juha Voipio for being my custos and for helping me with all the practicalities and bureaucracy of my thesis work. I wish to extend my gratitude to the members of my thesis committee, Drs. Soile Nymark and Vootele Voikar. Thank you for the support and invaluable insights in our meetings! I'm also very grateful to Dr. Katri Wegelius, the coordinator of our Doctoral Programme Brain & Mind, for all her knowledge and help (always applied with remarkable speed!) over the years. I will send my deepest gratitude to the animal caretakers in the Biocenter 3: Chrisse, Maria, Madara, Fanny and Sissi made a lot of the work presented in this thesis possible by taking care of the reversed light cycle and our frogs and mice. I would also like to thank Professor Almut Kelber for helping me to set out on this path many years ago and for all her support over the years. Dr. Carola Yovanovich I would like to thank for our time together when building the frog rig as well as for her great hospitality in Buenos Aires. Dr Magnus Lindström, thank you for organizing the wonderful meeting that is the Visionarium (the frog collaboration might not have existed without it).

Above all, I wish to thank my two supervisors, Professors Petri Ala-Laurila and Kristian Donner for taking me into their scientific family. Having not only one, but two dedicated and passionate scientists discussing one's work is a genuine privilege. It is enlightening and inspiring to see opposing views in science and the resulting scientific discourse in the pursue of truth. I have got to enjoy this privilege to the very last minutes of my thesis work, and hopefully, beyond. Thank you both for believing in me so wholeheartedly.

Petri, I don't think words can ever express how grateful I am to you for all the encouragement you have given me and the faith you put in me. Your passion and devotion towards the lab and to science is truly inspirational and, honestly, unparalleled. My plan for a long time was to do a PhD abroad but working in your lab quickly convinced me to want to stay. I don't think I will ever forget the awe I felt working in the lab in the first months. It was also a real privilege to participate in the building of a new, top research lab. Thank you for all the fun times in the lab together, for teaching me so many things and for pushing us to be ever better.

Kristian, your office has always been open and welcoming, I will always remember with fondness the laughs and conversations there. I am eternally grateful for your never-ending patience and for listening to my woes, scientific and otherwise. Your profound knowledge, not only of vision science, but of physiology and biology in a much broader sense is exceptional and helped me significantly in the writing of this thesis. Thank you for the countless emails in which you tirelessly replied to all my questions. I also want to thank you and Niki for opening your home to us so many times. The Rodieck seminar is something I will never forget.

Between the two PIs, Twinlabs as a scientific environment is extraordinary, but even more so because of the amazing lab members, past and present. Lina, you are one of the big reasons I made it this far. From the first days of teaching me to do watermaze experiments throughout the ups and downs of a PhD, we have shared the journey, along with many laughs and tears. Thank you for being there. Martta, your friendship means a world to me. It started with sharing an office and the first cup of coffee in the morning and came to be a great source of strength and emotional support. I'm so glad you came back from Norway just in time to share the last bit of the journey with me. Noora, I will never forget our frog collecting trips (when one might have to sacrifice one's pants). The first paper would not exist without your tireless frog jumping experiments. Collectively, I need to thank the 24h Helpline-chat for the peer-support and dealing with any problem, big or small, at any time.

Natali, the patching master. Thank you for the long hours together in the lab, for the long walks during the corona spring and for the wonderful conversations during both. Johan, thank you for the heroic job with bringing the third paper of this thesis to its full fruition, as well as for all the scientific help and discussions. Tuomas, our Slack conversations might not always be the most scientific but they have been great fun, and very instructive when buying an iPad or a camera. Working with you during the second paper of this

thesis was a true pleasure, thank you for that and for all the countless hours working with the watermaze. Markku, thank you for sharing the office and insights to science. Aarni and Jussi, thank you for all the fascinating science conversations over lunch and for all the help in the lab. Santtu, thank you for your energetic work with the behavioral experiments. Oliver, Alexandra, Janne and Kata, the newest members of the lab, thank you and best of luck to your future. Kata, thank you also for being such an enthusiastic Master's student, it has been a pleasure to work with you.

Sami, I still think of you as one of the foundation rocks of the lab. Thank you for all the help and support along the way. Sathish, you are one of the best teachers I know, and I hope you can continue to pursue that dream very soon. Thank you both for continuing to be part of the lab family, I hope this connection never breaks. Daisuke, thank you for innumerable hours patiently advising data analysis and for all the help in the lab. Anna, who can forget the first months on the Ferrari that is the Aalto-rig? Thank you for the dinners and for the many beautiful conversations, even through the Parisian night. Soile, you get a second thank you as the (fairy) godmother of our lab. Thank you for listening and for all the advice and encouragement.

Besides the scientific environment, I want to thank my lovely friends and family. To my goddaughters Heidi and Sanni, believe in yourself and you can achieve anything! Sanna and Kaisa, you are the sisters I never had. Your support from the beginning to the last moments has been indispensable. The days when you didn't have to listen to my frustrations and doubts and fears are few and far between, yet you always cheered me on. Reetta, I am so glad that even after 27 years we are still friends and can always pick up the conversation from where it was left. Satu, I count you as family (perhaps an aunt I never had), thank you for always being such a positive force in my life.

Franci, we started as idealistic, bright-eyed Master's students together and now we are finishing the journey together as, perhaps a bit less idealistic and more seasoned doctoral candidates (dare I say, as Doctors!). Thank you for sharing the ride, and for the wine-Tuesdays as well. Pia, Ilona and Ceci, though you are far away, you've been present in this journey. When working all hours in the lab, a time difference to Australia or Argentina can be a blessing. Thank you for all the care, laughs and shared memes along the years. An especially big thank you to Ilona for so enthusiastically proofreading various texts (including these Acknowledgements). I also wish to send my warmest regards to my NS&B 2018 colleagues and the Woods Hole community, I learned so much from you!

Mum, the best of mums, I would not be where I am nor who I am without you. Thank you for always encouraging me onwards and never doubting what I could achieve. I have learned that making a two-hour long phone call to you while walking in the woods can cure anything.

Finally, I would just like to add: It was hard at times but we had a lot of fun. Which, I suppose, is the way making science should be.

REFERENCES

Abrahamson, E. E., and Moore, R. Y. (2001). Suprachiasmatic Nucleus in the Mouse: Retinal Innervation, Intrinsic Organization and Efferent Projections. Brain Res. *916*, 172–191.

Adly, M. A., Spiwoks–Becker, I., and Vollrath, L. (1999). Ultrastructural Changes of Photoreceptor Synaptic Ribbons in Relation to Time of Day and Illumination. Investigative Ophthalmology & Visual Science *40*, 2165–2172.

Aho, A. C., Donner, K., and Reuter, T. (1993a). Retinal Origins of the Temperature Effect on Absolute Visual Sensitivity in Frogs. J. Physiol. *463*, 501–521.

Aho, A. C., Donner, K., Helenius, S., Larsen, L. O., and Reuter, T. (1993b). Visual Performance of the Toad (*Bufo bufo)* At Low Light Levels: Retinal Ganglion Cell Responses and Prey-Catching Accuracy. Journal of Comparative Physiology A *172*, 671–682.

Aho, A.-C., Donner, K., Hydén, C., Larsen, L. O., and Reuter, T. (1988). Low Retinal Noise in Animals with Low Body Temperature Allows High Visual Sensitivity. Nature *334*, 348–350.

Aho, A. C., Donner, K., Hydén, C., Reuter, T., and Orlov, O. Y. (1987). Retinal Noise, the Performance of Retinal Ganglion Cells, and Visual Sensitivity in the Dark-Adapted Frog. J. Opt. Soc. Am. A. *4*, 2321–2329.

Ala-Laurila, P., Pahlberg, J., Koskelainen, A., and Donner, K. (2004a). On the Relation Between the Photoactivation Energy and the Absorbance Spectrum of Visual Pigments. Vision Res. *44*, 2153–2158.

Ala-Laurila, P., and Rieke, F. (2014). Coincidence Detection of Single-Photon Responses in the Inner Retina at the Sensitivity Limit of Vision. Curr. Biol. *24*, 2888–2898.

Ala-Laurila, P., Cornwall, M. C., Crouch, R. K., and Kono, M. (2009). The Action of 11-Cis-retinol on Cone Opsins and Intact Cone Photoreceptors. J. Biol. Chem. *284*, 16492–16500.

Ala-Laurila, P., Donner, K., Crouch, R. K., and Cornwall, M. C. (2007). Chromophore Switch From 11-Cis-dehydroretinal (A2) to 11-Cis-retinal (A1) Decreases Dark Noise in Salamander Red Rods. J. Physiol. *585*, 57–74.

Ala-Laurila, P., Donner, K., and Koskelainen, A. (2004b). Thermal Activation and Photoactivation of Visual Pigments. Biophys. J. *86*, 3653–3662.

Ala-Laurila, P., Kolesnikov, A. V., Crouch, R. K., Tsina, E., Shukolyukov, S. A., Govardovskii, V. I., Koutalos, Y., Wiggert, B., Estevez, M. E., and Cornwall, M. C. (2006). Visual Cycle: Dependence of Retinol Production and Removal on Photoproduct Decay and Cell Morphology. J. Gen. Physiol. *128*, 153–169.

Altimus, C. M., Güler, A. D., Alam, N. M., Arman, A. C., Prusky, G. T., Sampath, A. P., and Hattar, S. (2010). Rod Photoreceptors Drive Circadian Photoentrainment Across a Wide Range of Light Intensities. Nat. Neurosci. *13*, 1107–1112.

Altimus, C. M., Güler, A. D., Villa, K. L., Mcneill, D. S., Legates, T. A., and Hattar, S. (2008). Rods-Cones and Melanopsin Detect Light and Dark to Modulate Sleep Independent of Image Formation. Proc. Natl. Acad. Sci. U. S. A. *105*, 19998–20003.

Ames, A., III (1992). Energy Requirements of CNS Cells as Related to Their Function and to Their Vulnerability to Ischemia: A Commentary Based on Studies on Retina. Can. J. Physiol. Pharmacol. *70 Suppl*, S158–64.

Ames, A., III, Li, Y. Y., Heher, E. C., and Kimble, C. R. (1992). Energy Metabolism of Rabbit Retina as Related to Function: High Cost of Na+ Transport. J. Neurosci. *12*, 840–853.

Amphibiaweb (2020). https://amphibiaweb.org (Berkeley, CA, USA: University of California).

Angueyra, J. M., and Rieke, F. (2013). Origin and Effect of Phototransduction Noise in Primate Cone Photoreceptors. Nat. Neurosci. *16*, 1692–1700.

Armstrong-Gold, C. E., and Rieke, F. (2003). Bandpass Filtering at the Rod to Second-Order Cell Synapse in Salamander (*Ambystoma tigrinum*) Retina. J. Neurosci. *23*, 3796.

Attneave, F. (1954). Some Informational Aspects of Visual Perception. Psychol. Rev. *61*, 183–193.

Attwell, D., and Laughlin, S. B. (2001). An Energy Budget for Signaling in the Grey Matter of the Brain. J. Cereb. Blood Flow Metab. *21*, 1133–1145.

Auffray, J.-C., and Britton-Davidian, J. (2012). The house mouse and its relatives. In Evolution of the house mouse, Piálek, J., M. Macholán, P. Munclinger, and S. J. E. Baird, eds. (Cambridge: Cambridge University Press), pp. 1-34.

Autrum, H. (1943). Über Kleinste Reize Bei Sinnesorganen. Biologisches Zentralblatt *63*, 209–236.

Awatramani, G. B., and Slaughter, M. M. (2000). Origin of Transient and Sustained Responses in Ganglion Cells of the Retina. J. Neurosci. *20*, 7087.

Baba, K., Pozdeyev, N., Mazzoni, F., Contreras-Alcantara, S., Liu, C., Kasamatsu, M., Martinez-Merlos, T., Strettoi, E., Iuvone, P. M., and Tosini, G. (2009). Melatonin Modulates Visual Function and Cell Viability in the Mouse Retina Via the Mt1 Melatonin Receptor. Proc. Natl. Acad. Sci. U. S. A. *106*, 15043–15048.

Bäckström, A. C., and Reuter, T. (1975). Receptive Field Organization of Ganglion Cells in the Frog Retina: Contributions from Cones, Green Rods and Red Rods. J. Physiol. *246*, 79–107.

Baden, T., Berens, P., Franke, K., Roman Roson, M., Bethge, M., and Euler, T. (2016). The Functional Diversity of Retinal Ganglion Cells in the Mouse. Nature *529*, 345–350.

Baden, T., Euler, T., and Berens, P. (2020). Understanding the Retinal Basis of Vision Across Species. Nat. Rev. Neurosci. *21*, 5–20.

Baden, T., Schubert, T., Chang, L., Wei, T., Zaichuk, M., Wissinger, B., and Euler, T. (2013). A Tale of Two Retinal Domains: Near-Optimal Sampling of Achromatic Contrasts in Natural Scenes Through Asymmetric Photoreceptor Distribution. Neuron *80*, 1206–1217.

Bae, J. A., Mu, S., Kim, J. S., Turner, N. L., Tartavull, I., Kemnitz, N., Jordan, C. S., Norton, A. D., Silversmith, W. M., Prentki, R., Sorek, M., David, C., Jones, D. L., Bland, D., Sterling, A. L. R., Park, J., Briggman, K. L., and Seung, H. S. (2018). Digital Museum of Retinal Ganglion Cells With Dense Anatomy and Physiology. Cell *173*, 1293–1306.e19.

Balasubramanian, V., and Sterling, P. (2009). Receptive Fields and Functional Architecture in the Retina. J. Physiol. *587*, 2753–2767.

Balkema, G. W., Cusick, K., and Nguyen, T. H. (2001). Diurnal Variation in Synaptic Ribbon Length and Visual Threshold. Vis. Neurosci. *18*, 789–797.

Barlow, H. B. (1953). Summation and Inhibition in the Frog's Retina. J. Physiol. *119*, 69–88.

Barlow, H. B. (1956). Retinal Noise and Absolute Threshold. J. Opt. Soc. Am. *46*, 634–639.

Barlow, H. B. (1957). Purkinje Shift and Retinal Noise. Nature *179*, 255–256.

Barlow, H. B. (1988). The Thermal Limit to Seeing. Nature *334*, 296–297.

Barlow, H. (1961). Possible principles underlying the transformations of sensory messages. In Sensory communication, Rosenblith, W. A., ed. (Cambridge, MA: MIT Press), pp. 217-234.

Barnard, A. R., Hattar, S., Hankins, M. W., and Lucas, R. J. (2006). Melanopsin Regulates Visual Processing in the Mouse Retina. Curr. Biol. *16*, 389–395.

Bassi, C. J., and Powers, M. K. (1986). Daily Fluctuations in the Detectability of Dim Lights By Humans. Physiol. Behav. *38*, 871–877.

Baylor, D. A., Lamb, T. D., and Yau, K. W. (1979). Responses of Retinal Rods to Single Photons. J. Physiol. *288*, 613–634.

Baylor, D. A., Matthews, G., and Yau, K. W. (1980). Two Components of Electrical Dark Noise in Toad Retinal Rod Outer Segments. J. Physiol. *309*, 591–621.

Baylor, D. A., Nunn, B. J., and Schnapf, J. L. (1984). The Photocurrent, Noise and Spectral Sensitivity of Rods of the Monkey *Macaca fascicularis*. J. Physiol. *357*, 575–607.

Behrens, C., Schubert, T., Haverkamp, S., Euler, T., and Berens, P. (2016). Connectivity Map of Bipolar Cells and Photoreceptors in the Mouse Retina. eLife *5*, e20041.

Bennett, C., Arroyo, S., and Hestrin, S. (2013). Subthreshold Mechanisms Underlying State-Dependent Modulation of Visual Responses. Neuron *80*, 350–357.

Berry, R. (2012). Foreword. In Evolution of the house mouse, Piálek, J., M. Macholán, P. Munclinger, and S. J. E. Baird, eds. (Cambridge: Cambridge University Press), pp. xiii-xxii.

Berson, D. M. (2003). Strange Vision: Ganglion Cells as Circadian Photoreceptors. Trends Neurosci. *26*, 314–320.

Berson, D. M., Dunn, F. A., and Takao, M. (2002). Phototransduction By Retinal Ganglion Cells That Set the Circadian Clock. Science *295*, 1070–1073.

Besharse, J. C., and Iuvone, P. M. (1983). Circadian Clock in *Xenopus* Eye Controlling Retinal Serotonin N-Acetyltransferase. Nature *305*, 133–135.

Bialek, W., and Owen, W. G. (1990). Temporal Filtering in Retinal Bipolar Cells. Elements of an Optimal Computation. Biophys. J. *58*, 1227–1233.

Bialek, W. (1987). Physical Limits to Sensation and Perception. Annu. Rev. Biophys. Biophys. Chem. *16*, 455–478.

Birch, D. G., Berson, E. L., and Sandberg, M. A. (1984). Diurnal Rhythm in the Human Rod Erg. Invest. Ophthalmol. Vis. Sci. *25*, 236–238.

Birge, R. R., Einterz, C. M., Knapp, H. M., and Murray, L. P. (1988). The Nature of the Primary Photochemical Events in Rhodopsin and Isorhodopsin. Biophys. J. *53*, 367–385.

Bloomfield, S. A., and Dacheux, R. F. (2001). Rod Vision: Pathways and Processing in the Mammalian Retina. Prog. Retin. Eye. Res. *20*, 351–384.

Bonhomme, F., and Searle, J. B. (2012). House mouse phylogeography. In Evolution of the house mouse, Piálek, J., M. Macholán, P. Munclinger, and S. J. E. Baird, eds. (Cambridge: Cambridge University Press), pp. 278-296.

Bowmaker, J. K. (2008). Evolution of Vertebrate Visual Pigments. Vision Res. *48*, 2022–2041.

Bridges, C. D. B. (1974). Effects of Light and Darkness on the Visual Pigments of Amphibian Tadpoles. Vision Res. *14*, 779–793.

Bringmann, A., Syrbe, S., Görner, K., Kacza, J., Francke, M., Wiedemann, P., and Reichenbach, A. (2018). The Primate Fovea: Structure, Function and Development. Prog. Retin. Eye. Res. *66*, 49–84.

Burns, M. E., and Lamb, T. D. (2004). Visual transduction by rod and cone photoreceptors. In The Visual Neurosciences, Chalupa, L., M., and J. Werner, S., eds. (Cambridge, MA: MIT Press), pp. 215-233.

Burns, M. E., Mendez, A., Chen, J., and Baylor, D. A. (2002). Dynamics of Cyclic GMP Synthesis in Retinal Rods. Neuron *36*, 81–91.

Burnside, B., and Ackland, N. (1984). Effects of Circadian Rhythm and Camp on Retinomotor Movements in the Green Sunfish, *Lepomis cyanellus*. Investigative Ophthalmology & Visual Science *25*, 539–545.

Busse, L., Cardin, J. A., Chiappe, M. E., Halassa, M. M., Mcginley, M. J., Yamashita, T., and Saleem, A. B. (2017). Sensation During Active Behaviors. J. Neurosci. *37*, 10826.

Cahill, G. M., and Besharse, J. C. (1993). Circadian Clock Functions Localized in *Xenopu*s Retinal Photoreceptors. Neuron *10*, 573–577.

Cameron, M. A., Barnard, A. R., Hut, R. A., Bonnefont, X., Van Der Horst, G. T., Hankins, M. W., and Lucas, R. J. (2008). Electroretinography of Wild-Type and Cry Mutant Mice Reveals Circadian Tuning of Photopic and Mesopic Retinal Responses. J. Biol. Rhythms *23*, 489–501.

Cameron, M. A., and Lucas, R. J. (2009). Influence of the Rod Photoresponse on Light Adaptation and Circadian Rhythmicity in the Cone Erg. Mol. Vis. *15*, 2209–2216.

Campbell, N. A., Reece, J. B., Molles, M., Urry, L. A., and Heyden, R. (2005). Biology: International edition (New York City, NY: Pearson).

Carandini, M., and Churchland, A. K. (2013). Probing Perceptual Decisions in Rodents. Nat. Neurosci. *16*, 824–831.

Cardin, J. A. (2019). Functional Flexibility in Cortical Circuits. Curr. Opin. Neurobiol. *58*, 175–180.

Cardinali, D. P., and Pévet, P. (1998). Basic Aspects of Melatonin Action. Sleep Medicine Reviews *2*, 175–190.

Carter-Dawson, L. D., and Lavail, M. M. (1979). Rods and Cones in the Mouse Retina. I. Structural Analysis Using Light and Electron Microscopy. J. Comp. Neurol. *188*, 245–262.

Caton, R. (1887). Researches on electrical phenomena of cerebral grey matter. In Transactions of the international medical congress: Ninth session, volume 3, Hamilton, J. B., ed. (Washington, DC.: Int. Med. Congress), pp. 246-249.

Chang, W. S., and Harris, W. A. (1998). Sequential Genesis and Determination of Cone and Rod Photoreceptors in *Xenopus*. J. Neurobiol. *35*, 227–244.

Chaurasia, S. S., Rollag, M. D., Jiang, G., Hayes, W. P., Haque, R., Natesan, A., Zatz, M., Tosini, G., Liu, C., Korf, H. W., Iuvone, P. M., and Provencio, I. (2005). Molecular Cloning, Localization and Circadian Expression of Chicken Melanopsin (Opn4): Differential Regulation of Expression in Pineal and Retinal Cell Types. J. Neurochem. *92*, 158–170.

Chiappe, M. E., Seelig, J. D., Reiser, M. B., and Jayaraman, V. (2010). Walking Modulates Speed Sensitivity in Drosophila Motion Vision. Curr. Biol. *20*, 1470–1475.

Clewett, D., Gasser, C., and Davachi, L. (2020). Pupil-Linked Arousal Signals Track the Temporal Organization of Events in Memory. Nat. Commun. *11*, 4007.

Contini, M., and Raviola, E. (2003). Gabaergic Synapses Made By a Retinal Dopaminergic Neuron. Proc. Natl. Acad. Sci. U. S. A. *100*, 1358–1363.

Cooper, A. (1979). Energy Uptake in the First Step of Visual Excitation. Nature *282*, 531–533.

Copenhagen, D. R., Hemilä, S., and Reuter, T. (1990). Signal Transmission Through the Dark-Adapted Retina of the Toad (Bufo Marinus). Gain, Convergence, and Signal/noise. J. Gen. Physiol. *95*, 717–732.

Cornwall, M. C., Jones, G. J., Kefalov, V. J., Fain, G. L., and Matthews, H. R. (2000). Signal Transmission Through the Dark-Adapted Retina of the Toad (*Bufo Marinus*). Gain, Convergence, and Signal/noise. J. Gen. Physiol. *316*, 224–252.

Country, M. W. (2017). Retinal Metabolism: A Comparative Look At Energetics in the Retina. Brain Res. *1672*, 50–57.

Crescitelli, F. (1958). The Natural History of Visual Pigments. Ann. N. Y. Acad. Sci. *74*, 230–255.

Crescitelli, F. (1972). The visual cells and visual pigments of the vertebrate eye. In Photochemistry of vision, Dartnall, H. J. A., ed. (Berlin, Heidelberg: Springer Berlin Heidelberg), pp. 245-363.

Cronin, T. W., Johnsen, S., Marshall, N. J., and Warrant, E. J. (2014). Visual Ecology (New Jersey: Princeton University Press).

Czeisler, C. A., Shanahan, T. L., Klerman, E. B., Martens, H., Brotman, D. J., Emens, J. S., Klein, T., and Rizzo, J. F. (1995). Suppression of Melatonin Secretion in Some Blind Patients By Exposure to Bright Light. N. Engl. J. Med. *332*, 6–11.

Dadarlat, M. C., and Stryker, M. P. (2017). Locomotion Enhances Neural Encoding of Visual Stimuli in Mouse V1. J. Neurosci. *37*, 3764.

Dalal, J. S., Jinks, R. N., Cacciatore, C., Greenberg, R. M., and Battelle, B. A. (2003). Limulus Opsins: Diurnal Regulation of Expression. Vis. Neurosci. *20*, 523–534.

Dall, S. R. X., Giraldeau, L.-A., Olsson, O., Mcnamara, J. M., and Stephens, D. W. (2005). Information and Its Use By Animals in Evolutionary Ecology. Trends in Ecology & Evolution *20*, 187–193.

Damsgaard, C., Lauridsen, H., Funder, A. M. D., Thomsen, J. S., Desvignes, T., Crossley, D. A., II, Møller, P. R., Huong, D. T. T., Phuong, N. T., Detrich, H. W., III, Brüel, A., Wilkens, H., Warrant, E., Wang, T., Nyengaard, J. R., Berenbrink, M., and Bayley, M. (2019). Retinal Oxygen Supply Shaped the Functional Evolution of the Vertebrate Eye. eLife *8*, e52153.

Dartnall, H. J. A. (1968). The Photosensitivities of Visual Pigments in the Presence of Hydroxylamine. Vision Res. *8*, 339–358.

Dartnall, H. J. A., and Lythgoe, J. N. (1965). The Spectral Clustering of Visual Pigments. Vision Res. *5*, 81–100.

Darwin, C. (1986). The Expression of the Emotions in Man and Animals; second edition edited by Francis Darwin (1890). (Charlottesville, Virginia, U.S.A.: InteLex Corp.).

De Franceschi, G., Vivattanasarn, T., Saleem, A. B., and Solomon, S. G. (2016). Vision Guides Selection of Freeze or Flight Defense Strategies in Mice. Curr. Biol. *26*, 2150–2154.

Deans, M. R., Volgyi, B., Goodenough, D. A., Bloomfield, S. A., and Paul, D. L. (2002). Connexin36 is Essential for Transmission of Rod-Mediated Visual Signals in the Mammalian Retina. Neuron *36*, 703–712.

Dearry, A., and Barlow, R. B., Jr (1987). Circadian Rhythms in the Green Sunfish Retina. J. Gen. Physiol. *89*, 745–770.

Denman, D. J., Luviano, J. A., Ollerenshaw, D. R., Cross, S., Williams, D., Buice, M. A., Olsen, S. R., and Reid, R. C. (2018). Mouse Color and Wavelength-Specific Luminance Contrast Sensitivity Are Non-Uniform Across Visual Space. eLife *7*, e31209.

Denman, D. J., and Contreras, D. (2016). On Parallel Streams Through the Mouse Dorsal Lateral Geniculate Nucleus. Front Neural Circuits *10*, 20.

Denton, E. J., and Wyllie, J. H. (1955). Study of the Photosensitive Pigments in the Pink and Green Rods of the Frog. J. Physiol. *127*, 81–89.

Devries, S. H. (2000). Bipolar Cells Use Kainate and AMPA Receptors to Filter Visual Information Into Separate Channels. Neuron *28*, 847–856.

Do, M. T., and Yau, K. W. (2010). Intrinsically Photosensitive Retinal Ganglion Cells. Physiol. Rev. *90*, 1547–1581.

Do, M. T. H. (2019). Melanopsin and the Intrinsically Photosensitive Retinal Ganglion Cells: Biophysics to Behavior. Neuron *104*, 205–226.

Donner, K., Copenhagen, D. R., and Reuter, T. (1990a). Weber and Noise Adaptation in the Retina of the Toad *Bufo marinus*. J. Gen. Physiol. *95*, 733–753.

Donner, K., Firsov, M. L., and Govardovskii, V. I. (1990b). The Frequency of Isomerization-Like "dark" Events in Rhodopsin and Porphyropsin Rods of the Bullfrog Retina. J. Physiol. *428*, 673–692.

Donner, K. O., and Reuter, T. (1976). Visual pigments and photoreceptor function. In Frog neurobiology: A handbook, Llinás, R., and W. Precht, eds. (Berlin, Heidelberg: Springer Berlin Heidelberg), pp. 251-277.

Donner, K. (1989). Visual Latency and Brightness: An Interpretation Based on the Responses of Rods and Ganglion Cells in the Frog Retina. Vis. Neurosci. *3*, 39–51.

Donner, K. (2020). Spectral and thermal properties of rhodopsins: Closely related but not tightly coupled

Donner, K., and Grönholm, M.-L. (1984). Center and Surround Excitation in the Receptive Fields of Frog Retinal Ganglion Cells. Vision Res. *24*, 1807–1819.

Donner, K., Hemilä, S., and Koskelainen, A. (1998). Light Adaptation of Cone Photoresponses Studied At the Photoreceptor and Ganglion Cell Levels in the Frog Retina. Vision Res. *38*, 19–36.

Donner, K., Koskelainen, A., Djupsund, K., and Hemilä, S. (1995). Changes in Retinal Time Scale Under Background Light: Observations on Rods and Ganglion Cells in the Frog Retina. Vision Res. *35*, 2255–2266.

Donner, K., and Yovanovich, C. A. M. (2020). A Frog's Eye View: Foundational Revelations and Future Promises. Seminars in Cell & Developmental Biology in press.

Dowling, J. E. (1976). Physiology and morphology of the retina frog neurobiology: A handbook. Llinás, R., and W. Precht, eds. (Berlin, Heidelberg: Springer Berlin Heidelberg), pp. 278-296.

Dowling, J. E., Boycott, B. B., and Wells, G. P. (1966). Organization of the Primate Retina: Electron Microscopy. Proc. R. Soc. Lond. B. Biol. Sci. *166*, 80–111.

Doyle, S. E., Grace, M. S., McIvor, W., and Menaker, M. (2002). Circadian Rhythms of Dopamine in Mouse Retina: The Role of Melatonin. Vis. Neurosci. *19*, 593–601.

Dräger, U. C., and Olsen, J. F. (1980). Origins of Crossed and Uncrossed Retinal Projections in Pigmented and Albino Mice. J. Comp. Neurol. *191*, 383–412.

Du Pont, J. S., and De Groot, P. J. (1976). A Schematic Dioptric Apparatus for the Frog's Eye (*Rana Esculenta*). Vision Res. *16*, 803–810.

Dunlap, J. C. (1999). Molecular Bases for Circadian Clocks. Cell *96*, 271–290.

Dyballa, L., Hoseini, M. S., Dadarlat, M. C., Zucker, S. W., and Stryker, M. P. (2018). Flow Stimuli Reveal Ecologically Appropriate Responses in Mouse Visual Cortex. Proc. Natl. Acad. Sci. U. S. A. *115*, 11304.

Ellis, E. M., Frederiksen, R., Morshedian, A., Fain, G. L., and Sampath, A. P. (2020). Separate on and Off Pathways in Vertebrate Vision First Arose During the Cambrian. Curr. Biol. *30*, R633–R634.

Ellis, E. M., Gauvain, G., Sivyer, B., and Murphy, G. J. (2016). Shared and Distinct Retinal Input to the Mouse Superior Colliculus and Dorsal Lateral Geniculate Nucleus. J. Neurophysiol. *116*, 602–610.

Erisken, S., Vaiceliunaite, A., Jurjut, O., Fiorini, M., Katzner, S., and Busse, L. (2014). Effects of Locomotion Extend Throughout the Mouse Early Visual System. Curr. Biol. *24*, 2899–2907.

Fain, G. L. (1975). Quantum Sensitivity of Rods in the Toad Retina. Science *187*, 838.

Faisal, A. A., and Laughlin, S. B. (2007). Stochastic Simulations on the Reliability of Action Potential Propagation in Thin Axons. PLoS Comput. Biol. *3*, e79.

Fechner, G. (1860). Elements of psychophysics. Vol. I. (Holt, Rinehart and Winston: New York).

Fein, A., and Szuts, E., Z. (1982). Photoreceptors, Their Role in Vision.

Field, G. D., Uzzell, V., Chichilnisky, E. J., and Rieke, F. (2019). Temporal Resolution of Single-Photon Responses in Primate Rod Photoreceptors and Limits Imposed By Cellular Noise. J. Neurophysiol. *121*, 255–268.

Field, G. D., and Sampath, A. P. (2017). Behavioural and Physiological Limits to Vision in Mammals. Philos. Trans. R. Soc. Lond. B. Biol. Sci. *372*, 20160072.

Field, G. D., and Rieke, F. (2002a). Nonlinear Signal Transfer From Mouse Rods to Bipolar Cells and Implications for Visual Sensitivity. Neuron *34*, 773–785.

Field, G. D., and Rieke, F. (2002b). Mechanisms Regulating Variability of the Single Photon Responses of Mammalian Rod Photoreceptors. Neuron *35*, 733–747.

Field, G. D., Sampath, A. P., and Rieke, F. (2005). Retinal Processing Near Absolute Threshold: From Behavior to Mechanism. Annu. Rev. Physiol *67*, 491–514.

Foster, R. G., Provencio, I., Hudson, D., Fiske, S., De Grip, W., and Menaker, M. (1991). Circadian Photoreception in the Retinally Degenerate Mouse (Rd/rd). J. Comp. Physiol. A *169*, 39–50.

Frank, B. D., and Hollyfield, J. G. (1987). Retinal Ganglion Cell Morphology in the Frog, *Rana Pipiens*. J. Comp. Neurol. *266*, 413–434.

Freedman, K., Becker, R. S., Hannak, D., and Bayer, E. (1986). Investigation Into the Spectroscopy and Photoisomerization of a Series of Poly (Ethylene Glycol) Peptide Schiff Bases of 11-Cis Retinal. Photochemistry and Photobiology *43*, 291–295.

Freedman, M. S., Lucas, R. J., Soni, B., Von Schantz, M., Muñoz, M., David-Gray, Z., and Foster, R. (1999). Regulation of Mammalian Circadian Behavior By Non-Rod, Non-Cone, Ocular Photoreceptors. Science *284*, 502–504.

Fu, Y., Kefalov, V., Luo, D.-G., Xue, T., and Yau, K.-W. (2008). Quantal Noise From Human Red Cone Pigment. Nat. Neurosci. *11*, 565–571.

Fu, Y., and Yau, K.-W. (2007). Phototransduction in Mouse Rods and Cones. Pflug. Arch. Eur. J. Phy. *454*, 805–819.

Fujiwara, T., Cruz, T. L., Bohnslav, J. P., and Chiappe, M. E. (2017). A Faithful Internal Representation of Walking Movements in the Drosophila Visual System. Nat. Neurosci. *20*, 72–81.

Gale, S. D., and Murphy, G. J. (2014). Distinct Representation and Distribution of Visual Information By Specific Cell Types in Mouse Superficial Superior Colliculus. J. Neurosci. *34*, 13458.

Gamlin, P. D. R., McDougal, D. H., Pokorny, J., Smith, V. C., Yau, K.-W., and Dacey, D. M. (2007). Human and Macaque Pupil Responses Driven By Melanopsin-Containing Retinal Ganglion Cells. Vision Res. *47*, 946–954.

Gekakis, N., Staknis, D., Nguyen, H. B., Davis, F. C., Wilsbacher, L. D., King, D. P., Takahashi, J. S., and Weitz, C. J. (1998). Role of the Clock Protein in the Mammalian Circadian Mechanism. Science *280*, 1564–1569.

Gooley, J. J., Lu, J., Fischer, D., and Saper, C. B. (2003). A Broad Role for Melanopsin in Nonvisual Photoreception. J. Neurosci. *23*, 7093–7106.

Govardovskii, V. I., Fyhrquist, N., Reuter, T., Kuzmin, D. G., and Donner, K. (2000). In Search of the Visual Pigment Template. Vis. Neurosci. *17*, 509–528.

Govardovskii, V. I., and Reuter, T. (2014). Why Do Green Rods of Frog and Toad Retinas Look Green. Journal of Comparative Physiology. A, Neuroethology, sensory, neural, and behavioral physiology *200*, 823–835.

Govardovskiĭ, V. I., and Zueva, L. V. (1974). Spectral Sensitivity of the Frog Eye in the Ultraviolet and Visible Region. Vision Res. *14*, 1317–1321.

Gozem, S., Schapiro, I., Ferré, N., and Olivucci, M. (2012). The Molecular Mechanism of Thermal Noise in Rod Photoreceptors. Science *337*, 1225.

Grace, M. S., Wang, L. A., Pickard, G. E., Besharse, J. C., and Menaker, M. (1996). The Tau Mutation Shortens the Period of Rhythmic Photoreceptor Outer Segment Disk Shedding in the Hamster. Brain Res. *735*, 93–100.

Greene, M., Kim, J., and Seung, H. (2016). Analogous Convergence of Sustained and Transient Inputs in Parallel on and Off Pathways for Retinal Motion Computation. Cell Reports *14*, 1892–1900.

Grimes, W. N., Baudin, J., Azevedo, A. W., and Rieke, F. (2018). Range, Routing and Kinetics of Rod Signaling in Primate Retina. eLife *7*, e38281.

Grubb, M. S., and Thompson, I. D. (2003). Quantitative Characterization of Visual Response Properties in the Mouse Dorsal Lateral Geniculate Nucleus. J. Neurophysiol. *90*, 3594–3607.

Grüsser, O.-J., and Grüsser-Cornehls, U. (1976). Neurophysiology of the anuran visual system frog neurobiology: A handbook. Llinás, R., and W. Precht, eds. (Berlin, Heidelberg: Springer Berlin Heidelberg), pp. 297-385.

Hailman, J. P., and Jaeger, R. G. (1974). Phototactic Responses to Spectrally Dominant Stimuli and Use of Colour Vision By Adult Anuran Amphibians: A Comparative Survey. Animal Behaviour *22*, 757–795.

Hailman, J. P. (1976). Oildroplets in the Eyes of Adult Anuran Amphibians: A Comparative Survey. J. Morphol. *148*, 453–468.

Hankins, M. W., Jones, R. J., and Ruddock, K. H. (1998). Diurnal Variation in the B-Wave Implicit Time of the Human Electroretinogram. Vis. Neurosci. *15*, 55–67.

Hannibal, J., and Fahrenkrug, J. (2004). Target Areas Innervated By PACAP-Immunoreactive Retinal Ganglion Cells. Cell Tissue Res. *316*, 99–113.

Hannibal, J., Georg, B., Hindersson, P., and Fahrenkrug, J. (2005). Light and Darkness Regulate Melanopsin in the Retinal Ganglion Cells of the Albino Wistar Rat. J. Mol. Neurosci. *27*, 147–155.

Hárosi, F. I. (1982). Recent Results From Single-Cell Microspectrophotometry: Cone Pigments in Frog, Fish, and Monkey. Color Research & Application *7*, 135–141.

Hartline, H. K. (1938). The Response of Single Optic Nerve Fibers of the Vertebrate Eye to Illumination of the Retina. Am. J. Physiol. *121*, 400–415.

Hattar, S., Kumar, M., Park, A., Tong, P., Tung, J., Yau, K. W., and Berson, D. M. (2006). Central Projections of Melanopsin-Expressing Retinal Ganglion Cells in the Mouse. J. Comp. Neurol. *497*, 326–349.

Hattar, S., Liao, H. W., Takao, M., Berson, D. M., and Yau, K. W. (2002). Melanopsin-Containing Retinal Ganglion Cells: Architecture, Projections, and Intrinsic Photosensitivity. Science *295*, 1065–1070.

Hayasaka, N., Larue, S. I., and Green, C. B. (2002). In Vivo Disruption of *Xenopus* Clock in the Retinal Photoreceptor Cells Abolishes Circadian Melatonin Rhythmicity Without Affecting Its Production Levels. J. Neurosci. *22*, 1600.

Hecht, S., Shlaer, S., and Pirenne, M. H. (1942). Energy, Quanta, and Vision. J. Gen. Physiol. *25*, 819–840.

Hemilä, S., and Reuter, T. (1981). Longitudinal Spread of Adaptation in the Rods of the Frog's Retina. J. Physiol. *310*, 501–528.

Hemilä, S. , Lerber, T., and Donner, K. (1998). Noise-Equivalent and Signal-Equivalent Visual Summation of Quantal Events in Space and Time. Vis. Neurosci. *15*, 731–742.

Henriksson, J. T., Bergmanson, J. P., and Walsh, J. E. (2010). Ultraviolet Radiation Transmittance of the Mouse Eye and Its Individual Media Components. Exp. Eye Res. *90*, 382–387.

Hensley, S. H., Yang, X. L., and Wu, S. M. (1993). Relative Contribution of Rod and Cone Inputs to Bipolar Cells and Ganglion Cells in the Tiger Salamander Retina. J. Neurophysiol. *69*, 2086–2098.

Herculano-Houzel, S. (2011). Scaling of Brain Metabolism With a Fixed Energy Budget Per Neuron: Implications for Neuronal Activity, Plasticity and Evolution. PLoS One *6*, e17514.

Hess, E. H., and Polt, J. M. (1960). Pupil Size as Related to Interest Value of Visual Stimuli. Science *132*, 349.

Hess, E. H., and Polt, J. M. (1964). Pupil Size in Relation to Mental Activity During Simple Problem-Solving. Science *143*, 1190.

Hinshelwood, C. N. (1933). The kinetics of chemical change in gaseous systems. (Oxford, United Kingdom: Clarendon Press).

Hisatomi, O., Kayada, S., Taniguchi, Y., Kobayashi, Y., Satoh, T., and Tokunaga, F. (1998). Primary Structure and Characterization of a Bullfrog

Visual Pigment Contained in Small Single Cones. Comp. Biochem. Physiol. B *119*, 585–591.

Hisatomi, O., Takahashi, Y., Taniguchi, Y., Tsukahara, Y., and Tokunaga, F. (1999). Primary Structure of a Visual Pigment in Bullfrog Green Rods. FEBS Lett. *447*, 44–48.

Hong, G., Fu, T. M., Qiao, M., Viveros, R. D., Yang, X., Zhou, T., Lee, J. M., Park, H. G., Sanes, J. R., and Lieber, C. M. (2018). A Method for Single-Neuron Chronic Recording From the Retina in Awake Mice. Science *360*, 1447–1451.

Hoy, J. L., Yavorska, I., Wehr, M., and Niell, C. M. (2016). Vision Drives Accurate Approach Behavior During Prey Capture in Laboratory Mice. Curr. Biol. *26*, 3046–3052.

Hubel, D. H., and Wiesel, T. N. (1959). Receptive Fields of Single Neurones in the Cat's Striate Cortex. J. Physiol. *148*, 574–591.

Hubel, D. H., and Wiesel, T. N. (1962). Receptive Fields, Binocular Interaction and Functional Architecture in the Cat's Visual Cortex. J. Physiol. *160*, 106–154.

Hubel, D. H. (1959). Single Unit Activity in Striate Cortex of Unrestrained Cats. J. Physiol. *147*, 226–238.

Huberman, A. D., and Niell, C. M. (2011). What Can Mice Tell Us About How Vision Works. Trends Neurosci. *34*, 464–473.

Huberman, A. D., Manu, M., Koch, S. M., Susman, M. W., Lutz, A. B., Ullian, E. M., Baccus, S. A., and Barres, B. A. (2008). Architecture and Activity-Mediated Refinement of Axonal Projections From a Mosaic of Genetically Identified Retinal Ganglion Cells. Neuron *59*, 425–438.

Ingle, D. (1976). Behavioral correlates of central visual function in anurans frog neurobiology: A handbook. Llinás, R., and W. Precht, eds. (Berlin, Heidelberg: Springer Berlin Heidelberg), pp. 435-451.

Ingram, N. T., Sampath, A. P., and Fain, G. L. (2016). Why Are Rods More Sensitive Than Cones. J. Physiol. *594*, 5415–5426.

Ivanova, T. N., and Iuvone, M. P. (2003a). Melatonin Synthesis in Retina: Circadian Regulation of Arylalkylamine N-Acetyltransferase Activity in Cultured Photoreceptor Cells of Embryonic Chicken Retina. Brain Res. *973*, 56–63.

Ivanova, T. N., and Iuvone, P. M. (2003b). Circadian Rhythm and Photic Control of Camp Level in Chick Retinal Cell Cultures: A Mechanism for Coupling the Circadian Oscillator to the Melatonin-Synthesizing Enzyme, Arylalkylamine N-Acetyltransferase, in Photoreceptor Cells. Brain Res. *991*, 96–103.

Jacob, F. (1977). Evolution and Tinkering. Science *196*, 1161.

Jaeger, R. G., and Hailman, J. P. (1973). Effects of intensity on the phototactic responses of adult anuran amphibians: A comparative survey. Z. Tierpsychol. *33*, 352 – 407.

Jin, N., Zhang, Z., Keung, J., Youn, S. B., Ishibashi, M., Tian, L.-M., Marshak, D. W., Solessio, E., Umino, Y., Fahrenfort, I., Kiyama, T., Mao, C.-A., You, Y., Wei, H., Wu, J., Postma, F., Paul, D. L., Massey, S. C., and Ribelayga, C. P. (2020). Molecular and Functional Architecture of the Mouse Photoreceptor Network. Science Advances *6*, eaba7232.

Jin, N. G., Chuang, A. Z., Masson, P. J., and Ribelayga, C. P. (2015). Rod Electrical Coupling is Controlled By a Circadian Clock and Dopamine in Mouse Retina. J. Physiol. *593*, 1597–1631.

Joesch, M., and Meister, M. (2016). A Neuronal Circuit for Colour Vision Based on Rod–Cone Opponency. Nature *532*, 236–239.

Johnson, C. H., and Golden, S. S. (1999). Circadian Programs in Cyanobacteria: Adaptiveness and Mechanism. Annu. Rev. Microbiol. *53*, 389–409.

Johnston, J., and Lagnado, L. (2012). What the Fish's Eye Tells the Fish's Brain. Neuron *76*, 257–259.

Kahneman, D., and Beatty, J. (1966). Pupil Diameter and Load on Memory. Science *154*, 1583.

Kaneko, M., Hernandez-Borsetti, N., and Cahill, G. M. (2006). Diversity of Zebrafish Peripheral Oscillators Revealed By Luciferase Reporting. Proc. Natl. Acad. Sci. U. S. A. *103*, 14614.

Keating, M. J., and Gaze, R. M. (1970). Observations on the 'Surround' Properties of the Receptive Fields of Frog Retinal Ganglion Cells. Quarterly Journal of Experimental Physiology and Cognate Medical Sciences *55*, 129–142.

Keenan, W. T., Rupp, A. C., Ross, R. A., Somasundaram, P., Hiriyanna, S., Wu, Z., Badea, T. C., Robinson, P. R., Lowell, B. B., and Hattar, S. S. (2016). A Visual Circuit Uses Complementary Mechanisms to Support Transient and Sustained Pupil Constriction. eLife *5*, e15392.

Kefalov, V. J., Estevez, M. E., Kono, M., Goletz, P. W., Crouch, R. K., Cornwall, M. C., and Yau, K. W. (2005). Breaking the Covalent Bond--a Pigment Property That Contributes to Desensitization in Cones. Neuron *46*, 879–890.

Kefalov, V., Fu, Y., Marsh-Armstrong, N., and Yau, K.-W. (2003). Role of Visual Pigment Properties in Rod and Cone Phototransduction. Nature *425*, 526–531.

Kerschensteiner, D., and Guido, W. (2017). Organization of the Dorsal Lateral Geniculate Nucleus in the Mouse. Vis. Neurosci. *34*, E008.

Kety, S. S. (1957). The general metabolism of the brain in vivo. In: Metabolism of the Nervous System, (Richter, D., Pergamon), pp. 221-237.

Kiani, R., Ala-Laurila, P., and Rieke, F. (2020). Seeing With a Few Photons: Bridging Cellular and Circuit Mechanisms With Perception. In: The Senses: A Comprehensive Reference (Second Edition), Fritzsch, B., ed. (Oxford: Elsevier), pp. 293-308.

Kito, Y., Suzuki, T., Azuma, M., and Sekoguti, Y. (1968). Absorption Spectrum of Rhodopsin Denatured With Acid. Nature *218*, 955–957.

Ko, G. Y.-P. (2018). Circadian Regulation in the Retina: From Molecules to Network. Eur. J. Neurosci. *51*, 194–216.

Ko, G. Y.-P., Ko, M. L., and Dryer, S. E. (2001). Circadian Regulation of cGMP-Gated Cationic Channels of Chick Retinal Cones: Erk Map Kinase and Ca2+/Calmodulin-Dependent Protein Kinase II. Neuron *29*, 255–266.

Koch, K., Mclean, J., Segev, R., Freed, M. A., Berry, M. J., 2nd, Balasubramanian, V., and Sterling, P. (2006). How Much the Eye Tells the Brain. Curr. Biol. *16*, 1428–1434.

Kock, J.-H., Mecke, E., Orlov, O. Y., Reuter, T., Väisänen, R. A., and Wallgren, E.C.J. (1989). Ganglion Cells in the Frog Retina: Discriminant Analysis of Histological Classes. Vision Res. *29*, 1–18.

Kojima, K., Matsutani, Y., Yamashita, T., Yanagawa, M., Imamoto, Y., Yamano, Y., Wada, A., Hisatomi, O., Nishikawa, K., Sakurai, K., and Shichida, Y. (2017). Adaptation of Cone Pigments Found in Green Rods for

Scotopic Vision Through a Single Amino Acid Mutation. Proc. Natl. Acad. Sci. U. S. A. *114*, 5437.

Kolb, H. (1979). The Inner Plexiform Layer in the Retina of the Cat: Electron Microscopic Observations. J. Neurocytol. *8*, 295–329.

Kolb, H., and Famiglietti, E. V. (1974). Rod and Cone Pathways in the Inner Plexiform Layer of Cat Retina. Science *186*, 47–49.

Kolker, D. E., and Turek, F. W. (2001). 61 - circadian rhythms and sleep in aging rodents. In Functional neurobiology of aging, Hof, P. R., and C. V. Mobbs, eds. (San Diego: Academic Press), pp. 869-882.

Kondrashev, S. (1976). The Influence of the Dimensions of Visual Stimuli on Mating Behaviour of Anuran Males. Zoologicheskii Zhurnal *55*, 1576–1579.

Kondrashev, S., Gnyubkin, V., Dimentman, A., and Orlov, O. (1976). Role of Visual Stimuli in the Breeding Behavior of Males of the Common Frog *Rana temporaria*, the Common Toad *Bufo bufo* and the Green Toad *Bufo viridis*. Zoologicheskii Zhurnal *55*, 1027–1037.

Koskelainen, A., Hemilä, S., and Donner, K. (1994). Spectral Sensitivities of Short- and Long-Wavelength Sensitive Cone Mechanisms in the Frog Retina. Acta Physiologica Scandinavica *152*, 115–124.

Lamb, T. D. (2013). Evolution of Phototransduction, Vertebrate Photoreceptors and Retina. Prog. Retin. Eye. Res. *36*, 52–119.

Land, M. F., and Nilsson, D.-E. (2012). Animal eyes (Oxford, UK: Oxford University Press, Incorporated).

Lasansky, A. (1973). Organization of the Outer Synaptic Layer in the Retina of the Larval Tiger Salamander. Philos. Trans. R. Soc. Lond. B. Biol. Sci. *265*, 471–489.

Laughlin, S. (1981). A Simple Coding Procedure Enhances a Neuron's Information Capacity. Z Naturforsch C Biosci *36*, 910–912.

Laughlin, S. B., De Ruyter Van Steveninck, R. R., and Anderson, J. C. (1998). The Metabolic Cost of Neural Information. Nat. Neurosci. *1*, 36–41.

Lavail, M. M. (1976). Rod Outer Segment Disk Shedding in Rat Retina: Relationship to Cyclic Lighting. Science *194*, 1071–1074.

Lavail, M. M. (1980). Circadian Nature of Rod Outer Segment Disc Shedding in the Rat. Invest Ophthalmol Vis Sci *19*, 407–411.

Lavoie, J., Gagné, A. M., Lavoie, M. P., Sasseville, A., Charron, M. C., and Hébert, M. (2010). Circadian Variation in the Electroretinogram and the Presence of Central Melatonin. Doc. Ophthalmol. *120*, 265–272.

Lázár, G. (1972). Role of the Accessory Optic System in the Optokinetic Nystagmus of the Frog. Brain Behav. Evol. *5*, 443–460.

Legates, T. A., Altimus, C. M., Wang, H., Lee, H.-K., Yang, S., Zhao, H., Kirkwood, A., Weber, E. T., and Hattar, S. (2012). Aberrant Light Directly Impairs Mood and Learning Through Melanopsin-Expressing Neurons. Nature *491*, 594–598.

Leskov, I. B., Klenchin, V. A., Handy, J. W., Whitlock, G. G., Govardovskii, V. I., Bownds, M. D., Lamb, T. D., Pugh, E. N., and Arshavsky, V. Y. (2000). The Gain of Rod Phototransduction: Reconciliation of Biochemical and Electrophysiological Measurements. Neuron *27*, 525–537.

Lettvin, J., Y., Maturana, H., R., McCulloch, W., S., and Pitts, W., H. (1959). What the Frog's Eye Tells the Frog's Brain. Proceedings of the IRE *47*, 1940–1951.

Li, L., and Dowling, J. E. (2000). Effects of Dopamine Depletion on Visual Sensitivity of Zebrafish. J. Neurosci. *20*, 1893–1903.

Liang, L., Fratzl, A., Mansour, O. E., Reggiani, J. D. S., Chen, C., and Andermann, M. L. (2020). Selective Gating of Retinal Information By Arousal. bioRxiv 2020.03.12.989913.

Liebman, P. A., and Entine, G. (1968). Visual Pigments of Frog and Tadpole (*Rana Pipiens*). Vision Res. *8*, 761–IN7.

Liebman, P. A., Parker, K. R., and Dratz, E. A. (1987). The Molecular Mechanism of Visual Excitation and Its Relation to the Structure and Composition of the Rod Outer Segment. Annu Rev Physiol *49*, 765–791.

Liu, D., and Dan, Y. (2019). A Motor Theory of Sleep-Wake Control: Arousal-Action Circuit. Annu. Rev. Neurosci. *42*, 27–46.

Liu, X., Zhang, Z., and Ribelayga, C. P. (2012). Heterogeneous Expression of the Core Circadian Clock Proteins Among Neuronal Cell Types in Mouse Retina. PLoS One *7*, e50602.

Lucas, R. (2013). Mammalian Inner Retinal Photoreception. Curr. Biol. *23*, R125–R133.

Luo, D. G., Yue, W. W., Ala-Laurila, P., and Yau, K. W. (2011). Activation of Visual Pigments By Light and Heat. Science *332*, 1307–1312.

Luo, D.-G., Xue, T., and Yau, K.-W. (2008). How Vision Begins: An Odyssey. Proc. Natl. Acad. Sci. U. S. A. *105*, 9855.

Lyubarsky, A. L., Daniele, L. L., and Pugh, E. N. J. (2004). From Candelas to Photoisomerizations in the Mouse Eye By Rhodopsin Bleaching in Situ and the Light-Rearing Dependence of the Major Components of the Mouse Erg. Vision Res. *44*, 3235–3251.

Ma, J.-X., Znoiko, S., Othersen, K. L., Ryan, J. C., Das, J., Isayama, T., Kono, M., Oprian, D. D., Corson, D. W., Cornwall, M. C., Cameron, D. A., Harosi, F. I., Makino, C. L., and Crouch, R. K. (2001). A Visual Pigment Expressed in Both Rod and Cone Photoreceptors. Neuron *32*, 451–461.

Maimon, G. (2011). Modulation of Visual Physiology By Behavioral State in Monkeys, Mice, and Flies. Curr. Opin. Neurobiol. *21*, 559–564.

Maimon, G., Straw, A. D., and Dickinson, M. H. (2010). Active Flight Increases the Gain of Visual Motion Processing in Drosophila. Nat. Neurosci. *13*, 393–399.

Makino, M., Nagai, K., and Suzuki, T. (1983). Seasonal Variation of the Vitamin A2-Based Visual Pigment in the Retina of Adult Bullfrog, *Rana catesbeiana*. Vision Res. *23*, 199–204.

Manglapus, M. K., Iuvone, P. M., Underwood, H., Pierce, M. E., and Barlow, R. B. (1999). Dopamine Mediates Circadian Rhythms of Rod–Cone Dominance in the Japanese Quail Retina. J. Neurosci. *19*, 4132.

Martersteck, E. M., Hirokawa, K. E., Evarts, M., Bernard, A., Duan, X., Li, Y., Ng, L., Oh, S. W., Ouellette, B., Royall, J. J., Stoecklin, M., Wang, Q., Zeng, H., Sanes, J. R., and Harris, J. A. (2017). Diverse Central Projection Patterns of Retinal Ganglion Cells. Cell Reports *18*, 2058–2072.

Masland, R. H. (2012). The Neuronal Organization of the Retina. Neuron *76*, 266–280.

Masri, R. A., Percival, K. A., Koizumi, A., Martin, P. R., and Grünert, U. (2019). Survey of Retinal Ganglion Cell Morphology in Marmoset. J. Comp. Neurol. *527*, 236–258.

Matthews, G. (1984). Dark Noise in the Outer Segment Membrane Current of Green Rod Photoreceptors From Toad Retina. J. Physiol. *349*, 607–618.

Maturana, H. R., Lettvin, J. Y., Mcculloch, W. S., and Pitts, W. H. (1960). Anatomy and Physiology of Vision in the Frog (*Rana Pipiens*). J. Gen. Physiol. *43*, 129–175.

Maximov, V. V., Orlov, O. Y., and Reuter, T. (1985). Chromatic Properties of the Retinal Afferents in the Thalamus and the Tectum of the Frog (*Rana temporaria*). Vision Res. *25*, 1037–1049.

McCormack, C. A., and McDonnell, M. T. (1994). Circadian Regulation of Teleost Retinal Cone Movements in Vitro. J. Gen. Physiol. *103*, 487–499.

McCormick, D. A., Nestvogel, D. B., and He, B. J. (2020). Neuromodulation of Brain State and Behavior. Annu. Rev. Neurosci. *43*, 391–415.

Mcginley, M., David, S., and McCormick, D. (2015a). Cortical Membrane Potential Signature of Optimal States for Sensory Signal Detection. Neuron *87*, 179–192.

McGinley, M., Vinck, M., Reimer, J., Batista-Brito, R., Zagha, E., Cadwell, C., Tolias, A., Cardin, J., and McCormick, D. (2015b). Waking State: Rapid Variations Modulate Neural and Behavioral Responses. Neuron *87*, 1143–1161.

McMahon, D. G., Iuvone, P. M., and Tosini, G. (2014). Circadian Organization of the Mammalian Retina: From Gene Regulation to Physiology and Diseases. Prog. Retin. Eye. Res. *39*, 58–76.

Melamed, E., Frucht, Y., Lemor, M., Uzzan, A., and Rosenthal, Y. (1984). Dopamine Turnover in Rat Retina: A 24-Hour Light-Dependent Rhythm. Brain Res. *305*, 148–151.

Miranda-Anaya, M., Bartell, P. A., and Menaker, M. (2002). Circadian Rhythm of Iguana Electroretinogram: The Role of Dopamine and Melatonin. J. Biol. Rhythms *17*, 526–538.

Moran, D., Softley, R., and Warrant, E. J. (2015). The Energetic Cost of Vision and the Evolution of Eyeless Mexican Cavefish. Science Advances *1*, e1500363.

Morin, L. P., and Studholme, K. M. (2014). Retinofugal Projections in the Mouse. J. Comp. Neurol. *522*, 3733–3753.

Munk, O. (1970). On the Occurrence and Significance of Horizontal Band-Shaped Retinal Areae in Teleosts. Vidensk Medd Dan Naturhist Foren *133*, 85–120.

Muntz, W. R. A. (1962a). Effectiveness of Different Colors of Light in Releasing Positive Phototactic Behavior of Frogs, and a Possible Function of the Retinal Projection to the Diencephalon. J. Neurophysiol. *25*, 712–720.

Muntz, W. R. A. (1962b). Microelectrode Recordings From the Diencephalon of the Frog (*Rana pipiens*) and a Blue-Sensitive System. J. Neurophysiol. *25*, 699–711.

Muntz, W. R. A. (1963). The Development of Phototaxis in the Frog (*Rana temporaria*). J. Exp. Biol. *40*, 371.

Muntz, W. R. A. (1964). Vision in Frogs. Sci. Am. *210*, 110–119.

Muntz, W. R. A., and Reuter, T. (1966). Visual Pigments and Spectral Sensitivity in *Rana temporaria* and Other European Tadpoles. Vision Res. *6*, 601–618.

Murphy, G. J., and Rieke, F. (2006). Network Variability Limits Stimulus-Evoked Spike Timing Precision in Retinal Ganglion Cells. Neuron *52*, 511–524.

Murphy, P. R., Vandekerckhove, J., and Nieuwenhuis, S. (2014). Pupil-Linked Arousal Determines Variability in Perceptual Decision Making. PLoS Comput. Biol. *10*, e1003854.

Musolf, K., and Penn, D. J. (2012). Ultrasonic vocalizations in house mice. In Evolution of the house mouse, Piálek, J., M. Macholán, P. Munclinger, and S. J. E. Baird, eds. (Cambridge: Cambridge University Press), pp. 253-277.

Naarendorp, F., Esdaille, T. M., Banden, S. M., Andrews-Labenski, J., Gross, O. P., and Pugh, E. N. J. (2010). Dark Light, Rod Saturation, and the Absolute and Incremental Sensitivity of Mouse Cone Vision. J. Neurosci. *30*, 12495–12507.

Nakahara, D., Nakamura, M., Iigo, M., and Okamura, H. (2003). Bimodal Circadian Secretion of Melatonin From the Pineal Gland in a Living CBA Mouse. Proc. Natl. Acad. Sci. U. S. A. *100*, 9584–9589.

Nelson, R., and Connaughton, V. (2020). Bipolar cell pathways in the vertebrate retina. (Webvision: Moran Eye Center).

Niell, C. M., and Stryker, M. P. (2010). Modulation of Visual Responses By Behavioral State in Mouse Visual Cortex. Neuron *65*, 472–479.

Nilsson, S. E. G. (1964). An Electron Microscopic Classification of the Retinal Receptors of the Leopard Frog (*Rana pipiens*). J. Ultrastruct. Res. *10*, 390–416.

Nir, I., Haque, R., and Iuvone, P. M. (2000). Diurnal Metabolism of Dopamine in the Mouse Retina. Brain Res. *870*, 118–125.

Niven, J. E., and Laughlin, S. B. (2008). Energy Limitation as a Selective Pressure on the Evolution of Sensory Systems. J. Exp. Biol. *211*, 1792.

O'Keefe, L. P., and Baker, H. D. (1987). Diurnal Changes in Human Psychophysical Luminance Sensitivity. Physiol. Behav. *41*, 193–200.

Orlov, O. Y., and Maximov, V. V. (1982). Colour Vision and Behaviour of Amphibians. In Sensory systems. Vision. (Leningrad, Russia: Nauka. [In Russian.]), pp. 114-125.

Pack, W., Hill, D. D., and Wong, K. Y. (2015). Melatonin Modulates M4-Type Ganglion-Cell Photoreceptors. Neuroscience *303*, 178–188.

Pahlberg, J., and Sampath, A. P. (2011). Visual Threshold is Set By Linear and Nonlinear Mechanisms in the Retina That Mitigate Noise: How Neural Circuits in the Retina Improve the Signal-to-noise Ratio of the Single-Photon Response. BioEssays *33*, 438–447.

Palczewski, K., Kumasaka, T., Hori, T., Behnke, C. A., Motoshima, H., Fox, B. A., Trong, I. L., Teller, D. C., Okada, T., Stenkamp, R. E., Yamamoto, M., and Miyano, M. (2000). Crystal Structure of Rhodopsin: A G Protein-Coupled Receptor. Science *289*, 739.

Pang, J.-J., Gao, F., Lem, J., Bramblett, D. E., Paul, D. L., and Wu, S. M. (2010). Direct Rod Input to Cone BCs and Direct Cone Input to Rod BCs Challenge the Traditional View of Mammalian BC Circuitry. Proc. Natl. Acad. Sci. U. S. A. *107*, 395.

Peichl, L., Sandmann, D., and Boycott, B. B. (1998). Comparative anatomy and function of mammalian horizontal cells development and organization of the retina: From molecules to function. Chalupa, L. M., and B. L. Finlay, eds. (Boston, MA: Springer US), pp. 147-172.

Peng, Y.-R., Shekhar, K., Yan, W., Herrmann, D., Sappington, A., Bryman, G. S., Van Zyl, T., Do, M. T. H., Regev, A., and Sanes, J. R. (2019). Molecular Classification and Comparative Taxonomics of Foveal and Peripheral Cells in Primate Retina. Cell *176*, 1222–1237.e22.

Perge, J. A., Koch, K., Miller, R., Sterling, P., and Balasubramanian, V. (2009). How the Optic Nerve Allocates Space, Energy Capacity, and Information. J. Neurosci. *29*, 7917.

Perry, V. H., and Cowey, A. (1984). Retinal Ganglion Cells That Project to the Superior Colliculus and Pretectum in the Macaque Monkey. Neuroscience *12*, 1125–1137.

Peters, J. L., and Cassone, V. M. (2005). Melatonin Regulates Circadian Electroretinogram Rhythms in a Dose- and Time-Dependent Fashion. J. Pineal Res. *38*, 209–215.

Pierce, M. E., Sheshberadaran, H., Zhang, Z., Fox, L. E., Applebury, M. L., and Takahashi, J. S. (1993). Circadian Regulation of Iodopsin Gene Expression in Embryonic Photoreceptors in Retinal Cell Culture. Neuron *10*, 579–584.

Pirenne, M. H. (1967). Vision and the eye (London: Chapman & Hall).

Piscopo, D. M., El-Danaf, R. N., Huberman, A. D., and Niell, C. M. (2013). Diverse Visual Features Encoded in Mouse Lateral Geniculate Nucleus. J. Neurosci. *33*, 4642–4656.

Pozdeyev, N. V., and Lavrikova, E. V. (2000). Diurnal Changes of Tyrosine, Dopamine, and Dopamine Metabolites Content in the Retina of Rats Maintained At Different Lighting Conditions. Journal of Molecular Neuroscience *15*, 1–9.

Prusky, G. T., West, P. W., and Douglas, R. M. (2000). Behavioral Assessment of Visual Acuity in Mice and Rats. Vision Res. *40*, 2201–2209.

Purves, D., Augustine, G. J., Fitzpatrick, D., Hall, W. C., LaMantia, A.-S., and White, L. E. (2012). Neuroscience. 5th edition (Sunderland: Sinauer Associates, Inc.).

Ramón Y Cajal, S. (1894). Die Retina der Wirbelthiere. Trans. by R. Greeff (Wiesbaden: Bergmann).

Reimer, J., Froudarakis, E., Cadwell, C., Yatsenko, D., Denfield, G., and Tolias, A. (2014). Pupil Fluctuations Track Fast Switching of Cortical States During Quiet Wakefulness. Neuron *84*, 355–362.

Remtulla, S., and Hallett, P. E. (1985). A Schematic Eye for the Mouse, and Comparisons With the Rat. Vision Res. *25*, 21–31.

Reppert, S. M., and Weaver, D. R. (2002). Coordination of Circadian Timing in Mammals. Nature *418*, 935–941.

Reuter, T. E., White, R. H., and Wald, G. (1971). Rhodopsin and Porphyropsin Fields in the Adult Bullfrog Retina. J. Gen. Physiol. *58*, 351–371.

Reuter, T. Visual pigments and ganglion cell activity in the retinae of tadpoles and adult frogs (*Rana temporaria* L.). Helsinki: Societas Pro Fauna et Flora Fennica; 1969. 64 p. Dissertation.

Rheaume, B. A., Jereen, A., Bolisetty, M., Sajid, M. S., Yang, Y., Renna, K., Sun, L., Robson, P., and Trakhtenberg, E. F. (2018). Single Cell Transcriptome Profiling of Retinal Ganglion Cells Identifies Cellular Subtypes. Nat. Commun. *9*, 2759.

Ribelayga, C., Cao, Y., and Mangel, S. C. (2008). The Circadian Clock in the Retina Controls Rod-Cone Coupling. Neuron *59*, 790–801.

Ribelayga, C., Wang, Y., and Mangel, S. C. (2004). A Circadian Clock in the Fish Retina Regulates Dopamine Release Via Activation of Melatonin Receptors. J. Physiol. *554*, 467–482.

Rieke, F., and Baylor, D. A. (1996). Molecular Origin of Continuous Dark Noise in Rod Photoreceptors. Biophys. J. *71*, 2553–2572.

Rieke, F., Warland, D., De Ruyter Van Steveninck, R., and Bialek, W. (1997). Spikes: Exploring the neural code (Cambridge, MA: MIT Press).

Röhlich, P., Van Veen, T., and Szél, Á. (1994). Two Different Visual Pigments in One Retinal Cone Cell. Neuron *13*, 1159–1166.

Röhlich, P., and Szél, Á. (2000). Photoreceptor Cells in the *Xenopus* Retina. Microscopy Research and Technique *50*, 327–337.

Román Rosón, M., Bauer, Y., Kotkat, A. H., Berens, P., Euler, T., and Busse, L. (2019). Mouse dLGN Receives Functional Input From a Diverse Population of Retinal Ganglion Cells With Limited Convergence. Neuron *102*, 462–476.e8.

Roth, M. M., Dahmen, J. C., Muir, D. R., Imhof, F., Martini, F. J., and Hofer, S. B. (2016). Thalamic Nuclei Convey Diverse Contextual Information to Layer 1 of Visual Cortex. Nat. Neurosci. *19*, 299–307.

Ruan, G.-X., Zhang, D.-Q., Zhou, T., Yamazaki, S., and McMahon, D. G. (2006). Circadian Organization of the Mammalian Retina. Proc. Natl. Acad. Sci. U. S. A. *103*, 9703.

Saalmann, Y. B., Pinsk, M. A., Wang, L., Li, X., and Kastner, S. (2012). The Pulvinar Regulates Information Transmission Between Cortical Areas Based on Attention Demands. Science *337*, 753.

Salay, L. D., Ishiko, N., and Huberman, A. D. (2018). A Midline Thalamic Circuit Determines Reactions to Visual Threat. Nature *557*, 183–189.

Saleem, A. B., Ayaz, A., Jeffery, K. J., Harris, K. D., and Carandini, M. (2013). Integration of Visual Motion and Locomotion in Mouse Visual Cortex. Nat. Neurosci. *16*, 1864–1869.

Salkoff, D. B., Zagha, E., McCarthy, E., and McCormick, D. A. (2020). Movement and Performance Explain Widespread Cortical Activity in a Visual Detection Task. Cereb Cortex *30*, 421–437.

Sampath, A. P., and Baylor, D. A. (2002). Molecular Mechanism of Spontaneous Pigment Activation in Retinal Cones. Biophys. J. *83*, 184–193.

Sampath, A. P., and Rieke, F. (2004). Selective Transmission of Single Photon Responses By Saturation At the Rod-to-rod Bipolar Synapse. Neuron *41*, 431–443.

Sandu, C., Hicks, D., and Felder-Schmittbuhl, M. P. (2011). Rat Photoreceptor Circadian Oscillator Strongly Relies on Lighting Conditions. Eur. J. Neurosci. *34*, 507–516.

Saxén, L. (1953). An Atypical Form of the Double Visual Cell in the Frog (*Rana temporaria* L.). Cells Tissues Organs *19*, 190–196.

Saxén, L. (1954). The Development of the Visual Cells. Ann. Acad. Sci. Fenn. (A IV) *23*, 1–95.

Scalia, F. (1976). The optic pathway of the frog: Nuclear organization and connections. In Frog neurobiology: A handbook, Llinás, R., and W. Precht, eds. (Berlin, Heidelberg: Springer Berlin Heidelberg), pp. 386-406.

Schmidt, T. M., Chen, S.-K., and Hattar, S. (2011). Intrinsically Photosensitive Retinal Ganglion Cells: Many Subtypes, Diverse Functions. Trends Neurosci. *34*, 572–580.

Schröder, S., Steinmetz, N. A., Krumin, M., Pachitariu, M., Rizzi, M., Lagnado, L., Harris, K. D., and Carandini, M. (2020). Arousal Modulates Retinal Output. Neuron *107*, 487–495.e9.

Schwartz, G., Taylor, S., Fisher, C., Harris, R., and Berry, M. J. (2007). Synchronized Firing Among Retinal Ganglion Cells Signals Motion Reversal. Neuron *55*, 958–969.

Seabrook, T. A., Burbridge, T. J., Crair, M. C., and Huberman, A. D. (2017). Architecture, Function, and Assembly of the Mouse Visual System. Annu. Rev. Neurosci. *40*, 499–538.

Sengupta, A., Baba, K., Mazzoni, F., Pozdeyev, N. V., Strettoi, E., Iuvone, P. M., and Tosini, G. (2011). Localization of Melatonin Receptor 1 in Mouse

Retina and Its Role in the Circadian Regulation of the Electroretinogram and Dopamine Levels. PLoS One *6*, e24483.

Sengupta, B., Stemmler, M., Laughlin, S. B., and Niven, J. E. (2010). Action Potential Energy Efficiency Varies Among Neuron Types in Vertebrates and Invertebrates. PLoS Comput. Biol. *6*, e1000840.

Shaw, A. P., Collazo, C. R., Easterling, K., Young, C. D., and Karwoski, C. J. (1993). Circadian Rhythm in the Visual System of the Lizard *Anolis carolinensis*. J. Biol. Rhythms *8*, 107–124.

Shichida, Y., Imai, H., Imamoto, Y., Fukada, Y., and Yoshizawa, T. (1994). Is Chicken Green-Sensitive Cone Visual Pigment a Rhodopsin-Like Pigment? A Comparative Study of the Molecular Properties Between Chicken Green and Rhodopsin. Biochemistry *33*, 9040–9044.

Shichida, Y., and Matsuyama, T. (2009). Evolution of Opsins and Phototransduction. Philos. Trans. R. Soc. Lond. B. Biol. Sci. *364*, 2881–2895.

Shichida, Y., and Imai, H. (1998). Visual Pigment: G-Protein-coupled Receptor for Light Signals. Cell. Mol. Life Sci *54*, 1299–1315.

Shimaoka, D., Harris, K. D., and Carandini, M. (2018). Effects of Arousal on Mouse Sensory Cortex Depend on Modality. Cell Reports *22*, 3160–3167.

Siddiqi, A., Cronin, T. W., Loew, E. R., Vorobyev, M., and Summers, K. (2004). Interspecific and Intraspecific Views of Color Signals in the Strawberry Poison Frog *Dendrobates pumilio*. J. Exp. Biol. *207*, 2471.

Simoncelli, E. P., and Olshausen, B. A. (2001). Natural Image Statistics and Neural Representation. Annu. Rev. Neurosci. *24*, 1193–1216.

Sinha, R., Hoon, M., Baudin, J., Okawa, H., Wong, R. O. L., and Rieke, F. (2017). Cellular and Circuit Mechanisms Shaping the Perceptual Properties of the Primate Fovea. Cell *168*, 413–426.e12.

Smeds, L., Takeshita, D., Turunen, T., Tiihonen, J., Westö, J., Martyniuk, N., Seppänen, A., and Ala-Laurila, P. (2019). Paradoxical Rules of Spike Train Decoding Revealed At the Sensitivity Limit of Vision. Neuron *104*, 576–587.e11.

Sonoda, T., and Schmidt, T. M. (2016). Re-Evaluating the Role of Intrinsically Photosensitive Retinal Ganglion Cells: New Roles in Image-Forming Functions. Integr. Comp. Biol. *56*, 834–841.

Soucy, E., Wang, Y., Nirenberg, S., Nathans, J., and Meister, M. (1998). A Novel Signaling Pathway From Rod Photoreceptors to Ganglion Cells in Mammalian Retina. Neuron *21*, 481–493.

Srinivasan, M. V., Laughlin, S. B., and Dubs, A. (1982). Predictive Coding: A Fresh View of Inhibition in the Retina. Proc. R. Soc. Lond. B. Biol. Sci. *216*, 427–459.

Steele, C. T., Tosini, G., Siopes, T., and Underwood, H. (2006). Time Keeping By the Quail's Eye: Circadian Regulation of Melatonin Production. Gen Comp Endocrinol *145*, 232–236.

Sterling, P. (2004). How retinal circuits optimize the transfer of visual information. In The visual neurosciences, Chalupa, L., M., and J. Werner, S., eds. (Cambridge, MA: MIT Press), pp. 234-259.

Sterling, P., and Laughlin, S. (2015). Principles of neural design (Cambridge, MA: MIT Press).

Stopka, P., Stopková, R., and Janotová, K. (2012). Mechanisms of chemical communication. In Evolution of the house mouse, Piálek, J., M. Macholán, P. Munclinger, and S. J. E. Baird, eds. (Cambridge: Cambridge University Press), pp. 191-220.

Storch, K.-F., Paz, C., Signorovitch, J., Raviola, E., Pawlyk, B., Li, T., and Weitz, C. J. (2007). Intrinsic Circadian Clock of the Mammalian Retina: Importance for Retinal Processing of Visual Information. Cell *130*, 730–741.

Strother, J. A., Wu, S.-T., Rogers, E. M., Eliason, J. L. M., Wong, A. M., Nern, A., and Reiser, M. B. (2018). Behavioral State Modulates the on Visual Motion Pathway of *Drosophila*. Proc. Natl. Acad. Sci. U. S. A. *115*, E102.

Szatko, K. P., Korympidou, M. M., Ran, Y., Berens, P., Dalkara, D., Schubert, T., Euler, T., and Franke, K. (2020). Neural Circuits in the Mouse Retina Support Color Vision in the Upper Visual Field. Nat. Commun. *11*, 3481.

Szél, Á., Csorba, G., Caffé, A. R., Szél, G., Röhlich, P., and Van Veen, T. (1994). Different Patterns of Retinal Cone Topography in Two Genera of Rodents, *Mus* and *Apodemus*. Cell Tissue Res. *276*, 143–150.

Szikra, T., Trenholm, S., Drinnenberg, A., Jüttner, J., Raics, Z., Farrow, K., Biel, M., Awatramani, G., Clark, D. A., Sahel, J.-A., Da Silveira, R. A., and Roska, B. (2014). Rods in Daylight Act as Relay Cells for Cone-Driven Horizontal Cell–Mediated Surround Inhibition. Nat. Neurosci. *17*, 1728–1735.

Takahashi, J. S. (2017). Transcriptional Architecture of the Mammalian Circadian Clock. Nat. Rev. Genet. *18*, 164–179.

Takeshita, D., Smeds, L., and Ala-Laurila, P. (2017). Processing of Single-Photon Responses in the Mammalian on and Off Retinal Pathways At the Sensitivity Limit of Vision. Philos. Trans. R. Soc. Lond. B. Biol. Sci. *372*, 20160073.

Tan, Z., Sun, W., Chen, T.-W., Kim, D., and Ji, N. (2015). Neuronal Representation of Ultraviolet Visual Stimuli in Mouse Primary Visual Cortex. Sci. Rep. *5*, 12597.

Tassi, P., Pellerin, N., Moessinger, M., Eschenlauer, R., and Muzet, A. (2000). Variation of Visual Detection Over the 24-Hour Period in Humans. Chronobiology International *17*, 795–805.

Toda, K., Bush, R. A., Humphries, P., and Sieving, P. A. (1999). The Electroretinogram of the Rhodopsin Knockout Mouse. Vis. Neurosci. *16*, 391–398.

Tosini, G., Baba, K., Hwang, C. K., and Iuvone, P. M. (2012). Melatonin: An Underappreciated Player in Retinal Physiology and Pathophysiology. Exp. Eye. Res. *103*, 82–89.

Tosini, G., Davidson, A. J., Fukuhara, C., Kasamatsu, M., and Castanon-Cervantes, O. (2007a). Localization of a Circadian Clock in Mammalian Photoreceptors. FASEB J. *21*, 3866–3871.

Tosini, G., and Menaker, M. (1998). The Tau Mutation Affects Temperature Compensation of Hamster Retinal Circadian Oscillators. Neuroreport *9*, 1001–1005.

Tosini, G., Iuvone, P. M., McMahon, D. G., and Collin, S. P. (2014). The Retina and Circadian Rhythms. Springer Series in Vision Research 238.

Tosini, G., Kasamatsu, M., and Sakamoto, K. (2007b). Clock Gene Expression in the Rat Retina: Effects of Lighting Conditions and Photoreceptor Degeneration. Brain Res. *1159*, 134–140.

Tosini, G., and Menaker, M. (1996). Circadian Rhythms in Cultured Mammalian Retina. Science *272*, 419.

Tosini, G., and Menaker, M. (1998). Multioscillatory Circadian Organization in a Vertebrate, *Iguana iguana*. J. Neurosci. *18*, 1105.

Trexler, E. B., Li, W., Mills, S. L., and Massey, S. C. (2001). Coupling From AII Amacrine Cells to on Cone Bipolar Cells is Bidirectional. J. Comp. Neurol. *437*, 408–422.

Tuthill, J., Nern, A., Rubin, G., and Reiser, M. (2014). Wide-Field Feedback Neurons Dynamically Tune Early Visual Processing. Neuron *82*, 887–895.

Van Der Velden, H. A. (1946). The Number of Quanta Necessary for the Perception of Light of the Human Eye. Ophthalmologica *111*, 321–331.

Vinck, M., Batista-Brito, R., Knoblich, U., and Cardin, J. (2015). Arousal and Locomotion Make Distinct Contributions to Cortical Activity Patterns and Visual Encoding. Neuron *86*, 740–754.

Von Schantz, M., Lucas, R. J., and Foster, R. G. (1999). Circadian Oscillation of Photopigment Transcript Levels in the Mouse Retina. Brain Res Mol Brain Res *72*, 108–114.

Vugler, A. A., Redgrave, P., Semo, M., Lawrence, J., Greenwood, J., and Coffey, P. J. (2007). Dopamine Neurones Form a Discrete Plexus With Melanopsin Cells in Normal and Degenerating Retina. Exp. Neurol. *205*, 26–35.

Wald, G. (1955). Visual Pigments and Vitamins a of the Clawed Toad, *Xenopus Laevis*. Nature *175*, 390–391.

Wang, Z., Asenjo, A. B., and Oprian, D. D. (1993). Identification of the Cl(-)-binding Site in the Human Red and Green Color Vision Pigments. Biochemistry *32*, 2125–2130.

Warrant, E. J. (2017). The Remarkable Visual Capacities of Nocturnal Insects: Vision at the Limits With Small Eyes and Tiny Brains. Philos. Trans. R. Soc. Lond. B. Biol. Sci. *372*, 20160063.

Warrant, E. J., and Nilsson, D.-E. (1998). Absorption of White Light in Photoreceptors. Vision Res. *38*, 195–207.

Wässle, H., Grünert, U., Röhrenbeck, J., and Boycott, B. B. (1989). Cortical Magnification Factor and the Ganglion Cell Density of the Primate Retina. Nature *341*, 643–646.

Wehner, R. (1987). 'Matched Filters' — Neural Models of the External World. Journal of Comparative Physiology A *161*, 511–531.

Wells, K. D. (2007). The ecology & behavior of amphibians (Chicago: University of Chicago Press).

Werblin, F. S., and Dowling, J. E. (1969). Organization of the Retina of the Mudpuppy, *Necturus maculosus*. II. Intracellular Recording. J. Neurophysiol. *32*, 339–355.

White, M. P., and Hock, P. A. (1992). Effects of Continuous Darkness on Erg Correlates of Disc Shedding in Rabbit Retina. Exp Eye Res *54*, 173–180.

Wiechmann, A. F., Vrieze, M. J., Dighe, R., and Hu, Y. (2003). Direct Modulation of Rod Photoreceptor Responsiveness Through a Mel1c Melatonin Receptor in Transgenic *Xenopus Laevis* Retina. Investig. Ophthalmol. Vis. Sci. *44*, 4522–4531.

Wienbar, S., and Schwartz, G. W. (2018). The Dynamic Receptive Fields of Retinal Ganglion Cells. Prog. Retin. Eye. Res. *67*, 102–117.

Wilby, D., and Roberts, N. W. (2017). Optical Influence of Oil Droplets on Cone Photoreceptor Sensitivity. J. Exp. Biol. *220*, 1997.

Wirz-Justice, A., Da Prada, M., and Remé, C. (1984). Circadian Rhythm in Rat Retinal Dopamine. Neurosci. Lett. *45*, 21–25.

Witkovsky, P., Veisenberger, E., Lesauter, J., Yan, L., Johnson, M., Zhang, D.-Q., McMahon, D., and Silver, R. (2003). Cellular Location and Circadian Rhythm of Expression of the Biological Clock Gene Period 1 in the Mouse Retina. J. Neurosci. *23*, 7670–7676.

Witpaard, J., and Keurs, H. E. D. J. T. (1975). A Reclassification of Retinal Ganglion Cells in the Frog, Based Upon Tectal Endings and Response Properties. Vision Res. *15*, 1333–IN6.

Wong-Riley, M. T. T. (2010). Energy Metabolism of the Visual System. Eye Brain. *2*, 99–116.

Yan, W., Laboulaye, M. A., Tran, N. M., Whitney, I. E., Benhar, I., and Sanes, J. R. (2020). Mouse Retinal Cell Atlas: Molecular Identification of Over Sixty Amacrine Cell Types. J. Neurosci. *40*, 5177.

Yanagawa, M., Kojima, K., Yamashita, T., Imamoto, Y., Matsuyama, T., Nakanishi, K., Yamano, Y., Wada, A., Sako, Y., and Shichida, Y. (2015). Origin of the Low Thermal Isomerization Rate of Rhodopsin Chromophore. Sci. Rep. *5*, 11081.

Yang, C.-Y., Hassin, G., and Witkovsky, P. (1983). Blue-Sensitive Rod Input to Bipolar and Ganglion Cells of the *Xenopus* Retina. Vision Res. *23*, 933–941.

Yeandle, S. (1958). Evidence of Quantized Slow Potentials in the Eye of Limulus. Am. J. Ophthalmol *46*, 82.

Yeandle, S., and Spiegler, J. B. (1973). Light-Evoked and Spontaneous Discrete Waves in the Ventral Nerve Photoreceptor of Limulus. J. Gen. Physiol. *61*, 552–571.

Yilmaz, M., and Meister, M. (2013). Rapid Innate Defensive Responses of Mice to Looming Visual Stimuli. Curr. Biol. *23*, 2011–2015.

Yokoyama, S. (2000). Molecular Evolution of Vertebrate Visual Pigments. Prog. Retin. Eye. Res. *19*, 385–419.

Zak, P. P., Ostrovsky, M. A., and Bowmaker, J. K. (2001). Ionochromic Properties of Long-Wave-sensitive Cones in the Goldfish Retina: An Electrophysiological and Microspectrophotometric Study. Vision Res. *41*, 1755–1763.

Zhang, D. Q., Wong, K. Y., Sollars, P. J., Berson, D. M., Pickard, G. E., and McMahon, D. G. (2008). Intraretinal Signaling By Ganglion Cell Photoreceptors to Dopaminergic Amacrine Neurons. Proc. Natl. Acad. Sci. U. S. A. *105*, 14181–14186.

Zhang, R., Lahens, N. F., Ballance, H. I., Hughes, M. E., and Hogenesch, J. B. (2014). A Circadian Gene Expression Atlas in Mammals: Implications for Biology and Medicine. Proc. Natl. Acad. Sci. U. S. A. *111*, 16219.

Zhu, H., Larue, S., Whiteley, A., Steeves, T. D. L., Takahashi, J. S., and Green, C. B. (2000). The *Xenopus* Clock Gene is Constitutively Expressed in Retinal Photoreceptors. Mol. Brain Res. *75*, 303–308.

ISBN 978-951-51-6548-0 (PRINT)
ISBN 978-951-51-6549-7 (ONLINE)
ISSN 2342-3161 (PRINT)
ISSN 2342-317X (ONLINE)
http://ethesis.helsinki.fi

HELSINKI 2020